Universidad de Salamanca

Instituto de Biología Funcional y Genómica (IBFG-CSIC)

MES-4 regulation through cell cycle during development in *Caenorhabditis elegans*

PhD thesis

Sara Amanda Rivera Martín

Salamanca, 2018

Memoria presentada por Sara Amanda Rivera Martín para optar al título de Doctor por la Universidad de Salamanca.

Este trabajo ha sido realizado en el Instituto de Biología Funcional y Genómica (IBFG-CSIC) bajo la supervisión del Doctor José Pérez Martín.

MINISTERIO
DE ECONOMÍA
Y COMPETITIVIDAD

CSIC

VNiVERSiDAD
D SALAMANCA

ibfg
INSTITUTO DE BIOLOGÍA
FUNCIONAL Y GENÓMICA

JOSE PEREZ MARTIN, DNI 28473540T, PROFESOR DE INVESTIGACIÓN DEL CSIC EN EL INSTITUTO DE BIOLOGIA FUNCIONAL Y GENOMICA (CSIC-USAL)

CERTIFICA:

Que la memoria titulada "MES-4 regulation through cell cycle during development in Caenorhabditis elegans " presentada por la Licenciada SARA AMANDA RIVERA MARTIN, ha sido realizada bajo su dirección en el Instituto de Biología Funcional y Genómica y reúne, a su juicio, originalidad y contenidos suficientes para que sea presentada ante el tribunal correspondiente y optar al grado de Doctor por la Universidad de Salamanca.

Y para que así conste, a efectos legales, expide el presente certificado en Salamanca a 4 de Marzo de 2018.

INSTITUTO DE BIOLOGIA FUNCIONAL Y GENOMICA
ibfg
SALAMANCA CSIC-USAL

Fdo.

José Pérez Martín

jose.perez@csic.es
http://www.ibfg.usal-csic.es

Zacarias Gonzalez 2
37007 SALAMANCA. ESPAÑA
TEL.: 923 294912; FAX: 923 224876

Acknowledgemnts

Antes que nada, me gustaría agradecer mi director de tesis, Pepe, su paciencia y dedicación. Gracias por confiar en mí, por todo el apoyo recibido durante estos años, y por ayudarme a crecer científicamente. Sin ti este trabajo no habría sido posible. Gracias también a Juan Cabello por su implicación en el proyecto desde el inicio, por sus ideas y su ayuda. A mis compañeros de laboratorio: a María, por estar siempre ahí, en las buenas y en las malas. Soninha, compañera de aventuras y desventuras tanto dentro como fuera del lab. Gracias a Adrián, el otro "gusanero", por hacer los días más amenos con sus imitaciones y chistes malos (casi tanto como los de Pepe). Y cómo olvidar a Paola y Antonio, cual Pepa y Abelino, siempre haciéndonos reír.

Gracias también a los compañeros del IBFG, en especial a Irene (2.6), por su apoyo y sus ideas, germen del inicio del estudio de Cdh1. Gracias también a Carmen, por su paciencia y dulzura, y por estar siempre disponible cuando el spinning empezaba a hacer de las suyas. Y no puedo olvidar a Vero por su apoyo y sus consejos en estos últimos meses de escritura.

I also want to thank Susan Strome for her support and for accepting me in the lab during my stay. Many thanks for the reagents and strains provided. Thanks also to all the Strome's lab, for their useful discussion and for making my stay wonderful. Special mention to Alec, who made the KEN box mutant as soon as he heard about that KEN box and to Kiyomi, who had the patience of teaching me the immunostaining technique.

Gracias también a mis amigos valencianos, siempre presentes aún en la distancia. Gracias por vuestro apoyo incondicional. Gracias en especial a Marta por estar siempre ahí para cualquier cosa con una sonrisa, incluso ahora desde el extranjero. A Robert y Eva, siempre dispuestos y con el corazón abierto. El doctorado es una aventura más que iniciamos juntos, y vosotros habéis sido tres pilares fundamentales a lo largo de estos años.

Quisiera agradecer también a "las viejas glorias" esos martes y jueves de desconexión total llenos de música, danza y risas. Y cómo no, mil gracias a Ángel por estar siempre a mi lado, por tu cariño y comprensión. Gracias por animarme en los peores días y entusiasmarte con mis alegrías, por haberme ayudado a crecer como persona y por compartir conmigo tu camino.

Por último, quiero dar las gracias a mi familia, en especial a aquellos que me han traído hasta aquí. Gracias de corazón a mis padres, por hacerme creer en mí misma. Gracias por haberme enseñado la importancia del trabajo bien hecho y del pensamiento crítico. Gracias por apoyarme, por enseñarme que lo que importa al final son aquellos que te acompañan en tu viaje. Vosotros habéis estado desde el inicio del mío, y esto no lo habría logrado sin vosotros.

Sin todos vosotros esta Tesis no habría sido posible.

Contents table

Abstract

During development of multicellular organisms differentiation and cell cycle need a tight coordination. This coordination is also orchestrated by changes in the chromatin landscape. From the initial divisions to the differentiated cells, chromatin switches from an "immature" state that enables stemness and high cell cycle activity, to a "differentiated" state, in which cells have exit cell cycle and are totally differentiated. In the worm *Caenorhabditis elegans* these two situations are easily distinguished, and regulation of MES proteins maintain this distinction. In this study we centered on the study of the histone methyltransferase MES-4/NSD family.

MES-4 maintains the "immature" chromatin landscape, being essential for the survival of germ cells. LIN-35/pRb inhibits *mes-4* transcription (Kudron *et al*., 2013; Wang *et al*., 2005a), and we found that a KEN box in the MES-4 protein sequence is the target of APC/C$^{FZR\text{-}1/Cdh1}$-dependent regulation. Therefore, MES-4 is regulated through cell cycle inhibitors LIN-35 and APC/C$^{FZR\text{-}1}$. This double regulation seems to be important during the development of the worm. Besides, FZR-1 and LIN-35 repression depends on the tissue and developmental stage, being FZR-1 more important in neurons in the head and tail of the worm in early stages, than LIN-35. On the contrary, both regulators cooperate in other tissues, such as the intestine. This cooperation allows a fine-tuned regulation of MES-4 levels during development.

Abbreviation list

APC/C: Anaphase Promoting Complex/Cyclosome

CDK: cyclin-dependent kinase

cDNA: coding DNA

C. elegans*: Caenorhabditis elegans*

CGC: *Caenorhabditis* Genetics Centre

CKI: cyclin-dependent kinase inhibitor

CRISPR: Clustered regularly interspaced short palindromic repeats

CYA/B/D: cyclin A, B, D

CYE-1: cyclin E

DNA: deoxyribonucleic acid

DNC: dorsal nerve cord

DSB: double strand break

DTC: distal tip cell

E. coli*: Escherichia coli*

EZH2:enhancer of zeste homologous2

Fig.: figure

FZR-1: Fizzy related

FZY-1: Fizzy

GFP: green fluorescent protein

GFP(KEN): GFP with extra-KEN box

GLD-1: Germline defective

GSC: germ stem cells

HR: homologous recombination

HTM: histone methyltransferase

HygR*:* hygromycin B resistance

kb: kilobase

LIN-35: abnormal cell lineage

MAPK: mitogen-activated protein kinase

mCherry: monomeric Cherry

MET-1: histone methyltransferase

MosSCI: Mos1-mediated single copy insertion

MES-4/2/3/6: maternal effect sterile

mRNA: messenger RNA

MuvB: Multivulva class B proteins

NHEJ: non-homologous end joining

NSD: nuclear receptor-binding SET domain

PAM: proto-spacer adjacent motif

P cells: precursors in the larva of neurons and VPCs

P lineage: precursor of the PGCs

PGC: precursor germ cell

pRb: Retinoblastoma protein

Q cells: neuroblasts

Rb: Retinoblastoma

RNA: ribonucleic acid

RNAi: RNA of interference

SCF: Skp1, Cullin, F-box protein

SEC: self-excising cassette

SL2: intergenic region between *glp-1 glp-2*

sgRNA: single guide RNA

SWI/SNF: switch/sucrose non-fermentable

TF: transcription factor

TZ: transition zone

V cells: seam cells

VNC: ventral nerve cord

VPC: vulval precursor cell

1. INTRODUCTION

1.1. Introduction to the Thesis

The correct development of multicellular organisms needs a high coordination between cell cycle and the successive differentiation steps. As the organism develops, cells progressively switch from an "immature" to a differentiated state. This loss of developmental plasticity coincides with an enlargement of cell cycle, most likely in G1 phase, and finally with cycle exit. It is generally though that an active cell cycle and differentiation factors antagonize each other (Busanello *et al*., 2012; Liu *et al*., 2017; Martins *et al*., 2017; Zhang *et al*., 1999). However, the establishment and maintenance of this transcriptional program in differentiating cells is mainly mediated though modifications in the chromatin landscapes (Doré *et al*., 2012; Hajkova *et al*., 2002; Meshorer *et al*., 2006; Ye *et al*., 2016).

Chromatin from the "immature" state is relaxed and allows plasticity and proliferation. This "open" chromatin landscape is an important feature of early embryos and germ cells. Germ cells would form the gametes and a new organism after fecundation. Therefore, they need to maintain this "immature" pluripotent mode. The rest of cells conform the soma, and they differentiate as the organism develops. Differentiated somatic cells have the opposite chromatin landscape, with chromatin "closed" at plasticity and cell cycle genes. Chromatin modifiers collaborate to set up and maintain these differentiated scenarios throughout the life of the organism (Petrella *et al*., 2011; Unhavaithaya *et al*., 2002). Uncontrolled alterations in chromatin lead to changes in plasticity and cell cycle, driving to developmental diseases and

cancer (Belinsky *et al*., 1998; Chai *et al*., 2005; Frigola *et al*., 2006; McClurg *et al*., 2018; Zhou *et al*., 2010).

In the same way that cell cycle favors plasticity and antagonizes differentiation, the initial hypothesis of this Thesis was that cell cycle should also favor an "open" chromatin landscape. This chromatin would change to a differentiated landscape coupled with cell cycle exit. The examples and significance of this interplay are scarce, and it merits a deeper understanding due to its importance in health and disease.

Discrepancy between germ and somatic landscapes regarding plasticity, chromatin and cell cycle enables the study of this crosstalk. This distinction is very well established in the nematode *Caenorhabditis elegans* due to the lack of stem cells in the adult except for the germline (Hirsh *et al*., 1976). Therefore, the aim of this Thesis was to gain insights in these connections using the nematode *Caenorhabditis elegans* as a model.

1.2. Caenorhabditis elegans as a model

This transparent free-living nematode has been widely used as a model system to study development since 1974 (Brenner, 1974). It has multiple advantages such as its suitability for genetic analyses, its small size or the invariant cell lineage.

This nematode reproduces primarily by self-fertilization of adult hermaphrodites, allowing the maintenance of a clonal population. Males

appear at low frequency in wild-type worms (<0.2%) and they can be used for genetic exchange. Hermaphrodites can produce around 300 self-fertilized eggs, but nearly 1,000 when mated with males (Hodgkin *et al.*, 1979).

C. elegans adult hermaphrodites are about 1 mm long and just 70 µm in diameter with a simple anatomy. As it is transparent, some of the internal organs, like the pharynx, intestine, and the reproductive system can be easily distinguished by sight (**Fig. 1**). It has also striated muscles, an epidermal, an excretory and a nervous system (anatomical details in Appendix I).

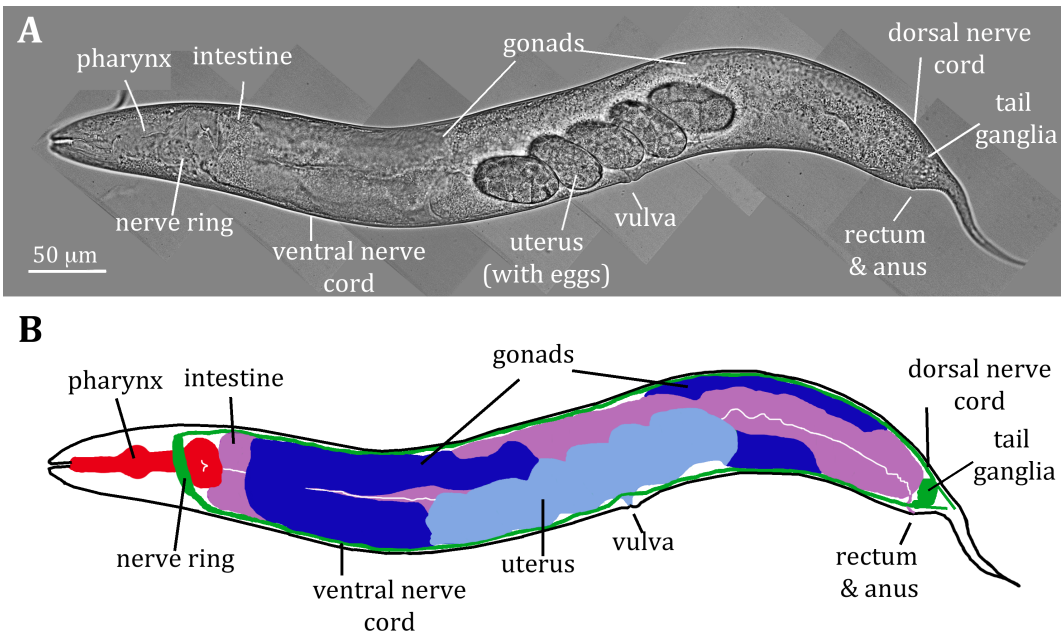

Figure 1. Scheme of adult worm anatomy

A. Image of an adult hermaphrodite wom with the different anatomical parts pointed out. **B.** Scheme of the picture shown in A. Gonads are represented in purple, each of them at one side of the intestine (pink). The uterus, with eggs at different developmental stages is seen in light blue. The eggs would be expelled throught the vulva. Ventral and dorsal nerve cords are represented in green, like the nerve ring around the pharynx (red).

Another advantage of this nematode is that it is easily cultured in the laboratory. The worm grows at temperatures ranging from 15 to 25°C over agar plates spotted with bacteria (its food). It has a short life cycle of approximately three days at 20°C, which diminishes as temperature rises (Byerly *et al*., 1976). The worm passes through an embryo phase, followed by four larval stages (L1-L4) and an adult stage (**Fig. 2**). The life cycle closes with egg self-fertilization (Byerly *et al*., 1976; Klass, 1977).

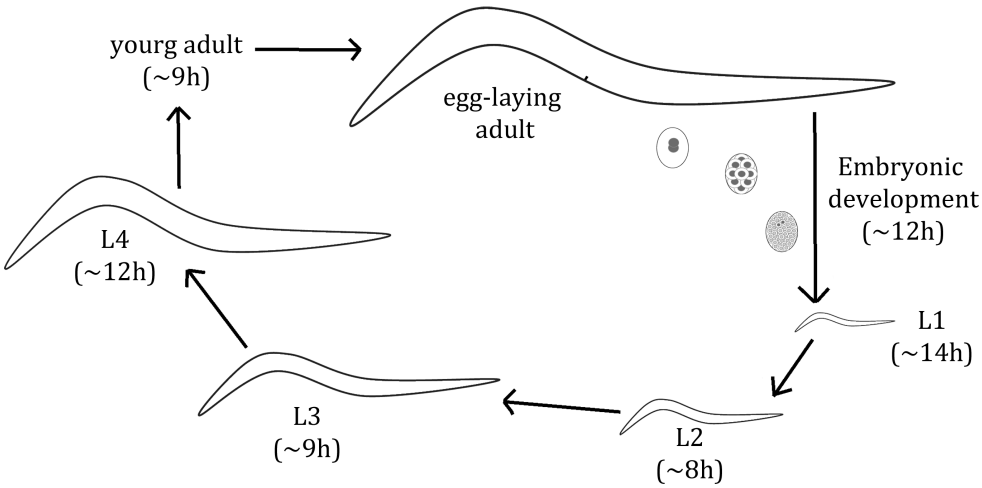

Figure 2. Life cycle of *C. elegans* at 20°C

Times were previously described (Byerly *et al*., 1976). The time from egg fertilization to the complete development of an egg-laying adult at 20°C is ~65 h. Eggs develope *in utero* before being layed.

1.2.1. Development: first distinction between germline and soma

Fertilization starts a series of controlled asymmetric cell divisions. Embryo development can be divided into two halves: a proliferative part in which the number of cells increases but they still retain some developmental

plasticity, and a phase of morphogenesis and differentiation. The first division allows separation of the germline (P lineage) from the soma. They would have highly different regulations and developments.

Development in soma is timely governed by two main mechanisms. The first one is the anterior-posterior axis fixation (assisted by maternal products and cell-cell interactions)(Kemphues *et al.*, 1988; Priess and Thomson, 1987). The second is the sequential activation of sets of genes that are specific for each lineage. Most them are transcription factors that allow tissue-specific differentiation (Mango *et al.*, 1994; Schnabel and Schnabel, 1990). From fertilization to the gastrulation, maternal-loaded products control cell fate and pattern specification. Gastrulation begins at the 26-cell stage. Throughout this phase, all the somatic cells continue dividing and forming the diverse lineage precursors. During gastrulation, cells start reorganizing in a tube-shape conformation, with the only germ cell and founder intestinal cells in the inside. Later on, in the middle of gastrulation, at the 100-cell stage, zygotic transcription starts, specifying tissue and organ identities. Coinciding with this, plasticity of the somatic blastomeres has been reported to drop (Fukushige and Krause, 2005; Quintin *et al.*, 2001).

Morphogenesis starts at the 550-cell stage, at the end of gastrulation (reviewed in (Labouesse and Mango, 1999)). Later on, the worm elongates (**Fig. 3**, next page) and starts moving inside the eggshell. The pharynx starts pumping before hatching (Sulston *et al.*, 1983).

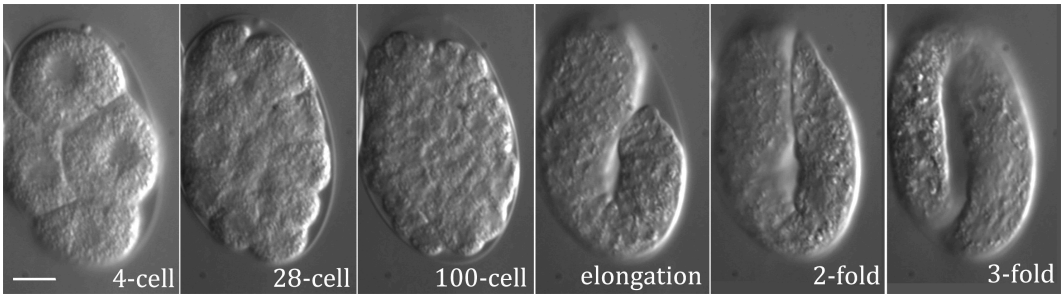

Figure 3. Embryo development

As embryo developes from the fertilized egg, cells divide, differentiate and reorganize in order to form a new organism. Images from Dr. Juan Cabello. Scale bar: 10 μm.

After embryonic development, larvae hatches. However, not all the somatic cells are terminally differentiated. Some of them complete differentiation at adulthood: hypodermal stem cells (seam cells) or the Q cells (neuroblasts). Other somatic cells are differentiated but immature, and proliferate during larval stages, such as intestine or muscle (Hedgecock and White, 1985; Sulston and Horvitz, 1977). Therefore, the newly hatched larva, while similar in overall organization to the mature adult contains 556 somatic nuclei (plus 2 germ cells), while the adult hermaphrodite contains 959 somatic nuclei and around 1000 germ cells per gonad arm (Hirsh *et al*., 1976; Sulston and Horvitz, 1977). This increase in cells (nuclei) is largely derived from precursor blast cells distributed along the body axis. They are the source for post-embryonic cell lineage development (Sulston and Horvitz, 1977).

The germline suffers a distinct developmental process. After the first division, the P lineage separates from the soma. It divides asymmetrically four times like a stem cells, giving rise each time to a new somatic precursor. The last division takes place at the 100-cells stage, giving rise to two precursor germ cells (PGCs). They would remain quiescent until the larva hatches (Sulston *et al*., 1983). PGCs inherit specific maternal factors in the germ plasma that allow the maintenance of their pluripotent state. This is similar to the formation of the PGCs in *Drosophila melanogaster* or *Xenopus laevis*, in contrast to PGC induction in mammals (reviewed in (Strome and Updike, 2015)).

Germline fate needs to be specified and safeguard early in development. This is accomplished by three ways: first, by a physical separation in the embryo from the first cell division. In addition, until the 100-cell stage, repression of RNA polymerase II impairs the expression of somatic genes in PGCs (Batchelder *et al*., 1999; Mello *et al*., 1992). Later on, PIE-1 repression alleviates, although transcription stills impaired. This is due to the third mechanism: chromatin modifications (Schaner *et al*., 2003; Wang *et al*., 2011). These modifications maintain the correct expression patterns along the worm's life, ensuring that only germ but not somatic genes are expressed in germline (Fong *et al*., 2002; Korf *et al*., 1998). This aspect is particularly relevant, since stemness allows germ cells to differentiate into diverse cell types inside the gonad if they are not protected (Patel *et al*., 2012; Tursun *et al*., 2011).

Once the larva hatches, the quiescent germline starts proliferation from the two PGCs at the L1 stage. It elongates and the tip migrates to conform the final U-shape. At L4 stage, meiosis starts producing sperm and, later, oocytes at the adult stage (Hirsh *et al*., 1976; Ward *et al*., 1983).

1.2.2. The adult germline: proliferation-differentiation interplay

Similar to soma, the germ cells also differentiate. They undergo meiosis, although this is not a terminal differentiation. Curiously, the proliferation-differentiation decisions, which occur in adulthood, are spatially separated, not temporally as in soma. This separation has facilitated the study of the coordination of both processes.

The hermaphrodite has two U-shaped gonads. They connect to the uterus through the spermatheca, where the sperm is stored. Fertilized eggs develop in the uterus before being expelled. Somatic gonad covers these parts, and all together comprises the worm's reproductive system (Kimble and Hirsh, 1979; Kimble and White, 1981). The two U-shaped gonad arms contain the only stem cells in the adult: the germ cells, also referred as germline. Germ cells in the gonad are distributed as a syncytium. The membrane that encloses cells opens to the central cytoplasm core (rachis). Despite this cytoplasm sharing, cell-cell signaling is restricted. This allows this spatial distribution of distinguishable zones in the adult gonad. Cells start being individualized at the proximal part of each arm (Hirsh *et al*., 1976).

There are two special cells of the somatic gonad called distal tip cells (DTCs). They are located at the distal part of each the gonad. Each DTC establishes a niche for the germ stem cells (GSC) (Crittenden *et al*., 2006; Kimble and White, 1981). This allows the existence of a highly mitotic zone or proliferative zone of around 230 cells (Crittenden *et al*., 2006). As cells divide and progress through the gonad, signals from the DTC are lower. At the most proximal part of the mitotic zone, germ cells start differentiation, entering meiotic S phase. These cells are indistinguishable from mitotic S phase cells. Later on, these nuclei enter leptotene-zygotene of the meiotic prophase at the transition zone (TZ), acquiring a half-moon shape (**Fig. 4**, next page).

At leptotene-zygotene, meiotic chromosome axes are assembled and homologous chromosomes paired. Prophase I continues through the pachytene, where recombination takes place (Dernburg *et al*., 1998). After pachytene, diplotene starts at the gonad loop, followed by diakinesis (**Fig. 4** A, next page). Six bivalent chromosomes (five autosomes and one X) are observed in diakinetic oocytes (**Fig. 4** A, next page). Blocked oocytes maturate before entering the spermatheca, and they resume meiosis after fertilization (McCarter *et al*., 1999). Important mRNAs for the embryo are maternally loaded in oocytes for being used during development.

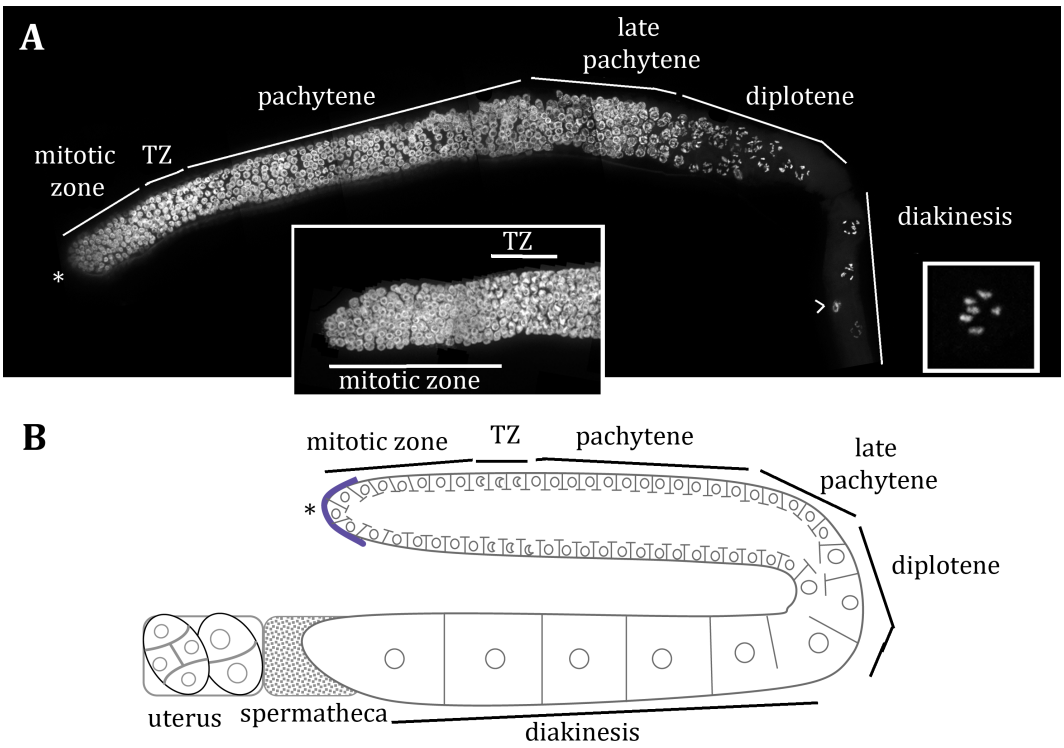

Figure 4. Germline organization

A. DAPI staining of a extruded hermaphrodite wild type gonad. Mitotic zone is observed near to the DTC (*). Zones are marked on the germline. Chromosomes are condensed and at diakinesis, bivalent chromosomes of the worm are observed. Arrowhead: nucleus of somatic gonad cell. **B.** Scheme of the gonad syncytium.

Most of the events leading to this differentiation imply post-transcriptional processing regulated through DTC signaling. RNA regulation is essential for germline sustainability. Indeed, 3' UTR regulation drives most of the expression patterns in this tissue. In the proliferation zone, mRNAs for meiotic products are inhibited, while mitotic mRNAs are completely eliminated in the pachytene (Merritt *et al*., 2008). In addition, proteasome

also regulates some proteins important for this transition and maintenance of the mitotic zone (Burger *et al*., 2013; Gupta *et al*., 2015; MacDonald *et al*., 2008). Alterations in these factors usually lead to changes in proliferation-differentiation decisions, changing the ratio of proliferative/differentiated cells (Morgan *et al*., 2013).

1.3. Chromatin regulators coordinate differentiation processes

Most of the changes occurring during differentiation processes are controlled by distinct transcriptional programs, which are specific for each cell type. Gene transcription requires binding of transcription factors (TFs) to regulatory DNA sequences in promoter and enhancer elements. Whether these TFs can bind and activate transcription would depend on the chromatin structure. In other words, the transcriptional changes involved in differentiation are not achieved by TFs alone, but rather in coordination with a large variety of chromatin factors. Furthermore, chromatin structure is responsible for the maintenance of the distinct cell types during development and along the worm's life.

Eukaryotic DNA is wrapped around histone octamers in nucleosome, conforming the chromatin. Two tetramers of both histone dimers H2A-H2B and H3-H4 combine to form the octamer (Thomas and Kornberg, 1975). Residues in the N-terminal tail of histones can be modified. These modifications consist on methylation, acetylation, ubiquitylation,

sumoylation, phosphorylation or ribosylation. Combinations of these marks conform a histone code (reviewed in (Munshi *et al*., 2009)). Several factors are able to read and interpret the histone code, modifying chromatin structure. There are two main groups of enzymes: the ones that add or remove marks to histone tails, and the ones that can alter the nucleosome positions for allowing or impeding the entrance of diverse factors. Activating modifications allow a relaxed transcriptionally active chromatin ("open" chromatin). Instead, repressing marks are found on silent zones, and are associated with compacted chromatin. Active and repressed loci are different between tissues, and they change throughout development. These dynamic modifications are critical for the correct cell fate determination and development of multicellular organisms (González-Aguilera *et al*., 2013; Ye *et al*., 2016).

In the worm, the most important repressive marks are di-/tri-methylations at lysine 9 of H3 (H3K9me2-3) and H3K27me3. All of them are placed at the promoter of regulated genes. Regarding active marks, they consist mainly in histone acetylation near the beginning of the genes, H3K4me2-3 at promoters, and H3K36me2-me3 at the body of highly transcribed genes (Liu *et al*., 2011). These activating and repressing marks are found in somatic and germ cells. However, the loci marked at each one are different, so the outcome at each chromatin landscape is characteristic. As the worm develops, differences between germline and soma become patent. In the adult, the chromatin landscape allows expression of plasticity

genes and represses somatic genes in the germline, while doing the opposite in soma. In addition, this chromatin and plasticity factors maintain an active cell cycle in the adult germline, contrary to non-dividing somatic cells.

1.3.1. Germline chromatin landscape: stemness maintenance

A correct expression pattern must be maintained in order to repress somatic fate in the germline and preserve plasticity. Chromatin regulation therefore plays a central role in keeping the ability of germ cells to produce all cell fates. In several organisms, the interplay of the repressive PcG (Polycomb group) and the activator trxG (Trithorax group) chromatin modifier complexes is responsible of cell fate maintenance (Coulson *et al*., 1998; Papp and Müller, 2006; Shen *et al*., 2009). In *C. elegans* the Polycomb Repressive Complex 2 (PRC2) and MES-4 proteins play similar regulatory roles (Gaydos *et al*., 2012).

MES-4 (maternal effect sterile 4) is one of the most important histone methyltransferases (HMTs) that make germline and soma chromatin landscapes distinguishable. Its regulation differs between soma and germline, playing a major role in establishing chromatin divergences between both. It is essential for germ cell fate maintenance and germline development, although its role in soma has not been established (Capowski *et al*., 1991; Rechtsteiner *et al*., 2010).

MES-4 is a large multidomain protein of the SET2 family that contains a conserved catalytic SET domain (Su(var)3-9, Enhacer-of-zeste, Trithorax).

It is a specific H3K36 HMT. However, opposite to its yeast counterpart Set2, its activity is independent on RNA polymerase II (Furuhashi *et al*., 2010). Its human orthologous are NSD1, NSD2 and NSD3, from the NSD (nuclear receptor-binding SET domain) family. They have important functions in development and disease (reviewed in (Morishita and di Luccio, 2011)).

In *C. elegans*, MES-4 preserves the germline transcriptional memory by maintaining H3K36me2-3 on germline genes (Bender *et al*., 2006; Fong *et al*., 2002). It has also a role in X-chromosome dosage compensation and silencing (Strome *et al*., 2014). It is synthetized in the germline, and is provided to the embryo maternally. Mutants develop to adults with this maternal protein supply. However, they are not fertile although they have no obvious defects in soma (Capowski *et al*., 1991).

Consistent with its roles in fertility, MES-4 is present mainly in the germline (**Fig. 5** A), while not detected in somatic cells of the adult worm. It is found in the mitotic zone. Protein levels start to drop at the transition zone, reappearing at late pachytene (**Fig 5,** A, B).

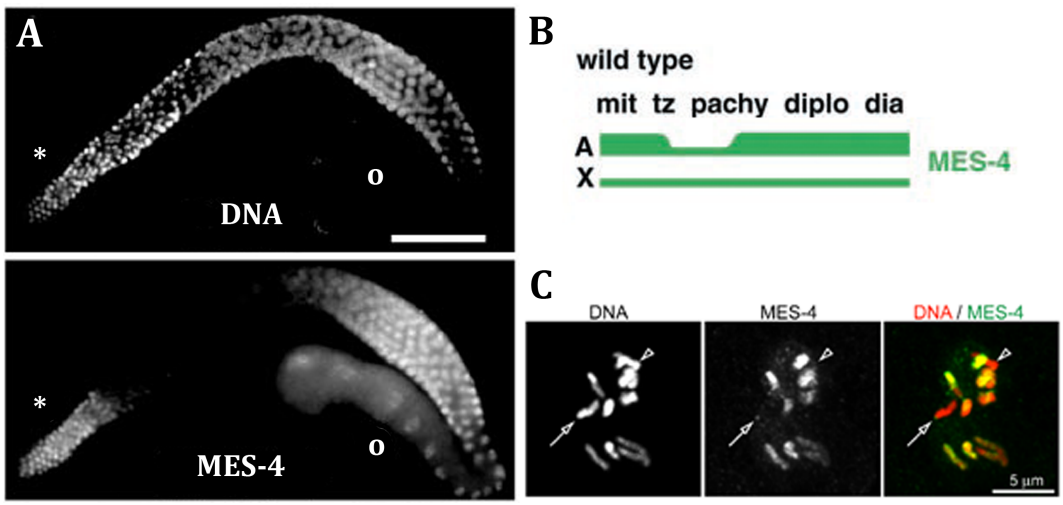

MES-4 is broadly associated to the autosomes (5+5 in the diploid nucleus) and the tip of the X chromosomes (**Fig.5** B, previous page) (Rechtsteiner *et al*., 2010). Additionally, during embryo development, the protein is present in all the cells until approximately the 100-cell stage. Then its level drops in somatic cells, while remains high in PGCs (Fong *et al*., 2002).

In the germline, MES-4 is bound to highly transcribed genes. These marked loci are maintained in the embryo in both, PGCs and somatic cells while MES-4 is present (Rechtsteiner *et al*., 2010). PGCs would maintain MES-4 and, therefore, these marked loci would contain H3K36me. Although PGCs are not transcriptionally active (Wang *et al*., 2011), the presence of MES-4 would allow a rapid activation of zygotic transcription after hatching. However, in the somatic cells of the embryo, some of these MES-4 marked genes are transcribed, but not all of them (Rechtsteiner *et al*., 2010). It has not been reported if these marks continue existing in later stages, or if they dilute with divisions due to the decay in MES-4. On the contrary, in germline, these marks persist through generations. Therefore, MES-4 is in charge of maintaining transcriptional memory in the germline. It maintains an open chromatin landscape that promotes the transcription of stemness factors.

Figure 5. MES-4 pattern in germline and DNA association (on the left)

A and B are adapted from (Fong *et al*., 2002). **A.** Germline stained with DAPI and anti-MES-4. Scale bar: 50 μm, *: mitotic zone, o: oocytes. **B.** Scheme of the pattern observed in A. The protein drops at pachytene. It is concentrated in autosomes (A) while not in X. **C**. From (Rechtsteiner *et al*., 2010). 12 chromosomes from a fertilized egg. MES-4 is present in the 10 autosomes, while only a at the tip of both X chromosomes (arrow and arrowhead). Scale bar: 5 μm.

Most of the genes controlled by MES-4 are proteins needed for germ fate protection against reprogramming. Most of them are part of the protective P granules (orthologous to polar granules for mammals and insects). These perinuclear ribonucleoprotein granules are able to bind and process mRNAs and small RNAs and are implicated in splicing, translation initiation, decapping, degradation and RNAi amongst others. Some of these conserved proteins are NANOS, VASA-related RNA helicases, Argonaute-related and Tudor domain-related proteins (reviewed in (Updike and Strome, 2010)).

The maintenance of transcriptional memory on these genes is linked with the epigenetic memory maintenance. MES-4 acts in contraposition to the conserved Polycomb Repressive Complex 2 (PRC2). This complex is composed by MES-2/EZH2 (enhancer of zeste homolog 2), MES-3 and MES-6 and it is the responsible for H3K27me3 repression in germline, like in other organisms (Korf *et al*., 1998). H3K36 methlylation impairs PRC2-mediated H3K27 methylation, so PRC2 is excluded from MES-4 marked zones (Gaydos *et al*., 2012; Yuan *et al*., 2011). This exclusion leads to the existence of alternating domains of these activating and silencing marks extended through the autosomes. However, a higher concentration of repressive marks is found on the X chromosome (Gaydos *et al*., 2012; Strome *et al*., 2014).

The mutual exclusion of PRC2 and MES-4 causes the spread of repressive marks in *mes-4* mutants. In these mutants, PRC2 has no H3K36-restriction; therefore, H3K27 methylation diminishes in the X-chromosome

and increases elsewhere, deregulating gene expression (**Fig. 6**, next page). In the absence of MES-4, germline active genes are down regulated while X-linked genes are up regulated (Gaydos *et al.*, 2012; Strome *et al.*, 2014). On the other hand, PRC2 mutants allow up-regulation of X-linked genes in a similar aberrant way. Both mutants lead to the misexpression of somatic genes in the germline (Gaydos *et al.*, 2012; Rechtsteiner *et al.*, 2010).

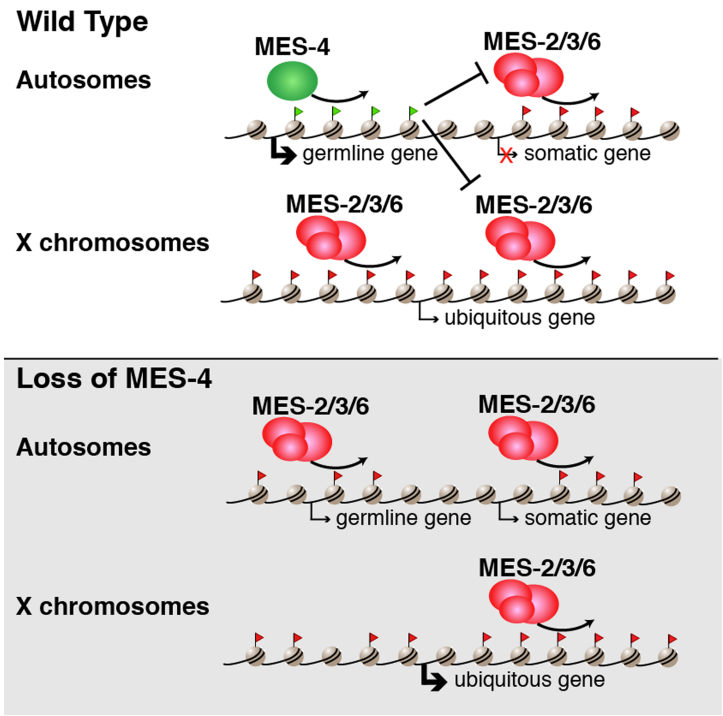

Figure 6. MES-4 *versus* Polycomb (Gaydos *et al.*, 2012)

H3K36 methylation by MES-4 impairs PRC2 from binding active zones in autosomes. This creates separated zones in the autosomes of repressive and active marks. PRC2 represses somatic genes in autosomes, and extends repressive marks on X chromosome. In *mes-4* mutants, PRC2 and its repressive mark are abnormally extended, causing a general misregulation of gene expression.

Alterations in chromatin leading to deregulation of gene expression have been implied in several cancers and developmental disorders. In consonance, deregulation of human NSD genes is associated with malignancies and developmental syndromes (Rayasam *et al*., 2003; Zhou *et al*., 2010). In the worm, PRC2 also has developmental roles in soma by repressing Hox genes; consequently mutants present somatic defects (Ross and Zarkower, 2003). Surprisingly, although MES-4 is present in somatic cells of the early embryo and also marks germline genes in somatic cells, the reported mutant phenotypes have been mainly related to germline (Bender *et al*., 2006; Fong *et al*., 2002; Garvin *et al*., 1998). However, recently, somatic problems have been referred for L1 mutant worms (quoted in (Ahringer and Gasser, 2018)). This more obvious function in the germline is linked with its differential regulation between soma and germline, marking two different chromatin landscapes.

1.3.2. Soma chromatin landscape: MES-4 regulation and the DRM complex

In soma, germline fate and MES-4 need to be repressed. Indeed, several mutants in chromatin-associated factors misexpress germline genes in soma dependent on MES-4. Some of them are Mi-2/NuRD complexes (nucleosome remodeling deacetylase) and the transcriptional repressor complex DRM (DP, Retinoblastoma-like, MuvB)/DREAM (DP, Retinoblastoma-like, E2F4, MuvB) (Erdelyi *et al*., 2017; Petrella *et al*., 2011; Wu *et al*., 2012). However, of those, only the DRM/DREAM complex has been

reported to directly regulate *mes-4* transcription (Goetsch *et al*., 2017; Kudron *et al*., 2013).

The DRM/DREAM is a transcriptional repressor complex that acts as a tumor suppressor regulating proliferation and differentiation. It regulates the transcription of key genes in cell cycle progression and cell fate specification (Ceol and Horvitz, 2001; Petrella *et al*., 2011; Sadasivam and DeCaprio, 2013). Alterations of this complex are linked to cancer and developmental problems in diverse organisms (Ferres-Marco *et al*., 2006; Fischer *et al*., 2017).

The mammalian DREAM contains a repressive heterodiemer E2F4/5-DP1/2, a protein from Retinoblastoma (Rb) family (pRb/p130/p107) and the multimeric subcomplex MuvB (multivulva class B proteins). It is formed by LIN9, LIN37, LIN52, LIN54 and RBAP48. MuvB complex has a dual role, acting as a repressor in the DREAM complex, but promoting cell cycle when interacts with Myb. In *C. elegans* their counterparts are EFL-1, DPL-1, LIN-35 and the MuvB proteins LIN-9, LIN-37, LIN-54 and LIN-53 respectively (**Fig. 7**) (Ceol and Horvitz, 2001; Lu and Horvitz, 1998). In contrast to mammals, *C. elegans* MuvB subcomplex acts mainly as a repressor, and there is no obvious Myb orthologous (Goetsch *et al*., 2017; Petrella *et al*., 2011). LIN-35 stabilizes the assembly of the complex (**Fig. 7**, next page).

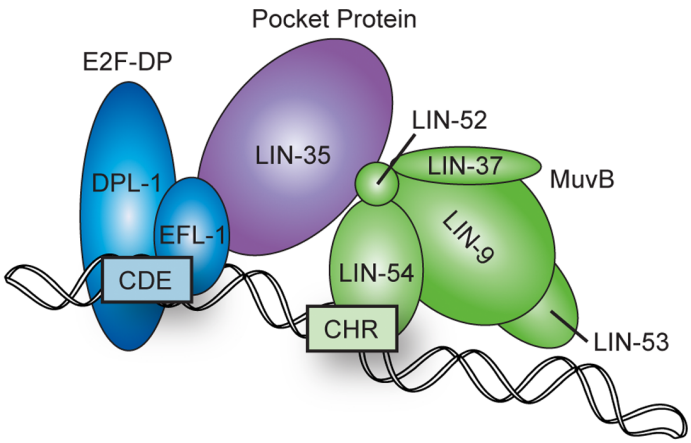

Figure 7. DRM complex assembly in C. elegans late embryo

From (Goetsch *et al.*, 2017). The DRM complex binds to its targets thorugh LIN-54 and EFL-1/DPL-1. They bind to two regulatory regions: a cell cycle genes homology region (CHR) and a cell cycle dependent element (CDE) respectively. The formation of the complex is stabilized by LIN-35.

The DRM complex controls genes linked with cell cycle, reproduction, larval and embryo development. Cell cycle genes are regulated from the beginning of development, while developmental genes are targeted at later stages (Goetsch *et al.*, 2017; Latorre *et al.*, 2015). In addition, DRM subunits have differential functions between germline and soma. Concretely, LIN-54 is enriched in *mes-4, mes-2* and *mes-6* promoters, although it does not regulate their expression in germline and early embryos (Tabuchi *et al.*, 2011). Indeed, no transcriptional regulation has been reported for *mes-4* in germline.

This is coherent with the diminished binding of LIN-35 in germline respect to soma (Kudron *et al*., 2013). Although the Muv subcomplex has a repressor activity and it can inhibit transcription on its own, LIN-35 stabilizes the DRM complex (Goetsch *et al*., 2017). Actually, LIN-35 binds to the promoter and down-regulates *mes-4* in somatic cells, while it is not bound to *mes-4* promoter in germ cells (Kudron *et al*., 2013). This soma-dependent regulation is consistent with the misregulation of germline genes in the soma of *lin-35* and DRM mutants in a MES-4-dependent manner (Wang *et al*., 2005a; Wu *et al*., 2012). Reasonably, as cells start differentiation, they need to repress plasticity marks such as MES-4-dependent H3K36 methylation that maintains the "immature" fate. Therefore, *mes-4* and its regulated genes would need to be silenced through development.

LIN-35/pRb has been widely studied due to its importance in cancer (reviewed in (Nevins, 2001)). It is important for fate choice in specific tissues and for maintaining the repression of cell cycle genes. LIN-35/pRb plays an important role in cell cycle exit and in transcriptional control through the repression of E2F transcriptional activation as part of the DRM/DREAM complex (reviewed in (van den Heuvel and Dyson, 2008)). Due to its role as a negative regulator in cell division, its activity is modulated through the cycle in order to allow proliferation or to repress it for enabling differentiation in mammals through chromatin alteration (Blais *et al*., 2007).

1.4. Cell cycle regulation in developmental processes

In metazoans, cell division and cell differentiation are intimately intertwined (reviewed in (Budirahardja and Gönczy, 2009)). These processes substantially overlap during the development of multicellular organisms. Developmental signals control cell cycle, determining cellular differentiation. Conversely, cell cycle regulation might control whether a cell is able to perceive the developmental signals for differentiation. In addition, terminal differentiation at the end of a particular developmental program is often characterized by a permanent cell cycle arrest. Therefore pathways controlling exit or entry into the cell cycle have dramatic consequences on the ability to differentiate.

Cell cycle is described as a series of highly controlled events that lead to cell division. In the canonical cycle, cells duplicate their genetic material in the synthesis phase (S) and divide physically during mitosis (M). S and M phases are separated by two gap phases: G1 and G2. These processes are highly controlled in order to allow progression into cell cycle in one direction. Cyclin dependent kinases (CDKs) with their respective cyclins drive the cell cycle by substrate phosphorylation (Nurse *et al*., 1976). They allow the expression of key genes for the next phase. CDK activity increases through cell cycle. CDK activity threshold and cyclin-substrate specificity ensure the on-direction flow of the events (Swaffer *et al*., 2016).

G1 phase is particularly important in the cell cycle because it determines whether a cell commits to division or to cell cycle exit. If a cell is marked to remain undivided, instead of moving onto the S phase, it will leave the G1 phase and move into a state of dormancy called the G0. Furthermore, it is widely accepted that major part of cells initiate fate decisions in G1 phase. This choice is made at every round of cell division by a mechanism known as restriction point (R-point) control (Pardee, 1974; Schwarz *et al*., 2018). The R-point serves as a molecular switch that controls cellular decisions between division and entry into the quiescent state (G0) or differentiation. This pathway involves the integration of extracellular mitogenic signals with the cell cycle machinery, converging on CDK activity. When this CDK activity reaches a threshold, cells are irreversibly committed to divide (Schwarz *et al*., 2018).

Why should cells preferentially make cell fate decisions in G1 phase and not in other cell cycle phases? The current idea is that transcriptional programs linked to cell identity can be rapidly reset following exit from M phase. The transition from M phase to G1 is associated with dramatic changes in nuclear architecture (Walter *et al*., 2003), including reformation of the nuclear envelope, chromosome decondensation and extensive chromosome repositioning in 3D space (Reddy *et al*., 2008). In addition, at G1 phase, chromatin marks are permissive for transcriptional changes. Developmental genes marked with negative H3K27me3 also acquire the positive H3K4me3 (Singh *et al*., 2015). This would allow that the presence of pro-differentiation

signals at G1 selectively activate transcription of these developmental genes. Consequently, an increase of G1 length would enable transcriptional changes driving to differentiation.

1.4.1. G1 length control in mammals and worms

The G1 length basically depends on how fast the CDK complex that triggers the G1/S transition reaches an activity threshold. In animals this complex is composed mainly of CDK2-cyclin E (Lukas *et al*., 1997). There are two key ways for controlling this complex at this transition: cyclin transcription and cyclin-CDK complex inhibition.

Cyclin E transcription depends on E2F/DP transcription factor (TF). E2F/DP also elicits transcription of other important genes for the G1/S and S phases in diverse organisms (DeGregori *et al*., 1995; Duronio and O'Farrell, 1995; Grishok and Sharp, 2005; Johnson *et al*., 1993; Ohtani *et al*., 1995). Retinoblastoma (Rb) family members negatively regulate E2F/DP. In *C. elegans* somatic cells, the solely member of the Rb family LIN-35/pRb (Lu and Horvitz, 1998) inhibits EFL-1/DPL-1-target genes acting in the DRM complex (Ceol and Horvitz, 2001; Goetsch *et al*., 2017). Consequently, the transcription of the E2F-regulated genes is off. This inhibition is bypassed through phosphorylation of LIN-35/pRb. CDK4/6-Cyclin D and their worm counterpart CDK-4/CYD-1 phosphorylate LIN-35/pRb (Kato *et al*., 1993; The *et al*., 2015), alleviating *cye-1* repression. Additional inhibition of pRb is achieved by CDK2-cyclin E and CDK2-cyclin A phosphorylation in mammals

(Hinds *et al*., 1992; Horton *et al*., 1995). Although in the worm there are no evidences, further phosphorylation of LIN-35/pRb by CDK-2/CYE-1, it has been proposed as a mechanism for total inactivation of LIN-35/pRb (The *et al*., 2015).

The second way of inhibiting CDK2-cyclinE activity consists on the binding of cyclin-dependent kinase inhibitors (CKIs) from the Cip/Kip family: p21/p27/p57 in mammals and CKI-1/CKI-2 in worms (Buck *et al*., 2009; Fujita *et al*., 2007; Harper *et al*., 1993; Polyak *et al*., 1994; Reynaud *et al*., 1999). In the worm, CKI-1 is the one that has the major role in proliferation in soma (Fukuyama *et al*., 2003; Hong *et al*., 1998). Although most of cell cycle elements are highly conserved between mammals and worms, CKI control differs. Mammalian CKIs can be phosphorylated by CDK-cyclin complexes (either CDK4/6-Cyclin D or CDK2-Cyclin E) and submitted to degradation (Hao *et al*., 2005; Sutterluty *et al*., 1999; Wang *et al*., 2005b). This degradation occurs mainly through the E3 ubiquitin ligase SCF (Skp1, cullin, F-box protein). SCF acting with the F-box proteins Skp2 and Csk1 is the main responsible for CKIs degradation in G1. In the worm, CKIs have been proposed as targets of CDK-4/CYD-1 (Boxem and van den Heuvel, 2001), although the link of CKD-4/CYD-1 with CKIs degradation has not been proved. Degradation of CKI-1 is also dependent of a cullin-containing E3 ubiquitin ligase. However, it is different from the SCF. There are five members of the cullin family in *C. elegans* (Kipreos *et al*., 1996). Of them, *cul-2* is key for CKI-1 degradation, being part of the E3 ubiquitin ligase $CRL2^{LRR-1}$

(Feng *et al*., 1999; Starostina *et al*., 2010). Despite this different regulation, in both, mammals and worms, CKIs are needed in in order to keep CDK2-cyclin E inactive during G1 phase until it reaches the adequate level. Therefore, during G1, CKIs are needed.

Another important complex controlling CDK2-cyclin E activity is the Anaphase Promoting Complex/Cyclosome (APC/C). APC/C is the E3 ubiquitin ligase in charge of degrading multiple substrates during cell cycle. This E3 ubiquitin ligase has two co-activators that dictate its substrate specificity at different cell cycle phases: Cdc20 and Cdh1. Cdc20 (FZY-1 in the worm) acts in early mitosis, and coordinates events leading to mitosis exit. Cdh1 (FZR-1 in the worm) activates APC/C at the end of mitosis and in G1 (reviewed in (Zhang *et al*., 2014)). In mammals, APC/C^{Cdh1} controls levels of activated CDK2-cyclin E during G1 impairing CKI degradation through ubiquitination of Skp2-Csk1 (Bashir *et al*., 2004). In the worm, FZR-1/Cdh1 has been proposed as a negative regulator of cyclins E and A, as overexpression of both cyclins induce similar phenotypes to the *fzr-1* mutant, and these phenotypes are increased in a *fzr-1* mutant background (Fay *et al*., 2002). However, it seems that this regulation is not through CKIs, as APC/C^{FZR-1} does not impede CKIs degradation. On the contrary, *fzr-1* RNAi increased CKI-1 levels in soma, suggesting a non-conserved regulation of CKI-1 through APC/C (The *et al*., 2015).

The ability of FZR-1/Cdh1 to interact with the APC/C complex is regulated through phosphorylation. CDK4/6-cyclin D phosphorylation of

Cdh1/FZR-1 impedes its interaction with APC/C complex in mammals and worms (The *et al.*, 2015; Wan *et al.*, 2017). In addition, Cdh1 is further phosphorylated by CDK2-cyclin E in mammals (Keck *et al.*, 2007) and this regulation has also been proposed in worms (The *et al.*, 2015).

In summary, the control of CDK-2/CYE-1 at multiple levels ensures low activity of this complex through G1. The little amount of the CDK-cyclin complex formed after LIN-35/pRb inactivation is inhibited by CKIs until it reaches a threshold activity. At this point, CDK-2/CYE-1 activity would bypass inhibitors, and it would be able to phosphorylate its targets. Therefore, the activity of inhibitors would drop as cyclin E levels rise to promote G1/S transition and proliferation (**Fig. 8**).

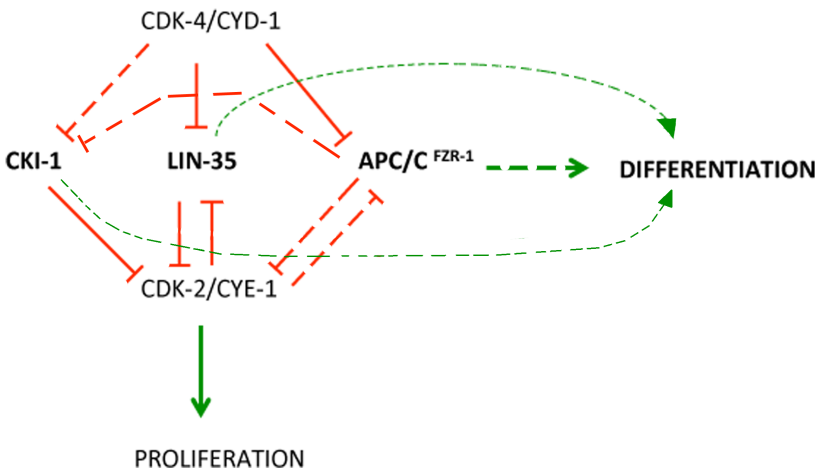

Figure 8. Shcematic representation of G1/S transition regulatory network in *C. elegans*

Representation of the main regulatory pathways of the G1/S transition. In bold: main inhibitors present at high levels during G1 before the R-point. These inhibitors promote differentiation in several organisms. Red dashed lines: repressions that take place in other organisms and have been suggested for *C. elegans*. Mechanisms of FZR-1-dependent control of CKI-1 levels is currently unknown.

As development proceeds, the cell cycle complexity increases and the G1 becomes now a prime target for regulation by developmental cues. This regulation is often directed through the repression of both CDK complexes and the activation of the mentioned cell cycle inhibitors. In fact, these G1 inhibitors have been reported to influence differentiation in several organisms (Burger *et al*., 2013; Calo *et al*., 2010; Fujita *et al*., 2007; Kostic *et al*., 2003; Wan *et al*., 2011).

1.4.2. Integration of cell cycle and differentiation signals through G1 regulators in the germline

In rapidly dividing cells of early mouse embryos, G1 is very short compared to cell cycle (Calder *et al*., 2012). *Drosophila* embryos lack gap phases during first divisions, adding them later (Edgar and O'Farrell, 1990). Similarly, *C. elegans* germ cells at the mitotic zone of the gonad have a rapid cell cycle with a long S and G2, a short M phase and an almost absent G1 (Fox *et al*., 2011). For all these rapid cyling cells, cyclin E is key for stemness regulation. Therefore, stem and germ cells of diverse organisms maintain high levels of CDK-cyclin E activity, favoring plasticity (Berger *et al*., 2010; Fox *et al*., 2011; Stead *et al*., 2002). Moreover, in *C. elegans*, CYE-1 coordinates differentiation and cell cycle in both, germ and somatic cells (Fox *et al*., 2011; Fujita *et al*., 2007). In order to allow differentiation, these cells would need to down regulate CYE-1.

In *C. elegans* germline, CYE-1 is present at high levels at the mitotic zone, and decreases at the onset of meiotic differentiation, being almost

undetectable at pachytene (Brodigan *et al*., 2003). This high CYE-1 levels are independent from the cell cycle phase, being CDK-4/CYD-1 less important at the mitotic zone (Fox *et al*., 2011). This is consistent with germ cells being continuously receiving proliferating signals, and with a strong impairment of inhibitors affecting this CDK-2/CYE-1.

This continuous signaling comes from the distal tip cell (DTC), which maintains the mitotic niche at the germline. The DTC initiates a Notch-signaling cascade that activates GLP-1/Notch receptor in the germ cells. This would favor mitosis and inhibit meiosis products mainly by mRNA regulation (Crittenden *et al*., 2002). One of the proteins inhibited at the tip is GLD-1. GLD-1 is a negative regulator of *cye-1* mRNA that restricts CYE-1 to the GLP-signaling zone (Biedermann *et al*., 2009). Conversely, CYE-1 also phosphorylates and inhibits GLD-1 at the tip (Jeong *et al*., 2011), limiting its action to CYE-1 depleted zones. This dual regulation takes place with multiple proteins in the germline and maintains the balance between proliferation and differentiation.

Regarding other CYE-1 inhibitors, *lin-35* mutants have known defects in fertility, with reduced fertility (Fay *et al*., 2002). However, no role in proliferation-differentiation decisions in the germline has been reported. Moreover, most of its downstream targets are being expressed in the germline (Kudron *et al*., 2013). On the other hand, CKIs are inhibited at the mitotic zone. CKI-2 is down-regulated through GLP-1-dependent pathway (Kalchhauser *et al*., 2011), while CKI-1 is degraded through $CRL2^{LRR\text{-}1}$

(Starostina *et al*., 2010). CKI activity therefore is inhibited by different means at the mitotic zone. Additionally, $SCF^{PROM-1/FBXO47}$ has been related to CYE-1 degradation in the germline, as mutants in this E3 ubiquitin ligase components show a lighter decay of CYE-1 at pachytene (Fox *et al*., 2011). About APC/C^{FZR-1}, the phenotypes for mutant alleles and *fzr-1* RNAi reported implied reduced fertility, similarly to *lin-35* mutants. However, these *fzr-1* mutants and RNAi seem to retain some FZR-1 activity, as direct injection of *fzr-1* RNAi in the gonads showed a stronger phenotype, with sterility of half of the injected worms (Fay *et al*., 2002). Additionally, these worms showed defects in the uterus, vulva and gonads, with missing or abnormal sperm and oocytes. This shows the importance of FZR-1 for fertility, although its targets remain undetermined. In contrast, in somatic cells, FZR-1 has been linked with cyclin E and A regulation, as an overexpression of either mimicked *fzr-1* mutant phenotype (Fay *et al*., 2002). How this repression is achieved and if it happens also in the germline is still unknown.

As cells progress through the mitotic region, GLP-1 influence decreases. Consequently, GLD-1 levels and CKI-2 levels start rising and inhibit CDK-2/CYE-1. CKI-1 levels also raise (Feng *et al*., 1999), helping to this inhibition. Further inhibition of *cye-1* mRNA (Biedermann *et al*., 2009), and the SCF-dependent control of CYE-1 (Fox *et al*., 2011) would lead to a drop in protein levels prior to the pachytene. At late pachytene CYE-1 levels raise again (Brodigan *et al*., 2003), coinciding with a drop of GLD-1 levels.

After fecundation, oocytes would resume meiosis and give rise to an entire organism, showing that these cells recover their high plasticity.

1.4.3. Integration of cell cycle and differentiation signals through G1 regulators in soma

Rapid embryonic cycles follow fertilization, with high CYE-1 levels in all the nuclei, except when they enter mitosis that CYE-1 is diffused through the cytoplasm (Brodigan *et al*., 2003). CYE-1 in the embryo disappears at the comma stage (Brodigan *et al*., 2003). At this stage all the cell divisions are completed and morphogenesis starts. This CYE-1 decay would be coherent with an increase of G1 inhibitors. In most organisms, as cells differentiate, cell cycle progressively enlarges, adding gap phases and opening to differentiation and quiescence options (Calder *et al*., 2012; Pauklin and Vallier, 2013). In mammals, the enlargement of G1 phase is linked with increased amounts of G1 inhibitors (Jacobs *et al*., 2002; Li and Kirschner, 2014). As development proceeds, G1 inhibitors gain importance not only due to their cell cycle function. Mutations in these cell cycle inhibitors usually lead to developmental problems not only linked with cell cycle, but with poor differentiation or impaired morphogenesis. Concretely, LIN-35/Rb mutants in the worm present a dedifferentiation of the intestine in L1 stage at high temperatures (Petrella *et al*., 2011). In addition, somatic cells misexpress germline genes (Wang *et al*., 2005a). However, under standard grown conditions, *lin-35* mutants are almost wild type except for some extra cells in specific tissues (Fay *et al*., 2002). In addition, *cki-1* mutants have defects in

morphogenesis (Fukuyama *et al*., 2003). Combination of *lin-35* mutation with mutations in *cki-1* and *fzr-1* reveals redundant control pathways (Boxem and van den Heuvel, 2001; Fay *et al*., 2002). Although FZR-1/Cdh1 in mammals is highly implied in differentiation (Bar-On *et al*., 2010; Cuende *et al*., 2008; Naoe *et al*., 2013), this role has not been explored in the worms.

1.4.4. Chromatin and cell cycle interplay during differentiation

G1 inhibitors roles in differentiation are related to cell cycle interaction with key TF for differentiation/stemness and chromatin-associated enzymes. Mammalian G1 cyclins are essential for maintaining pluripotency of embryonic stem cells by protecting the transcription factors Sox2, Oct4 and Nanog from degradation (Liu *et al*., 2017). In addition, pRb is implied in chromatin remodeling during cell cycle exit in both, an irreversible and a reversible way (Blais *et al*., 2007). The irreversible way would reassemble the post-mitotic cell cycle exit in differentiated muscle cells. These chromatin changes are due to pRb interaction with an unknown HMT. Additionally, pRb interacts with HDAC1 (Histone deacetylase 1) (Brehm *et al*., 1998). In the worm, the Switch/Sucrose nonfermentable (SWI/SNF) chromatin remodeling complex acts with LIN-35 /pRb to promote cell cycle exit in *C. elegans* (Cui *et al*., 2004; Ruijtenberg and van den Heuvel, 2015). Moreover, different SWI/SNF subunits show functions in mitotic progression and cell cycle delay in the worm (Krüger *et al*., 2015).

pRb is also implied in PRC2 control in human cells. EZH2 (MES-2 in the worm) is a direct target of E2F in humans cells, being repressed by Rb-E2F (Bracken *et al*., 2003). In addition, EZH2 is positively regulated through phosphorylation. CDK1 and CDK2 phosphorylate EZH2, promoting its binding to non-coding RNAs, thus enhancing its repressive activity. This allows plasticity maintenance (Chen *et al*., 2010; Kaneko *et al*., 2010). In addition, SCF (Skp1, Cullin, F-box) ubiquitin-ligase degrades the HMT PR-Set7 in *Drosophila* (SET-1 in the worm) (Zouaz *et al*., 2018). This cell cycle-dependent degradation controls a proper chromatin compaction. Cell cycle also controls changes of bivalent chromatin domains at G1, allowing changes in the expression pattern and therefore, the exit from pluripotency (Singh *et al*., 2015).

In the worm, the direct regulation of modifying enzymes through cell cycle has not been extensively studied. One exception is the known role of LIN-35/pRb in *mes-4* inhibition in soma. However, in the germline, besides LIN-54 binding to its promoter and PRC2 control of MES-4 location to autosomes, not too much is known about its regulation. Due to MES-4 implication in plasticity and a the well established germline model for plasticity-cell cycle studies, germline analysis of MES-4 would give clues to its regulation and if it is mediated through cell cycle. Moreover, the cell cycle-dependent regulation of its opposing partner PRC2 and the progressive degradation of MES-4 in soma through development make MES-4 an

interesting chromatin modifier to study regulation of plasticity in soma during development.

2. OBJECTIVES

We hypothesize that as cells differentiate the chromatin landscape changes. These changes are mediated through cell cycle in order to couple cell division with differentiation. This thesis centers in the study of the HMT MES-4 in the model organism *Caenorhabditis elegans* as a tool for understanding the link between cell cycle, plasticity and chromatin through development.

3. MATERIALS AND METHODS

3.1. C. elegans strains used and maintenance

Strains were grown at 20°C except indicated. Worms were cultured using standard methods (Brenner, 1974). They were grown in nematode growth media (NGM) plates seeded with *Escherichia coli* OP50.

Table 1. Worm strains

STRAIN	GENOTYPE	ORIGIN
N2	wild-type Bristol	CGC
EG6699	*ttTi5605 II; unc-119(ed3) III*	CGC
EG8081	*unc-119(ed3) III; oxTi177[ttTi5605 + NeoR(+) + unc-18(+)] IV*	CGC
EG8082	*unc-119(ed3) III; oxTi365 [ttTi5605 + NeoR(+) + unc-18(+)] V*	CGC
MT15488	*lin-35(n4760) I*	CGC
SS1420	*mes-4(bn185(mes-4[K10A, E11A, N12A]::GFP(KEN)::HA::6xHIS)) V*	Susan Strome
CONSTRUCTED		
STRAIN	GENOTYPE	ORIGIN
JPM45	*mes-4(sal3[mes-4::mCherry + FRT tbb-2utr HygR FRT]) V*	CRISPR in N2
JPM47	*lin-35(n4760) I; mes-4(sal3[mes-4::mCherry + FRT tbb-2utr HygR FRT]) V*	JPM45, MT15488
JPM75	*mes-4(sal8[mes-4::GFP^SEC^3xFlag::mes-4utr]) V*	CRISPR in N2
JPM76	*mes-4(sal9[mes-4::GFP::3xFlag::mes-4utr]) V*	SEC excised from JPM75
JPM94	*lin-35(n4760) I; mes-4(sal9[mes-4::GFP::3xFlag::mes-4utr]) V*	JPM76, MT15488

Table 1 cont. Worm strains

STRAIN	GENOTYPE	ORIGIN
JPM77	*mes-4(sal10[mes-4(K10A, E11A, N12A)::GFP^SEC^3xFlag ::mes-4utr]) V*	CRISPR in SS1420
JPM78	*mes-4(sal11[mes-4(K10A, E11A, N12A)::GFP::3xFlag::mes-4utr]) V*	SEC excised from JPM77
JPM95	*lin-35(n4760) I; mes-4(sal11[mes-4(bn185)::GFP::3xFlag ::mes-4utr]) V*	JPM78, MT15488
JPM99	*salIs4[QUAS::GFP:unc-54utr + unc-119(+)] II; salIs3[Prps-27:: QS::SL2::QF::unc-54utr + unc-119(+)] IV*	JPM5, JPM98
JPM68	*salIs3[Prps-27::QS::SL2::QF::unc-54utr + unc-119(+)]IV; salIs16[QUAS::mes-4::mCherry::tbb-2 utr + FRT HygR FRT + unc-119(+)] V*	JPM5, JPM79
JPM71	*salIs3[Prps-27::QS::SL2::QF::unc-54utr + unc-119(+)]IV; salIs17 salIs17[QUAS::mes-4(sal4(mes-4[K10A, E11A, E12A]):: mCherry::tbb-2 utr + FRT HygR FRT + unc-119(+)] V*	JPM5, JPM80
JPM51	*salIs13[QUAS::mes-4::mCherry]II; salIs25[Peft-3::QS::SL2::QF::unc-54utr + unc-119(+)]IV*	JPM50, JPM48
JPM52	*salIs14 [QUAS::mes-4(sal4[K10A, E11A, E12A]):: mCherry] II; salIs15[Peft-3::QS::SL2::QF::unc-54utr + unc-119(+)]IV*	JPM50, JPM49

CGC: *Caenorhabditis* Genetics Center (University of Minnesota, USA)

CRISPR: Clustered Regularly Interspaced Short Palindromic Repeats

HygR: hygromycin resistance gene

GFP(KEN): GFP with an extra KEN box

SEC: self-excising cassette

SL2: intergenic region between *glp-1 glp-2*

3.2. DNA procedures

PCR and worm DNA extraction

DNA from single worms was extracted using standard methods (Williams *et al.*, 1992). PCR was used for obtaining DNA fragments for plasmid construction and for checking strains. Two polymerases were used, Taq (own production) and VELOCITY polymerase (BIOLINE):

Table 2. PCR reaction mix

	Taq	VELOCITY
Buffer 10x	1x	----
Buffer 5x	-----	1x
dNTPs	200 µM	200 µM
Primers	1 µM	0.5 µM
polymerase	0.5 µL/25 µL	0.25 µL/25 µL
DNA	~ 120 ng	~ 10 ng

All primers used for checking or plasmid construction are listed in Appendix II. The protocol applied depended on the final use of PCR product. Taq polymerase was used for strain checking and VELOCITY for high fidelity amplifications for plasmid construction. Thermocycler was programmed for each polymerase:

Table 3. Amplification cycles

	Taq		VELOCITY	
Denaturalization	94°C	5 min	98°C	2 min
30 x	94°C	30 s	98°C	30 s
	60°C	30 s	55°C	30 s
	68°C	4 min	72°C	30 s/kb
Final extension	68°C	7 min	72°C	10 min

Cloning, mutations and plasmid checking

PCR amplified fragments were purified from gel (QIAquick extraction Kit – QIAgen). Then, they were ligated to pGEM-T plasmid using pGEM®-T Easy Vector Systems (Promega) or pJET (ClonJET PCR Clonning Kit – Thermo Scientific). For pGEM-T ligation, fragment was treated with Taq polymerase for 10 minutes at 72°C in order to allow 3'-A addition. Ligations were transformed into *Escherichia coli* DH5α by the heat shock method (Hanahan, 1983). Transformants were checked by restriction enzyme digestion and sequenced (Nucleus-University of Salamanca or GATC Biotech). Fragments were assembled first *in silico* (Serial Cloner 2.5) and then by standard cloning methods (Ausubel *et al*., 1997). Enzymes for digestions were acquired from New England Biolabs. T4 DNA ligase used was from Roche and isolation of DNA fragments from gel was carried out according to QIAquick Gel Extraction Kit (QIAGEN). Alkaline phosphatase treatment was done following manufacturer indications (Roche). T4 and Klenow polymerases were used for blunt end obtaining following manufacturer indications (Roche).

Table 4. Adgene plasmids used for this study

NAME	ADGENE PLASMID	COMMENTS
pCFJ601-*Peft-3::Mos1* transposase	# 34874	MosSCI transposase (Erik Jorgensen)
pCFJ350-ttTi5605_MCS	# 34866	MosSCI Universal insertion plasmid (Erik Jorgensen)

Table 4. Cont. Adgene plasmids used for this study

NAME	ADGENE PLASMID	COMMENTS
pCFJ90-*Pmyo-2:: mCherry::unc-54utr*	# 19327	MosSCI co-injection markers (Erik Jorgensen)
pGH8-*Prab-3:: mCherry::unc-54utr*	# 19359	
pMA122-*peel-1* negative selection	# 34873	
pCFJ104-*Pmyo-3:: mCherry::unc-54utr*	# 19328	
Peft-3::cas9-SV40_NLS::tbb-2utr	# 46168	CRISPR-Cas9 (John Calarco)
p*U6::unc-119_sgRNA*	# 46169	CRISPR-Cas9 (sgRNA) (John Calarco)
pDD282-*GFP^SEC^3xFlag*	# 66823	SEC cassette (Bob Goldstein)
pL4440	#1654	RNAi vector (Adrew Fire Kit, 1999-unpublished)
XW08-*Punc-4-QF::SL2:: mcherry::unc-54utr*	# 65832	QS system (Kang Shen)
XW09 *Punc-4-QS::SL2:: mcherry::unc-54utr*	# 65833	
XW12-*QUAS::GFP::unc-54utr*	# 65834	

CRISPR: Clustered regularly interspaced short palindromic repeats

MosSCI: Mos-1 Single Copy Insertion

SEC: self-excising cassette

sgRNA: single guide RNA

Plasmids constructed in this study are listed in Table 5.

Table 5. Constructed plasmids

NAME	COMMENTS
p*U6::mes-4_sgRNA*	*U6::unc-119_sgRNA* PCR: MES4sg primers + pJET Standard cloning method Used for *mes-4* CRISPR

Table 5. Cont. Constructed plasmids

NAME	COMMENTS
p*U6::TEV_sgRNA*	*U6*::*unc-119_sgRNA* PCR: TEV sg primers + pJET Standard cloning method Used for *mes-4* CRISPR extra-KEN box mutation in SS1420
p*mes-4::mCherry*	*mes-4::mCherry^tbb-2utr + HygR^mes-4utr* Standard cloning method Used for *mes-4* CRISPR
p*mes-4::GFP^SEC*	*mes-4::GFP^3xmyc::let-858utr sqt-1(d) hsp::Cre HygR^ 3xFlag::mes-4utr* Punctual mutation protocol and standard cloning methods used for *mes-4* CRISPR (no extra-KEN box)
p*Prps-27::QS::SL2::QF*	*Prps-27::QS::SL2::QF::unc-54utr + unc-119(+)* Standard cloning method Used as part of the inducible expression system
p*Peft-3::QS::SL2::QF*	*Peft-3::QS::SL2::QF::unc-54utr + unc-119(+)* Standard cloning method Used as part of the inducible expression system
p*QUAS::mes-4:*::mCherry	*QUAS::mes-4::mCherry^tbb-2utr + HygR + unc-119(+)^mes-4utr* Standard cloning method Used for induced *mes-4* overexpression
p*QUAS::mes-4(sal4)*::mCherry	*QUAS::mes-4(sal4[K10A, E11A, N12A])::mCherry ^tbb-2utr + HygR + unc-119(+)^mes-4utr* Standard cloning method and directed mutagenesis Used for induced mutant *mes-4* overexpression

CRISPR: Clustered regularly interspaced short palindromic repeats

HygR: hygromycin B resistance

sgRNA: single guide RNA

All plasmids for transformation were purified using QIAGEN Maxi Kit or QIAGEN Mini Kit. NanoVue plus spectrophotometer was used for measuring DNA concentration before worm transformation.

3.3. RNA procedures

Worms were frozen in a microcentrifuge tube with glass beads. Total RNA extraction was made with acidic phenol solution. After adding phenol, a first pulse of 30 seconds was given in a FastPrep for allowing cell rupture. Phases were divided by centrifugation. Aqueous phase was mixed with a chloroform:isoamyl alcohol solution (24:1), centrifuged and isolated again.

RNA obtained was passed through the High Pure RNA Isolation Kit (Roche Diagnostics GmbH). It was quantified using a NanoVue Plus spectrophotometer (GE Healthcare). cDNA was synthetized using the High Capacity cDNA Reverse Transcription Kit (Applied Biosystems). 1 µg of total RNA was added per sample. The cDNA obtained was used for amplifying *cdk-2* for RNAi with cdk2-1/cdk2-2 primers.

3.4. C. elegans strain construction methods

CRISPR/Cas9

Clustered regularly interspaced short palindromic repeats (CRISPR) method (Dickinson *et al*., 2015; Dickinson *et al*., 2013; Friedland *et al*., 2013) was used for tagging endogenous *mes-4* with mCherry and GFP. Briefly, a single guide RNA (sgRNA) directed Cas9 nuclease to a specific sequence in

the genome. This sgRNA has a constant and a variable part. The constant sequence recruits Cas9. The variable part is the specific target sequence. Cas9 makes a DSB at the target site. A template with homology to the place near the insertion is co-injected with Cas9 and the sgRNA plasmids. At some percentage the break is repaired by homologous recombination (HR) using this external template. That leads to the integration into the genome of the sequence of interest.

MosSCI: integration of cassettes for inducible expression

Mos1-mediated single-copy insertion (MosSCI) and its modification (Universal MosSCI) allow insertion of a frame of interest in specific sites in the genome (Frøkjær-Jensen *et al*., 2012; Frøkjær-Jensen *et al*., 2008).

Briefly, Jorgensen group constructed strains with the Mos1 transposon in specific loci in the genome flanked by specific sequences. These strains are microinjected with a mix of plasmids including the transposase gene and a template plasmid with our insert of interest. The template is flanked by sequences homologous to the insertion locus. Transposase expression in germline promotes Mos1 excision, creating a double strand break (DBS). Then, the DBS can be repaired by homologous recombination using the co-injected template. The result of HR repair is the integration of the desired insert into a specific locus. The Universal MosSCI differs from the previous one in the use of the same insertion sequences for every site in the genome. Therefore, with only one backbone (the one used

for chromosome II in the previous MosSCI), different sites in the genome can be targeted.

In this work, for chromosome II insertion, EG6699 MosSCI strain is used. For chromosomes IV and V, EG8081 and EG8082 respectively were used (Universal MosSCI).

Microinjections for MosSCI and CRISPR/Cas9

For microinjections, a Nikon ECLIPSE Ti microscope equipped with a FemoJet® Microinjector and a PatchMan® NP2 micromanipulator (both from Eppendorf) was used. Femtotips® II Capillaries were used as needles. Continuous pressure was set up to 2500 hPa, and injection time 0.2 seconds.

Transformants were isolated following the protocol described for each case. Positives were confirmed by PCR. Two backcrosses into wild-type N2 were performed for CRISPR/Cas9 tagged worms.

Crosses

In order to obtain worms with combined genotype, crossed were made. Males were induced by heatshock at 32°C for 5-6 hours. Crosses were performed by the standard method (Fay, 2005). For backcrosses into the wild type strain (N2), N2 males were crossed to the strain of interest. Males from the F1 were crossed again to N2 hermaphrodites, and progeny was checked. Transgenes, tags and mutations were followed by PCR.

3.5. Study of endogenous mes-4

sgRNA, Cas9 and templates

For mCherry and GFP tags in wild-type bacground, the sgRNA and Cas9 used were the same. Homologous sequences were almost the same, but different primers were used due to the construction method. The sgRNA was constructed by amplification of p*U6::unc-119_sgRNA* plasmid. In this amplification, a mutation was included, changing the *unc-119* specific sequence by the sequence of interest. sgRNA for changing GFP tag in SS1420 background was different, targeting the TEV sequence.

mes-4::mCherry tagging

The template was entirely constructed by standard cloning methods. Hygromycin resistance (*HygR*) with *rps-27* promoter and *unc-54utr* flanked by FRT sites was obtained from our laboratory's collection: pFRT_*HygR*_FRT. *SbfI* site before the promoter allowed the introduction of *tbb-2utr* between the FRT sites. UTR was amplified from pCFJ601- *Peft-3::Mos1 transposase* by tbb2Sbf-1/-2 primers.

For *mes-4* homology arms, 1.24 kb of the last exon of the gene and 1.26 kb of *mes-4utr* were amplified from genomic DNA with the oligo pairs MES4-cherry2/3 and MES4-cherry4/5 respectively. pCFJ90-*Pmyo-2::mCherry::unc-54utr* was used for mCherry amplification with Cherry-1/Cherry-2. It was cloned into pFRT_*tbb2-Hyg*_FRT plasmid. Finally, both

homology arms were added to this construction, giving rise to the final injection template plasmid (**Fig. 9**).

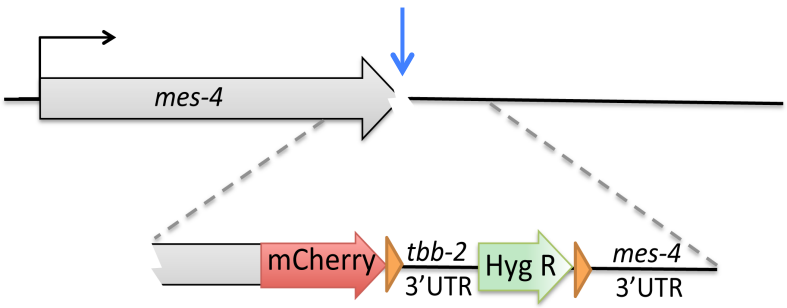

Figure 9. *mes-4::mCherry*

Template for reparation would recombine with endogenous *mes-4* for reparation of the DBS induced by Cas9-sgRNA (blue arrow at the end of *mes-4* gene). Left and right arms are homologous to *mes-4* last exon and 3'UTR respectively. The ORF is followed by in phase mCherry (red). HygR (green) and *tbb-2utr* are flanked by FRT sites (orange).

sgRNA sequence was designed by hand, and it was found at the end of the last exon of the gene. The Cas9 recognition site (proto-spacer adjacent motif – PAM) was not included in the sgRNA: 5' CGA GTT CAA AAA GAG ACA AA (**CGG**) 3' (PAM in bold). Two amplifications were made with CRSP-3/MES4-sg1 and MES4-sg2/CRSP-4. The products were mixed, amplified again with CRSP-3/CRSP-4 and cloned into pJET, obtaining the p*U6::mes-4_sgRNA* plasmid. In order to avoid a new directed DSB in the recombined locus, the 5' homologous arm had been modified to avoid Cas9 recognition. One base from the target sequence plus one base from the PAM were changed: A**CGG** to g**CGa** (switches in lowercase).

mes-4::GFP tagging

The plasmid backbone for template construction comes from a previously constructed plasmid from our laboratory: p*mes-4::mKate2^SEC^ 3xFlag*. In order to change mKate2 by GFP, p*mes-4::mKate2^SEC^ 3xFlag* and pDD282(GFP^SEC^3xFlag) were digested with *Bsu36I/EcoRV* for substituting mKate2 by GFP, obtaining *pmes-4::GFP(KEN)^SEC^3xFlag.*

Due to the presence of a predicted KEN box in the sequence of the plasmid (last K of GFP and first two amino acids of TEV site), it was mutated in order to avoid any interference. The initial plasmid was mutated through a punctual mutation protocol that allowed elimination of the TEV site (**Fig. 10**, next page). Briefly, part of the GFP was extracted from the original plasmid with *SwaI/EcoRV* and cloned into pJET in order to facilitate the mutation checking. TEV(*SacI*)fwd/TEV(*BstXI*)rev primers were used for amplifying the fragment to mutate from this pJET-GFP plasmid, directly avoiding TEV site. This PCR fragment was cloned into pJET-GFP by *SacI/BstXI* digestion and it was sequenced. Reconstructed pJET-GFP without TEV was used for p*mes-4::GFP^SEC* mutation by changing the original fragment in the construction by the mutated one through *BamHI* ligation.

Plasmids before microinjections were sequenced for making sure that this additional KEN box was not present.

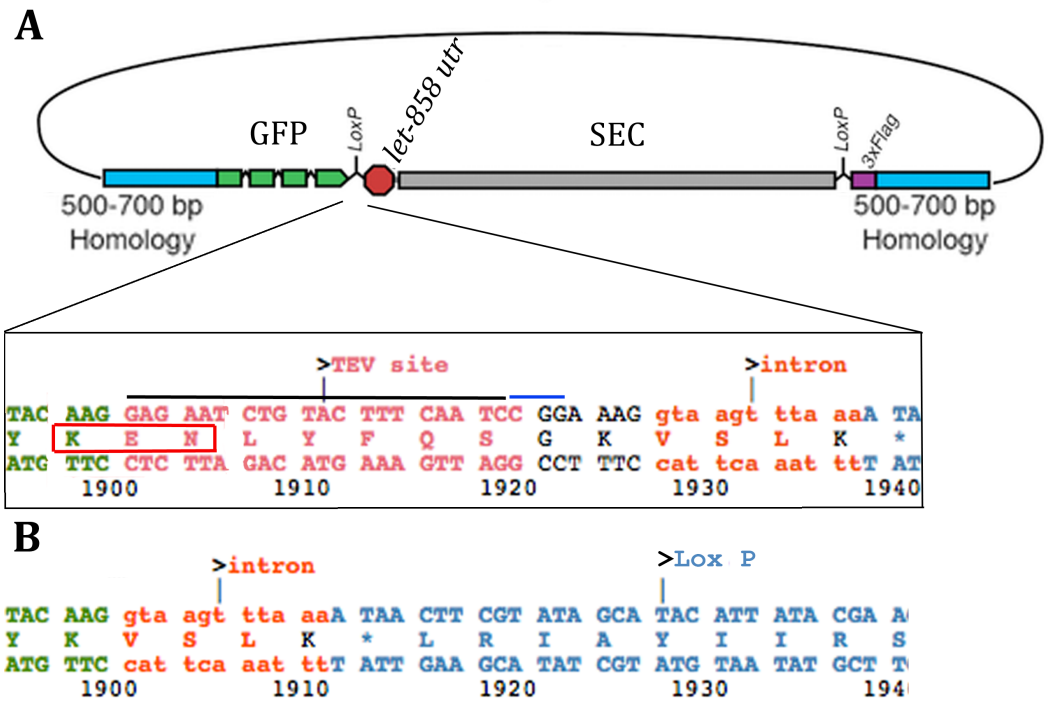

Figure 10. Extra-KEN box mutation

A. Image modified from (Dickinson *et al.*, 2015). Original plasmid and sequence where the KEN box was localized. sgRNA target and PAM sequences for SS1420 strain mutation represented by black and blue lines respectively. KEN box in red. **B.** TEV elimination. KEN box, sgRNA target and PAM sequences are not present.

The sgRNA was the same used for mCherry tag, and the changes in homology arm sequence for avoiding PAM recognition were the same. However, so as to change the tag in the SS1420*[mes-4(bn185(mes-4::[K10A, E11A, N12A]::GFP(KEN)::HA::6xHis)]*, which had the extra-KEN box, a second sgRNA was designed. The PAM (in bold) was located at the end of the TEV sequence; therefore, the sgRNA and PAM would not be in the repair template:

5’ GAG AAT CTG TAC TTT CAA TC (**CGG**) 3’. Two amplifications were made with CRSP-3/TEV sg1 and TEV sg2/CRSP-4. The products were mixed, amplified again with sgMES4-3/sgMES4-4 and cloned into pJET, obtaining the p*U6::TEV_sgRNA* plasmid.

Microinjections and strain obtaining

For microinjections, standard procedure was followed except for the avoidance of co-injection markers. N2 worms were injected only with Cas9, sgRNA and the template plasmids. Transformants were isolated following the protocol described (Dickinson *et al*., 2015). The only difference was that transformants were followed by hygromycin resistance and roller phenotype only. Positives were confirmed by PCR with MES4-cherry1/cherry LIN REV for mCherry-tagged worms, and MES4-cherry1/GFP rev SEC for GFP-tagged worms.

A heatshock was given to GFP worms in order to allow the excision of the selectable cassette. Loss of this cassette was followed by PCR with GFP utr DIR/MES4-cherry6 and HYGRO1/MES4-cherry6. Worms carrying *mes-4(sal3[mes-4::mCherry + FRT tbb-2utr HygR FRT])V,* the strain with *mes-4(sal9[mes-4::GFP::3xFlag::mes-4utr])V* and the strain with *mes-4(sal11[mes-4(K10A, E11A, N12A)::GFP::3xFlag::mes-4utr])V* were backcrossed twice into N2 background. MES4-cherry1/6 primers allowed distinguishing between tagged and untagged versions of the protein in order to look for homozygotes. The strains obtained were: JPM45(*mes-4(sal3[mes-4::mCherry + FRT tbb-2utr HygR FRT]) V*), JPM76(*mes-4(sal9[mes-4::GFP::3xFlag::mes-*

4utr])V) and JPM78(*mes-4(sal11[mes-4(K10A, E11A, N12A)::GFP::3xFlag::mes-4utr]) V*). Now onwards, these strains would be named as: *mes-4::mCherry, mes-4::GFP* and *mes-4(AAA)::GFP* respectively.

The three strains were crossed into MT15488(*lin-35(n4760) I*) mutant background. The tag and mutation were followed by PCR. For the tag, the primers were the previously described and n4760F/n4760R for *lin-35* mutation. Strains obtained were: JPM47, JPM94 and JPM95. From now, these strains would be named as: *mes-4::mCherry;lin-35*, *mes-4::GFP; lin-35* and *mes-4(AAA)::GFP;lin-35* respectively.

Fertility assay

A fertility assay was performed in order to assess that tagged protein was functional, as MES-4 is implied in fertility. L4 worms were placed in individual plates and allowed to lay eggs at 20°C and 25°C. Every day, mothers were passed to a new plate. Laid eggs were allowed to hatch at 20°C for one extra day. Larvae were counted everyday. Worms were followed until no fertile eggs were laid –usually five days. 8-15 worms for each condition (strain and temperature) were analyzed. This was performed for *mes-4::GFP* and *mes-4::mCherry* in comparison with N2. On the other hand, *mes-4(AAA)::GFP*, *mes-4::GFP;lin-35* and *mes-4(AAA)::GFP;lin-35* were also compared against *mes-4::GFP*. Statistical analyses were performed for both assays (detailed in Statistics section).

Analysis of protein sequence

MES-4 and MET-1 sequence was obtained from wormbase (WS258) (www.wormbase.org). Group-based Prediction System for APC/C recognition motifs (GPS-ARM) version 1.0 was used for D-box and KEN-box prediction (Liu *et al*., 2012). KEN-boxes have a 95% of accuracy, 100% of specificity and 93.18% of sensitivity. While for D-boxes it is 87.29%, 95.39% and 63.51% respectively. Default thresholds were used: medium and low for D- and KEN-box respectively. However, high threshold was applied for KEN-boxes. Protein blast of MES-4 against human proteome was performed using the NCBI Blast server (https://blast.ncbi.nlm.nih.gov/). The first sequences obtained from this blast that were annotated (NSD family proteins) were loaded onto the GPS-ARM program.

RNAi silencing by feeding

L4 and L1 worms were silenced, and changes in MES-4 pattern were studied in gonad (silencing from L4) and soma (silencing from L1).

Bacterial strains used

RNAi clones, except for *fzr-1, cdk-2* and control were obtained from Kamath and Aringher's library (Kamath and Ahringer, 2003). Primers used for the Aringher's library were aligned against the genome of *C. elegans* in order to validate the target sequence. Plasmids from bacterial strains in the collection were extracted. They were checked by digestion for confirming the target and transformed again into HT115(D3) strain (from CGC). Clones used

for the RNAi were: proteasomal subunits (*pas-4, pas-5, pbs-4, pbs-5, pbs-6*, *pbs-7*), APC adaptor *fzy-1*, *cye-1* and *ckd-1.*

For *fzr-1(RNAi)* 870 bp were amplified from genomic DNA using the primers fzr1-1/fzr1-2. The blunt ended fragment was integrated into *EcoRV* site in L4440. 1,16 kb from *cdk-2(RNAi)* were amplified from cDNA with cdk2-1/cdk2-2 and digested with *EcoRV*. The final fragment of 942 bp was integrated into L4440 *EcoRV* site. The plasmids were transformed into HT115 (DE3) bacteria. Bacteria transformed with the empty L4440 vector was used as a control RNAi strain.

RNAi protocol

RNAi was performed as previously described (Timmons and Fire, 1998). Briefly, bacteria were inoculated in LB-ampicillin media. Next day, cultures were concentrated 25x and spread over RNAi plates (NGM already containing 50 μg/mL of IPTG and 100 μg/mL of ampicillin). Double stranded RNA expression was induced at room temperature overnight.

L1 or L4 were placed on the plates and allowed to grow at 25°C overnight, and at 20°C for another day. Then, they were prepared for live microscopy (grown L1s) or gonad extrusion (grown L4s). Extruded gonads were treated for immunostaining or tube fixation and DAPI staining. For L1 RNAi, synchronization was achieved by the bleach-alkaline method (Porta-de-la-Riva *et al*., 2012).

From 8-10 worms were analyzed per sample. At least five replicates were made for gonad and somatic patterns for *mes-4::mCherry* and *mes-4::mCherry;lin-35* (somatic patterns not shown in results). Regarding RNAi of the strains *mes-4::GFP, mes-4::GFP;lin-35* and *mes-4(AAA)::GFP*, between 10 and 20 worms were analyzed for somatic and germline patterns. For RNAi of SS1420, 20 worms were analyzed.

Developmental analysis

For analyzing embryos, gravid worms from the strains *mes-4::GFP, mes-4::GFP;lin-35, mes-4(AAA)* and *mes-4(AAA);lin-35* were allowed to lay eggs for 16h at 20°C. Next day, eggs were collected from the plate, and the gravid worms were opened for harvesting eggs at early developmental stages. All the embryos were stained with DAPI. Around 30-60 eggs were analyzed per strain. A total of 8-10 eggs for each developmental time and strain were imaged.

Regarding larvae analysis, worms the from the strains *mes-4::GFP, mes-4::GFP;lin-35, mes-4(AAA)* and *mes-4(AAA);lin-35* were synchronized by bleaching and eggs allowed to hatch in M9 media in the absence of food. Next day, bacteria were added to half of the starved L1 worms in a microcentrifuge tube, and allowed to grow. Three hours later, both, starved and feed, were collected, washed and imaged. No DAPI staining was performed for larvae, although DAPI signal was acquired in order to distinguish autofluorescence. Around 15 L1s were imaged per condition and strain.

3.6. Inducible expression of mes-4 in soma

QS inducible system: method overview

The method used for controllable expression in soma at a specific time is a modification from the one previously described (Wei *et al*., 2012). It was used in this thesis for inducing ectopic expression of *mes-4* and *mes-4(sal4[K10A, E11A, N12A])*.

Briefly, the gene of interest is under the inducible promoter: *QUAS*. An activator (QF) and a repressor (QS) bind to this promoter. If only the activator is present, the gene of interest would be transcribed. On the other hand, when the activator and the repressor are being expressed, *QUAS* promoter would be repressed. Only when quinic acid is added *QUAS* would be released from repression. This would give temporal control. Tissue specificity would come from QS and QF promoters.

The main handicap in this system was the non-homogeneous expression of the gene of interest (**Fig. 11** B, next page). This is a consequence of having macroarrays formed and not homogenously distributed amongst cells. The authors solved this problem using the MosSCI system for single copy integration of the activator and the reporter. However, repressor and activator constructs were introduced separately. This would occupy at least two chromosome of the worm; therefore, combination of genes for ectopic expression would be more restricted.

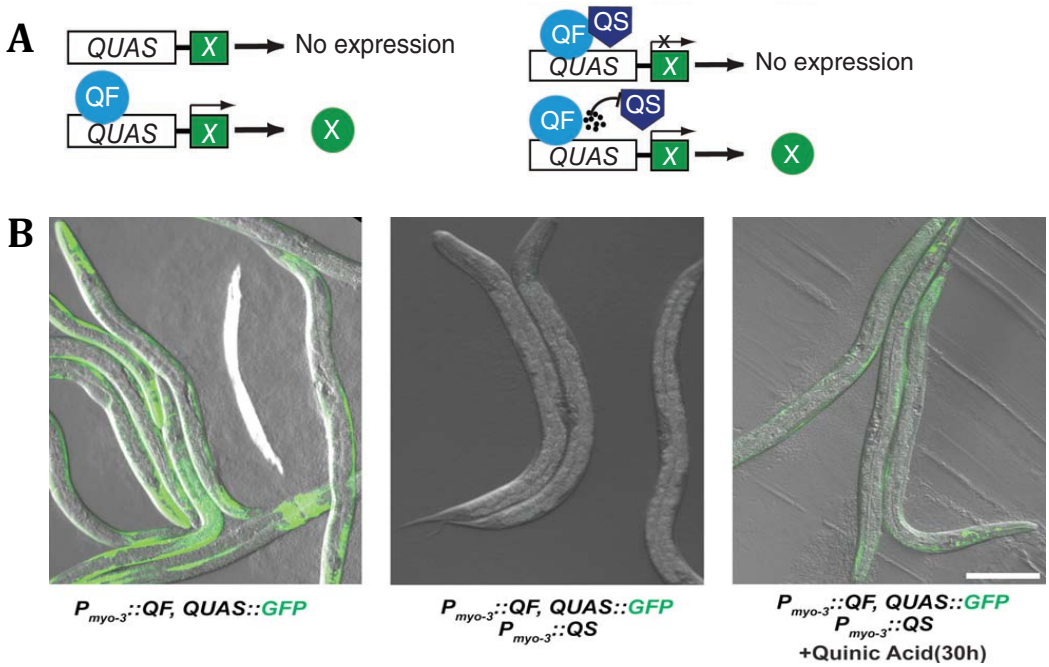

Figure 11. QS inducible expression system

Adapted from (Wei *et al.*, 2012). **A** The gene of interest (green) is expressed when the activator (QF) is present. QS repression of the QUAS promoter is alleviated by adding quinic acid. **B.** GFP is detected in worms with the activator or only when quinic acid is added. Note GFP reporter only in muscle due to *myo-3* promoter driving expression of QF and QS only in this tissue.

In this Thesis, a change was introduced: both, repressor and activator, were under the same promoter, separated by a SL2 intergenic region (Huang *et al.*, 2001). This construction was integrated by MosSCI system in chromosome IV. Additionally, two promoters were tested: *Prps-27* and *Peft-3*. In order to confirm that the modified system worked, *QUAS::GFP* reporter worm was used. The genes of interest under *QUAS* promoter were integrated in chromosomes V (for *mes-4*) and chromosome II (for the GFP reporter and *mes-4*), as shown in **Fig. 12** (next page).

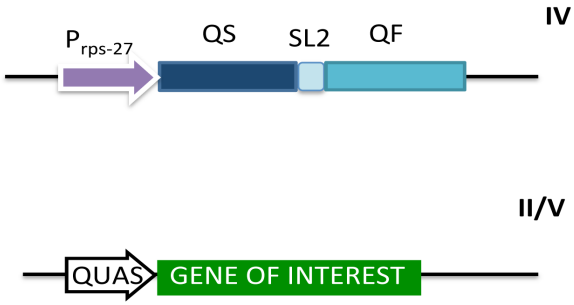

Figure 12. Integrated inducible system.

Scheme of the QS system and the chromosomes where it has been integrated. *Prps-27* promoter gives tissue specificity. QS: repressor, QF: activator, SL2: intergenic region between *gpd-2* and *gpd-3* previously described (Huang *et al.*, 2001). *QUAS*: inducible promoter. These parts were integrated into chr IV, II or V.

Plasmid construction

All constructions were introduced into the insertion plasmid, the same for chromosomes II, IV and V. This insertion plasmid was pCFJ350-*SfiI,* modified from pCFJ350-ttTi5605_MCS. This variation consisted on the addition by *AflII/SbfI* ligation of 1.9 kb flanked by *SfiI* sites. This facilitated integration of constructions into the insertion plasmid by *SfiI* ligation in a specific orientation.

Prps-27::QS-QF/Peft-3::QS-QF

QF and QS were obtained from XW08 and XW09 respectively. SL2 was amplified from genomic with SL2 *KpnI*/SL2 *SacI.* It corresponded to the intergenic region between *gdl-2* and *gdp-3* (Huang *et al.*, 2001), and was integrated into XW09 plasmid in substitution of SL2-Cherry. QF was ligated to this new XW09_SL2 by *NheI* digestion. Promoter was changed by *Prps-27,* that was ligated to the QS-QF plasmid from pdestRG5271Neo (Giordano-

Santini *et al*., 2010). The plasmid for integration was obtained by *SpeI/NotI* ligation to pCFJ350-*SfiI*. It was integrated in EG8081 (IV) obtaining JPM5 strain. In adition, *Peft-3* substituted the previous promoter in order to obtain the strain JPM50.

QUAS::GFP

The reporter plasmid used was XW12-*QUAS::GFP::unc-54utr.* It was inserted into pCFJ350-*SfiI* with *NotI* and used for EG6699 microinjection (II), obtaining JPM50 worms.

QUAS::mes-4::mCherry

Two plasmids were constructed for *mes-4* overxpression, both with the same tag and UTR than the p*mes-4::mCherry* construction (the one for CRISPR/Cas9 transformation). The first construction had a wild-type protein. The second one introduced a KEN box mutation to AAA.

For both, a plasmid p*QUAS-tbb2* was constructed. *QUAS* was amplified with QUAS(*SfiI)*DIR/ QUAS(*PacI*)REV from XW12 plasmid and cloned into pGEM-T. 3' UTR of *tbb-2* was amplified with tbb2-1/tbb2-2 primers, and integrated into pGEM-T. Digestion with *NdeI/SpeI* allowed ligation to p*QUAS.* For construction of the control plasmid with wild-type gen, a frame of 0.9 kb of *mes-4* was amplified with 1MES4/2MES4 primers, ligated to p*QUAS-tbb2*. It was introduced into pCFJ350-*SfiI* by *SfiI* digestion. This new vector was ligated with *PflMI/AgeI* to a plasmid from our laboratory's collection: pCFJ350_*Prps-27::mes-4::mCherry.* It had the same mCherry and *HygR* than CRISPR construction. The final vector contained *QUAS* promoter, *mes-4*

reconstructed gene tagged with mCherry, followed by *tbb-2utr* and hygromicin resistance.

Mutation of *mes-4* KEN-box was performed by PCR directed mutation with the primers QUAS(*SfiI)*DIR/mes4(AAA)REV and mes4(AAA)REV/ 2MES4. The template used was p*QUAS-1-tbb2.* Both PCRs were mixed and the final amplification with QUAS(*SfiI)*DIR/2MES4 contained the mutation. It was ligated to pGEM-T and digested for *mes-4* assembling in the same way than the wild-type form. As the KEN-box is in the first amino acids of the protein, only the first fragment was different between constructions (**Fig. 13**, next page).

Strain used for integration was EG8082 in chromosome V.

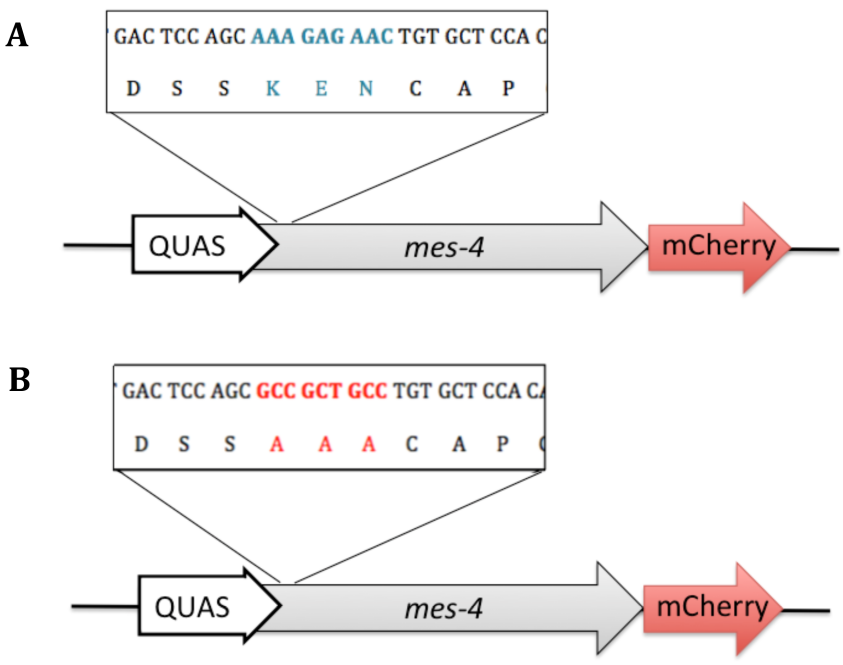

Figure 13. Plasmids for *mes-4* overexpression

A. Wild-type *mes-4* with mCherry tagging. **B**. KEN box mutation to AAA.

Microinjection and strain obtaining

For microinjections, standard procedure was followed, with addition of co-injection markers (Frøkjær-Jensen *et al*., 2012; Frøkjær-Jensen *et al*., 2008). Transformants were isolated following the protocol described. Positives were confirmed by PCR.

Standard crosses were made for obtaining worms with both parts of the inducible system.

Induction

A stock solution of 300mg/mL of quinic acid was made by dissolving D-(-)-quinic acid (Sigma-Aldrich, 98%, Catalog # 138622) in Mili-Q water. It was neutralized with 5M NaOH to pH6-7. This solution was used to add quinic acid to plates containing worms to a final concentration of 9.2 mg/mL. After 24 hours at 25°C or 20°C worms were analyzed under the microscope or the dissecting scope. Worms carrying a the GFP reporter, the *mes-4::mCherry* or the mutated version *mes-4(AAA)::mCherry* were induced and observed. For observation of adults and larvae phenotypes, they were induced at 20 °C. For RNAi, they were induced at 25 °C.

RNAi silencing by feeding

Bacterial strains used for control and *fzr-1* RNAi were constructed in the lab (detailed before). RNAi was performed as previously described

(Timmons and Fire, 1998). L4 worms were treated with RNAi. After one day of silencing, worms were passed to new RNAi plates with quinic acid. The plate was maintained at 25°C. The next day, F1 was analyzed by live imaging. Images from L2 silenced worms were analyzed.

3.7. Microscopy and image processing

Live imaging

Worms or eggs were mounted in a 2% agarose pad with a drop of microscope mounting media (0.1% levamisole – Sigma 31742-250MG –, 0.1% Tween 20 in M9). A drop of VECTASHIELD (Vector laboratories, H-1000) was added, and a cover slip was placed over the sample. It was sealed with nail polish.

Tube fixation and DAPI staining

In order to observe DNA at the same time than the tags in the germline (mCherry and GFP), gonad dissection, fixation and staining with DAPI were performed. Briefly, gonads were extruded and transferred to a microcentrifuge tube. Three washes with PBST were done by centrifugation 30 s at 2000 rpm. Afterwards, methanol was added and samples were incubated at -20°C for 5 min. This was followed by three washes with PBST. DAPI (100 ng/mL) was added to the samples and incubated at room temperature for 30 min. DAPI solution was washed again, and worms mounted as for live microscopy.

Immunostaining

L4 N2 worms treated with a control and *fzr-1* RNAi with the previously described protocol were stained with antibodies anti-MES-4. Protocol used from immunostaining was the one used in the laboratory of Professor Susan Strome, adapted for germlines (Strome and Wood, 1983). Dissected gonads were fixed by freeze cracking on poly-Lysine coated slides followed by methanol and acetone incubations at 4°C (10 minutes each). Then, slides are let to dry and blocked in 1.5% ovalbumin, 1.5% BSA in PBS at room temperature for 30 minutes. Samples were incubated with primary antibody (554_Rabbit-anti-MES-4 1:400 dilution, a gift from Prof. Susan Strome) overnight at 4°C in PBST (1xPBS, 0.1% tween-20).

Next day, slides were washed three times with PBST, blocked again for 10 minutes and incubated with secondary antibody (anti-Rabbit Invitrogen 1:300) and DAPI (1:1000) for 2 hours in dark. Slides were washed again, and mounted in a polyvinyl alcohol solution for imaging one day after. Briefly, this solution was prepared by mixing 1.2 g of polyvinyl alcohol (Sigma), 2.2 mL of glycerol, 3.0 mL of distillated water and 6.0 mL of 0.1M Tris buffer (pH 8.8). 15 worms of each condition were analyzed, and it was repeated twice.

Imaging conditions

For the reporter of the Q repressive system images were captured with a Nikon Eclipse 90i equipped with an ORCA ER camera (Hammatsu) and a 10x/0.30 Plan Fluor objective. GFP filter (525 nm) and an exposure time of

100 ms was enough to capture fluorescence. All the other images were captured using an Olympus IX81 confocal spinning disk (Yokogawa CSU-X1 disk unit) equipped with a Photometrics Evolve EM-CCD camera. MetaMorph program was used for imaging. Z-stack with the oil immersion 60x objective (60x PLAN apo 1.42) was done for each channel. For embryo imaging, 100x objective was used (100x PLAN apo 1.4). Top and bottom slides were adjusted by transmitted light and slides in Z were taken every 1 μm. Excitation wavelengths of solid-state lasers were: 405 nm (DAPI), 491 nm (GFP) and 561 nm (mCherry). All the conditions are listed in the next table:

Table 6. Imaging conditions

channel & excitation wavelength	5Hz, 3x EM-gain (300)		led/ laser power
	live imaging exposure time (ms)	immunostaining/tube fixation exposure time (ms)	
bright-field	100	100	2.0
mCherry 561nm	endogenous: 800 ectopic: 500	800	50%
DAPI 405nm	200	100	50%
GFP 491nm	800	immunostaining: 200 tube fixation: 800	50%

Acquisition in the DAPI channel in live imaging was performed in order to distinguish autofluorescence of the intestine (as the worms had no DAPI staining).

Image processing

Maximum intensity projection of z-stacks was made in ImageJ 1.47v in all the cases except indicated. The images were converted to RGB format and saved as tiff. In Adobe Photoshop CS5, channels were merged and complete images of the worms or larvae were mounted. When needed, brightness-contrast was adjusted between images from the same worm to ensure that they had the same background and intestine autofluorescence inside the same animal from frame to frame. For gonads, channels are shown separated in order to allow better visualization.

Nuclei counting

Complete worm images were opened with Adobe Photoshop CS5. Brightness was adjusted to maximum level. Visible nuclei were counted in L2 worms of every condition. Only L2 were evaluated, for this reason, although around 20 worms were observed, only 3-4 worms for *Peft-3* promoter and 6-8 worms for the *Prps-27* promoter were finally analyzed. Data was analyzed with Prism 5. Besides the small size sample, data behavior was quite similar for both promoters, and statistical analysis was performed.

3.8. Statistical analysis

Data from fertility assays or nuclei counting were introduced into Prism 5.0a (GraphPad) program. For each experiment, mean, standard deviation (SD) and standard error of the mean (SEM) were calculated. For the first fertility assay, a two-way ANOVA was made in order to compare

between variables and their interaction. However, for the mutants, variance was different amongst samples, therefore, an unpaired t-test with Welch's correlation was performed for comparisons. Assumptions made by the program were tested. Regarding quantification of *mes-4* positive nuclei in induced worms, an unpaired t-test was performed, as the interest was to see differences between treatment and no treatment (RNAi) for the same strain. For all the analysis, the confidence interval was 95%.

4. RESULTS

4.1. Study of endogenous MES-4 in the germline

MES-4 regulation has a very specific pattern in the germline: the protein is present at the mitotic zone, and its levels drop at the transition zone, reappearing at late pachytene and oocytes (Fong *et al*., 2002). This pattern suggested that there might be some regulation and, therefore, our first aim was exploring this possibility.

The described drop in protein levels could be due to transcriptional or post-transcriptional regulation. Regarding transcription, the most important regulator of *mes-4*, which is *lin-35*, is not binding the promoter in the germline (Kudron *et al*., 2013). In contrast, post-transcriptional regulation at 3' UTR level determines the patterns of most of the germline genes in the gonad (Merritt *et al*., 2008). Therefore, the starting point was examining this UTR regulation. In order to carry out this analysis and enabling posterior studies, two GFP-tagged versions of the endogenous *mes-4* were constructed. A slightly modified SEC cassette was used for CRISPR/Cas9 microinjections (see materials and methods). The first strain contained *mes-4::GFP* with the ubiquitous *let-858 utr*. The second strain had *mes-4::GFP* with its own 3' UTR. Gonads of both strains were extruded and stained with DAPI for analyzing. Protein patterns were compared amongst them and to the previously described. In addition, MES-4 tagged protein attachment to condensed chromosomes was observed in oocytes (**Fig. 14**, next page).

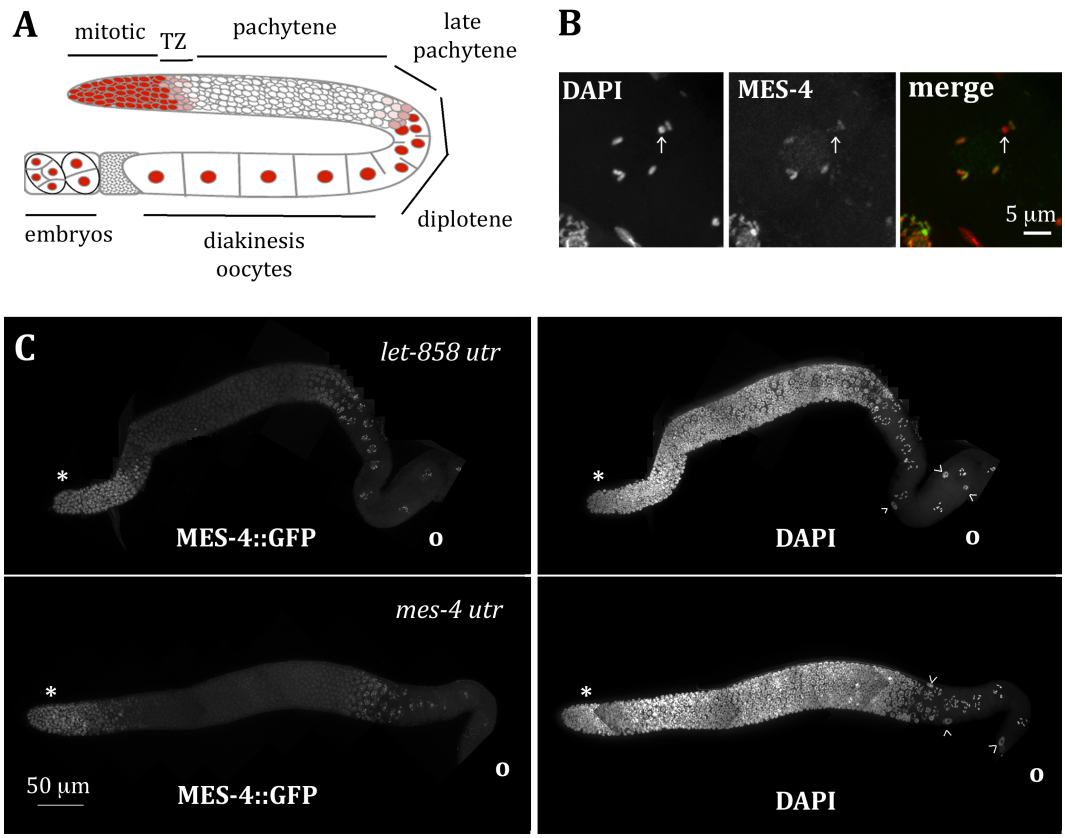

Figure 14. MES-4::GFP pattern and UTR regulation

A. Scheme of MES-4 pattern in the gonad. **B.** Oocyte from a worm with its own UTR. MES-4::GFP was in five of the six bivalent chromosomes. The sixth would be the X chromosome (arrow). This was reproduced for both strains. Red: DAPI; Green: MES-4. **C.** Extruded gonads for both strain with *let-858 utr* (top) and its own utr (bottom). MES-4 protein (left) and DAPI staining (right). *: mitotic region. o: oocytes in diakinesis. Arrowhead: nuclei of somatic gonad.

As observed in the image patterns in the gonads were similar amongst them and to the described (Fong *et al.*, 2002). Protein levels at pachytene decreased in both strains regardless their 3' UTR. Moreover, MES-4 was attached to five of the six bivalent chromosomes in diakinesis (**Fig. 14** B). The

non-stained chromosome would be the X-chromosome. Similarity of MES-4 distribution in these strains suggested that UTR regulation was not playing an important role in MES-4 pattern in the gonad.

Once UTR regulation was shown to be not essential, an additional tool was constructed. The endogenous *mes-4* was tagged with mCherry and the ubiquitous 3' UTR *tbb-2 utr*. This new strain presented the same pattern in the gonad (**Fig. 15**).

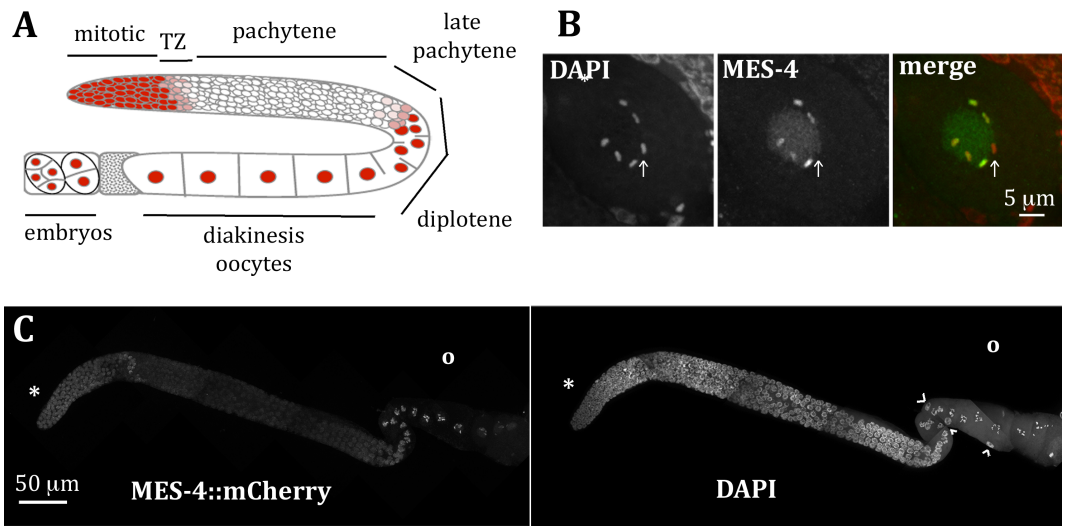

Figure 15. MES-4::mCherry

A. Scheme of MES-4 pattern in the gonad. **B.** Oocyte with MES-4::mCherry in five of the six bivalent chromosomes. The sixth would be the X chromosome (arrow). Red: DAPI; Green: MES-4. **C.** Extruded gonad. MES-4 protein (left) and DAPI staining (right). *: mitotic region. o: oocytes in diakinesis. Arrowhead: nuclei of somatic gonad.

The strains with *mes-4::mCherry::tbb-2 utr* and *mes-4::GFP::mes-4 utr* were used as tools on this Thesis. In order to make sure that they were

reliable, both tagged proteins should be functional, and the strain genetic background should be indistinguishable from the wild type. Genetic background and temperature have a recognized influence in progeny production (Petrella, 2014). Moreover, MES-4 is important for fertility (Garvin *et al.*, 1998). For these reasons, offspring from both strains was compared to the wild type offspring at 20°C and 25°C. All the data and statistics are found in Appendix III. A two-way ANOVA analysis was performed. Assumptions made by the program for this analysis were verified (Appendix III). Data summary and ANOVA results are shown below:

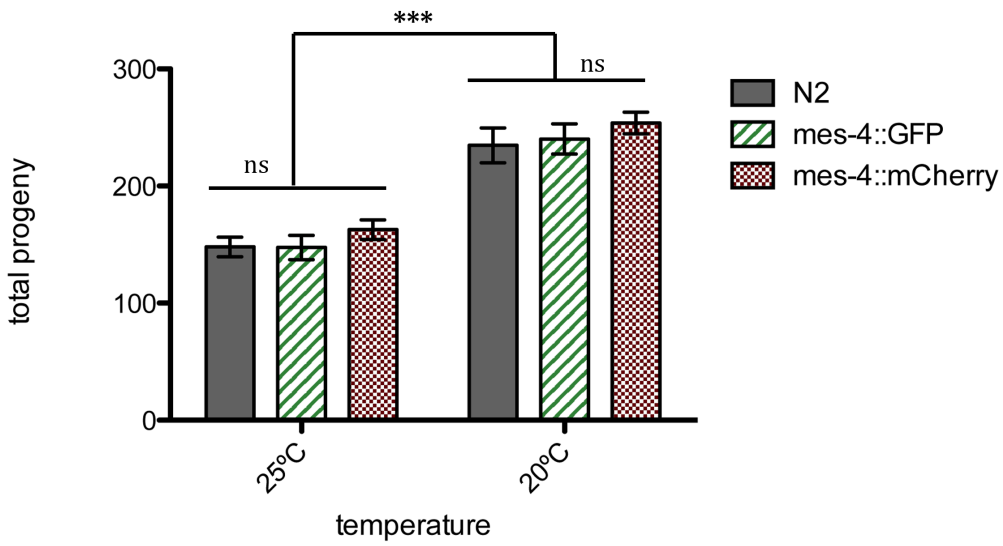

Figure 16. Fertility assay

Total progeny number for wild type N2, *mes-4::GFP* and *mes-4::mCherry* at 20°C and 25°C. Error bars represent the standard error of mean (SEM). N=13-15. Differences between strains were not significant (ns). Variation in fertility observed between 20°C and 25°C was explained by temperature. *** = p value <0.0001; ns: no significant, with a two-way ANOVA.

No differences between strains were detected. However, as expected, a reduction in fertility at 25°C was observed for all the strains compared to 20°C with a p value <0.0001. This suggested that both tagged proteins were functional and their background comparable to the wild type, arising as two reliable tools.

As 3' UTR regulation seemed not to be essential, these two strains were used for exploring other regulatory possibilities.

4.1.1. Regulation of protein drop in the pachytene

P-granules and some germline proteins are regulated through the proteasome in soma and germline (Gupta *et al*., 2015; MacDonald *et al*., 2008; Updike and Strome, 2009). Hence we sought to analyze whether protein stability could address MES-4 pattern.

The proteasome is a multimeric complex formed by a barrel-shaped proteolytic core (20S) and two regulatory lids (19S). The proteolytic core is composed by alpha and beta subunits. In *C.* elegans, there are seven of each, named PAS-1/-7 and PBS-1/7 respectively, and all of them have reported roles in fertility and development (reviewed in (Papaevgeniou and Chondrogianni, 2014)). Most of these subunits were present in Arhinger's RNAi library. Therefore, of these subunits, RNAi of *pas-4, pas-5*, *pbs-4, pbs-5, pbs-6* and *pbs-7* was performed and compared against a control RNAi. L4 worms were placed on RNAi bacteria and adults were analyzed two days after. For this first screening worms were imaged *in vivo,* without fixation

and DAPI staining in order to avoid fluorescence lost (**Fig. 17**). *In vivo* images were better seen in *mes-4::mCherry* strain, therefore this was the strain used:

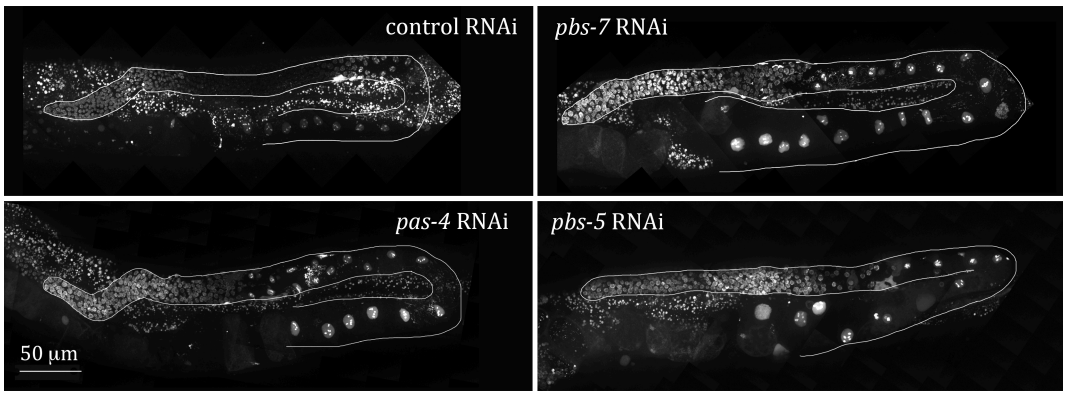

Figure 17. Proteasome RNAi in *mes-4::mCherry::tbb-2 utr*

Cherry fluorescence in the gonad of *in vivo* adults. No DAPI staining. From left to right: control RNAi, *pbs-7* RNAi, *pas-4* RNAi and *pbs-5* RNAi. Germlines surrounded. Intestine autofluorescence is observed as small dots.

An extension of MES-4 signal through pachytene was observed (**Fig.17**). This pattern was reproduced by all subunits tested, indicating a possible regulation through the proteasome. The next step was narrowing the circle to possible E3 ubiquitin ligases.

There are many E3 ubiquitin ligases that target their substrates for proteasome degradation, however, a KEN box was found in MES-4 protein sequence using the GPS-ARM program (Liu *et al*., 2012) (**Fig. 18** A, next page). A KEN box is a recognition site for FZR-1/Cdh1 and FZY-1/Cdc20, both co-activators of the E3 ubiquitin ligase APC/C (Pfleger and Kirschner, 2000; Sczaniecka *et al*., 2008). This suggested a possible degradation via APC/C-proteasome. In order to confirm the prediction and verify which co-activator

was responsible for MES-4 drop, RNAi against FZR-1/Cdh1 and FZY-1/Cdc20 was performed and their patterns compared to the control and the ones obtained with proteasome RNAi (**Fig. 18** B).

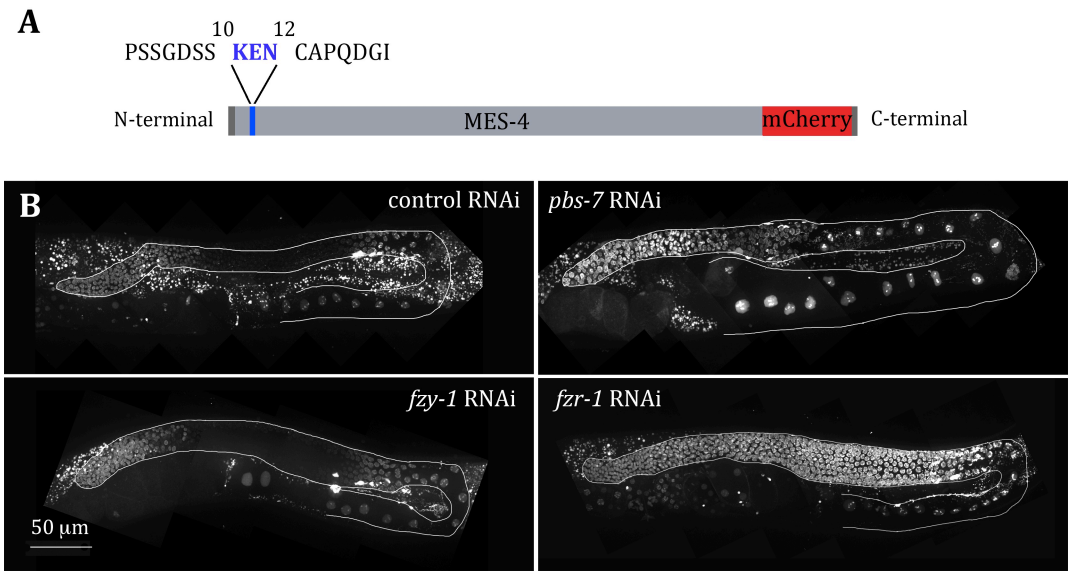

Figure 18. KEN box analysis

A. Scheme of the predicted KEN box position by GPS-ARM. **B.** RNAi experiments on *mes-4::mCherry* strain. MES-4::mCherry signal was observed *in vivo*. Intestine autofluorescence was also detected. Gonads were surounded in white. **B.** RNAi from left to right: control, proteasome RNAi (*pbs-7* in this case), FZY-1/Cdc20 and FZR-1/Cdh1. Both, control and proteasome RNAi images were taken from the previous experiment for comparison.

As shown in **Fig. 18** (B), MES-4 levels were extended through the gonad only in *fzr-1*/Cdh1, but not in *fzy*-1/Cdc20 RNAi. Indeed, the pattern observed using *fzr-1* RNAi was more defined than the one obtained by proteasome RNAi. Moreover, MES-4 pattern extension through the gonad after *fzr-1* RNAi was reproduced in *mes-4::GFP::mes-4 utr* strain and with

immunostaining of wild type worms treated with control and *fzr-1* RNAi (**Fig. 19**).

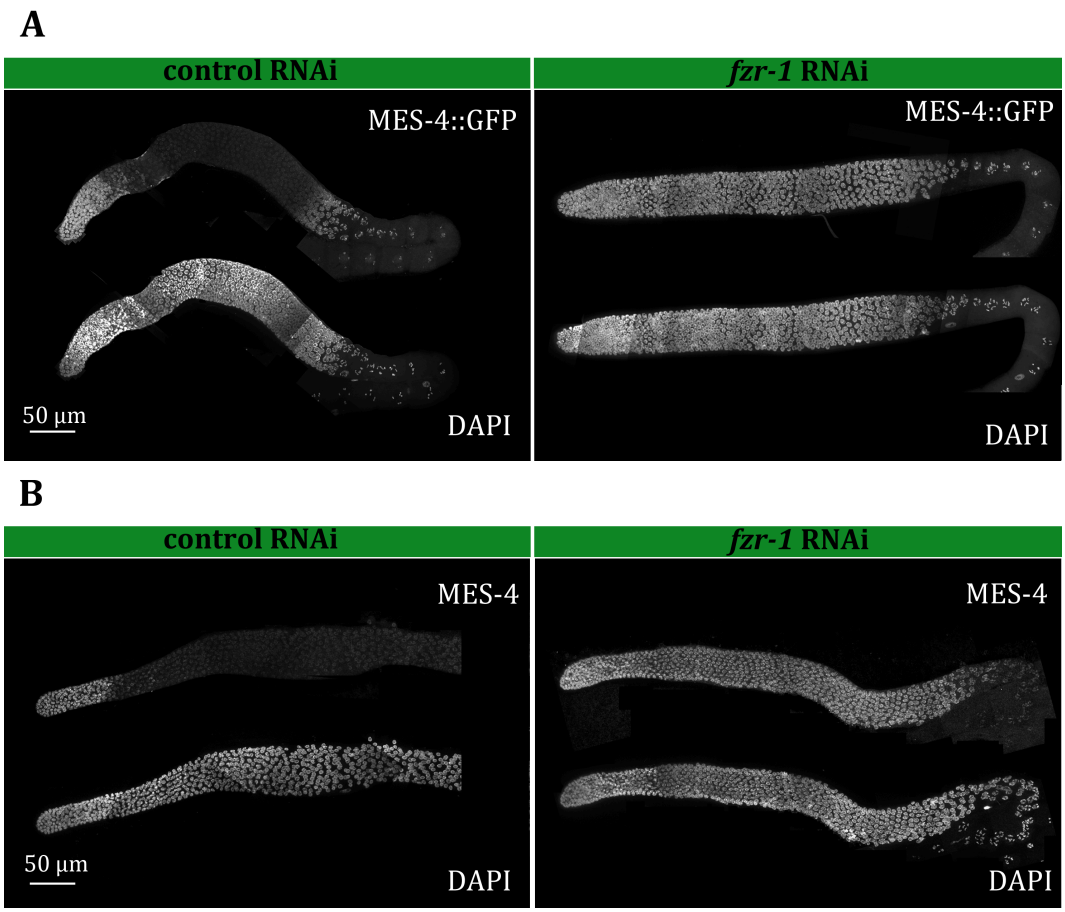

Figure 19. Control and *fzr-1* RNAi in *mes-4::GFP* and N2 immunostaining

A. *mes-4::GFP* gonads treated with control (left) and *fzr-1* (right) RNAi. Images MES-4::GFP signal and DAPI are combined for both. **B.** Immunostaining of N2 gonads treated with control (left) and *fzr-1* (right) RNAi. Images MES-4::GFP signal and DAPI are combined for both. Wild type gonad showed only to the pachytene region.

Taking these results together, MES-4 was likely to be regulated through the APC/C-proteasome system in an FZR-1-dependent manner. Although, this

KEN box was not conserved in human orthologous (BlastP showed that the first 120 residues were not conserved), other KEN box (residues 1077-1079) and D-box (2223-2226) appear in NSD1.

4.1.2. Endogenous KEN box mutation

The question that arouse at that point was if this was a direct or an indirect regulation. Due to the presence of a predicted KEN box in the protein, the next step was its mutation in order to unveil if this was a direct regulation. From here onwards, the tag used would be GFP, unless specified, as it has its own UTR, and a higher resistance to fixation steps.

Two approaches were taken in collaboration with Susan Strome's laboratory. The first one was the mutation of the endogenous KEN box to AAA box. The second was adding an extra-KEN box within the tag in order to see if the wild type pattern was recovered in the endogenous KEN-box mutant. For this purpose, we took advantage of a predicted KEN box found at the end of the tag construction in the SEC cassettes (at the TEV site – see materials and methods). This KEN box was predicted with the GPS-ARM tool. The final strain with the extra-KEN box was: SS1420 *[mes-4(AAA)::GFP(KEN)]*. SS1420 strain was engineered for giving JPM78 *[mes-4(AAA)::GFP]* with no extra box. The strain carrying *mes-4::GFP* described in the previous section was used as a control.

When these strains were analyzed, the KEN box mutant phenocopied the *fzr-1* RNAi previously observed (RNAi shown in **Fig. 19,** previous page).

MES-4 was extended through the pachytene (**Fig. 20,** A). However, when an extra KEN box was added to this mutant (**Fig. 20**, B), the phenotype was intermediate between the control *mes-4::GFP* and the mutant *mes-4(AAA)::GFP*. Protein levels at pachytene still drop, although less than in the wild type. Moreover, when it was treated with *fzr-1* RNAi, MES-4 levels increased (**Fig. 20** B).

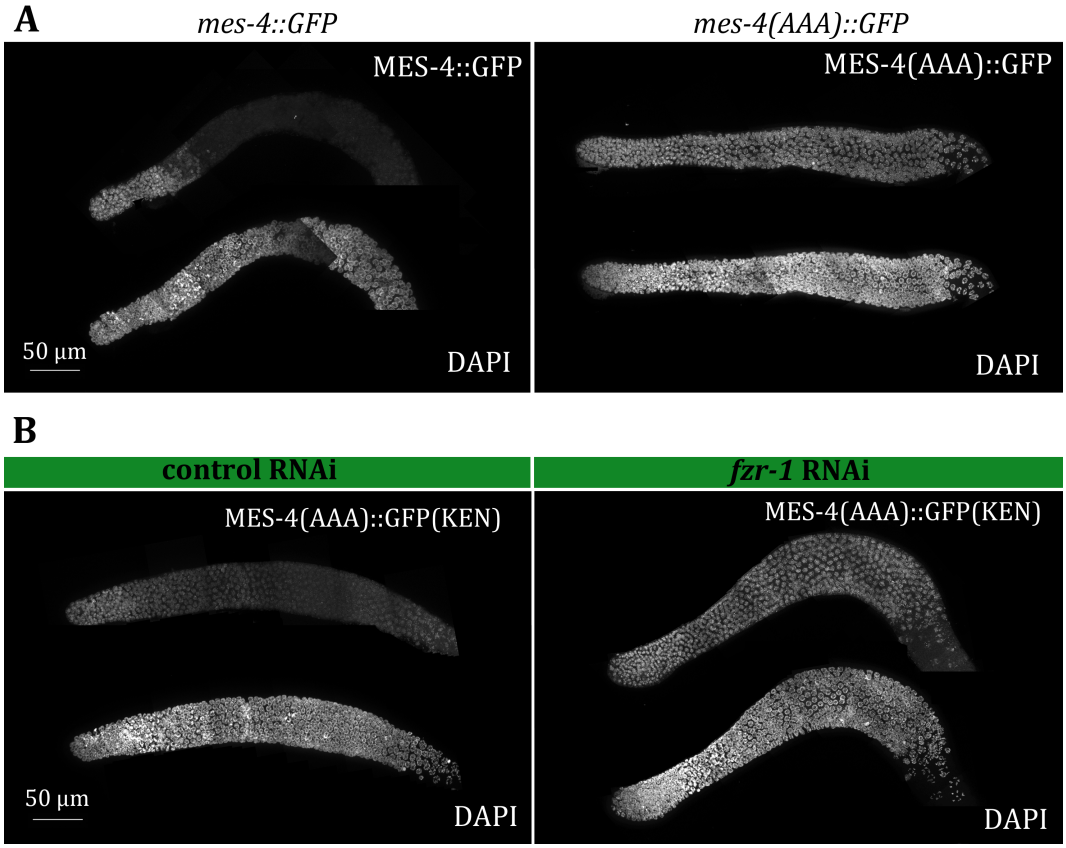

Figure 20. KEN box analysis

A. Wild type with no extra-KEN box and mutant *mes-4(AAA)* with no extra KEN box. **B.** Control and *fzr-1* RNAi of gonads mutant *mes-4(AAA)* with an extra-KEN box. Left: MES-4. Right:DAPI

These experiments confirmed that MES-4 was a direct target of APC/C^{FZR-1} in the germline through its KEN box. From here onwards, *mes-4(AAA)::GFP* strain would be referred as: *mes-4(AAA),* AAA mutant or KEN. The *mes-4::GFP* would be used as wild type (WT), unless specified.

4.1.3. Cell cycle regulation of MES-4

This direct regulation of MES-4 through FZR-1 suggested that FZR-1 was active at the pachytene. But how was FZR-1 activity regulated through the germline? As APC/C^{FZR-1} is an important negative cell cycle regulator, it might be regulated through cell cycle, therefore, we centered in cell cycle regulators.

Concretely, CYE-1 pattern was similar to the one described for MES-4, being high at the mitotic tip, with a drop at pachytene and increasing again at late pachytene and oocytes (Brodigan *et al*., 2003). We hypothesized that CYE-1 could be inhibiting FZR-1 and, consequently, MES-4 pattern would be the same than CYE-1. In fact, Cyclin E negatively regulates Cdh1 in mammals by phosphorylation (Keck *et al*., 2007). Moreover, although in the worm this CYD-1/CDK-4 is in charge of this phosphorylation, CYE-1/CDK-2 has been suggested as a second layer of regulation, acting in a similar way than in mammals (The *et al*., 2015). Besides, CYE-1/CDK-2 and not CYD-1/CDK-4 is one of the major regulators in germline events (Fox *et al*., 2011). For this reasons, we sought to study the possibility of FZR-1 regulation through CYE-1-/CDK-2. In addtion, as cyclin E can interact with CDK1 in mammals

(Santamaría *et al*., 2007), and has been suggested to interact with CDK-1 in the worm (Yoon *et al*., 2012), the effect of *cdk-1* RNAi was also analyzed.

If CYE-1/CDK-2 or CDK-1 were controlling FZR-1 activity, RNAi of *cye-1, cdk-2* or *cdk*-1 would decrease MES-4 levels at the mitotic tip, as FZR-1 would extend its action to this zone. Moreover, in order to study if the RNAi effect was affecting MES-4 through FZR-1, the *mes-4(AAA)* mutant was compared with the wild type (**Fig. 21**).

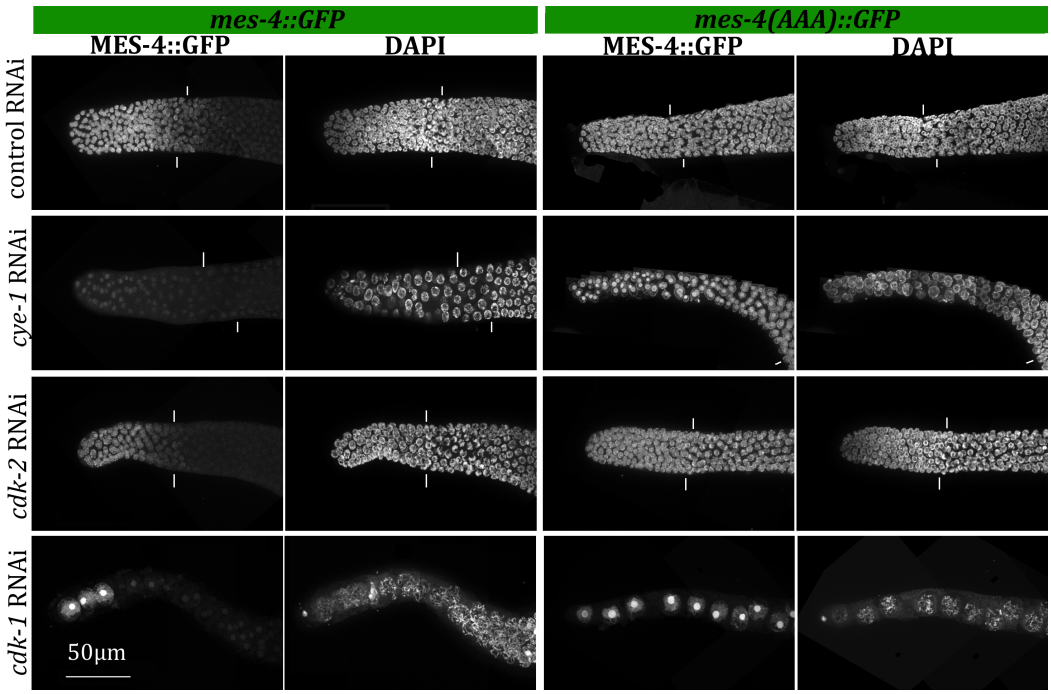

Figure 21. *cye-1* and *cdk-2* RNAi

RNAi in wild type (left) and AAA mutants (right). The distal tip of the gonads is represented for MES-4::GFP and DAPI stainings. The gonads in the top is the control RNAi, *cye-1, cdk-2* and *cdk-1* RNAi follow it respectively. The transition zone is marked between two vertical lines at the point where leptotene-zygotene nuclei first appear (when detected).

As observed in **Fig. 21** (previous page), in the wild type (left panel), MES-4 was reduced at the tip after *cye-1, cdk-2* and *cdk-1* RNAi. This decay in MES-4 levels in the wild type was not observed in the *mes-4(AAA)* mutant (right panel), suggesting that *cye-1/cdk-2/cdk-1* RNAi were probably acting through FZR-1.

On the other hand, the effect in MES-4 levels observed with *cdk-2* RNAi was not as pronunced as the observed for *cye-1* and *cdk-1* RNAi (as observed in the nuclei size at the mitotic zone). This was not due to a inefficienty of the RNAi, as at late pachytene, *cdk-2* RNAi presented enlarged nuclei, similar to those in *cye-1* RNAi. This suggested that CYE-1 could be acting also with CDK-1. Additionally, MES-4 decay in wild type worms treated with *cye-1* and *cdk-2* RNAi, was observed before the transition zone (where cells with a moon-shape are first observed). On the contrary, MES-4 in the wild type starts dropping at the transition zone. For *cdk-1* RNAi, the transition zone could not be assessed, as nuclei morphology was highly different. In addition, a higher accumulation of MES-4 was observed in the most distal nuclei of *cdk-1* RNAi gonads, even in the *mes-4(AAA)* mutant. This difference could be due to a stronger cell cycle exit and the accumulation of MES-4 protein on those cells.

These results suggest that CYE-1 (possibly acting with CDK-2 or CDK-1) could be targeting FZR-1 for degradation as in other organisms. The analysis of the influence of other cell cycle regulators in MES-4 decay would

give light to this cell cycle interaction using MES-4 as a reporter of FZR-1 activity.

4.2. MES-4 regulation in soma

We now wondered if MES-4 regulation through FZR-1 was conserved in soma. In somatic cells, there is an additional regulation at transcriptional level. LIN-35/pRb acting within the DRM/DREAM complex is known to repress *mes-4* (Goetsch et al., 2017; Kudron et al., 2013). For these reasons, in order to analyze MES-4 in soma, LIN-35 should be taken into account.

Wild type (WT) L1 larvae and *lin-35* mutant L1 larvae, both carrying *mes-4::GFP* were treated with a control and *fzr-1* RNAi. After the treatment, most of the larvae were at L4 stage, and they were analyzed. The phenotype of the *lin-35;fzr-1(*RNAi) was distinguishable from the WT;*fzr-1(*RNAi), WT;control(RNAi) and *lin-35;*control(RNAi). Generally *lin-35;fzr-1*(RNAi) were smaller and had defects in vulva formation more frequently (74/83) in comparison to *lin-35;*control(RNAi) (20/116), WT;*fzr-1(*RNAi) (2/53), or WT;control(RNAi) (0/51).

Worms in F**ig. 22** (next page) are at the L4 stage. As observed, MES-4 was not detected in somatic cells of the WT;control (RNAi). On the contrary, it was present in intestinal nuclei of WT;*fzr-1(*RNAi) and *lin-35;*control(RNAi). However, in the *lin-35;fzr-1(*RNAi), both regulators were removed, and MES-4 was observed in most of the somatic cell types: muscle, hypodermal cells, intestine and cells from the developing vulva. Despite this

increase in MES-4 signal, not all the cells of the worm contained MES-4. Only few neurons of the head and tail ganglia and the ventral nerve cord (VNC) were positive for MES-4. This is probably be due to the lower RNAi efficiency in neurons in comparison to other tissues (Asikainen *et al.*, 2005). Additionally, *lin-35;fzr-1(*RNAi) worms that reached adulthood were unfertile. Uterus was empty and the worms exhibit protruding vulva.

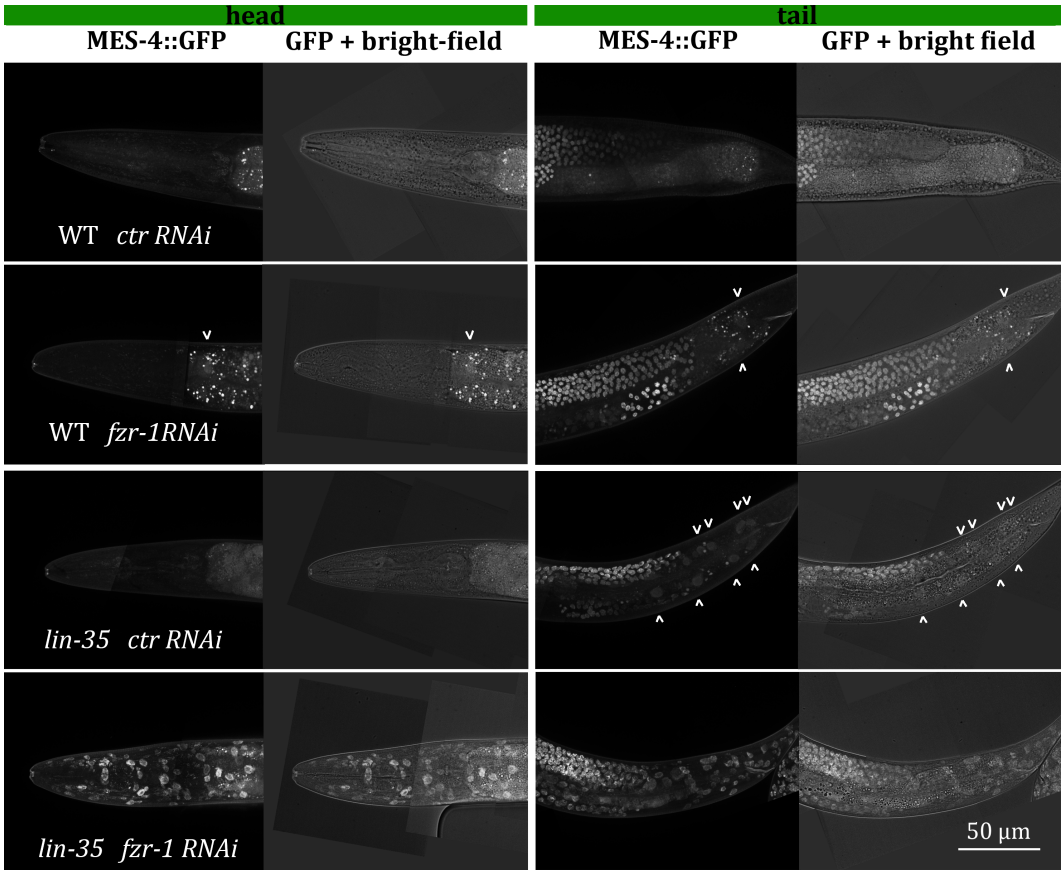

Figure 22. MES-4 misexpression in soma of L4 worms

All the worms carry *mes-4::GFP.* Live imaging of L4 worms and z projection are shown for the GFP channel. Brightness is adjusted for better visualization of the nuclei. No DAPI staining. Autofluorescence of the intestine is observed. The head on the left and tail on the right. Arrowhead: intestinal nuclei positive for MES-4. In the *lin-35* mutant treated with *fzr-1* RNA, nuclei are easily visible.

Figure 23. Expression of MES-4 in the double mutant *mes-4(AAA);lin-35* (next page)

A. Head from *mes-4(AAA)* on the left, *lin-35;fzr-1*(RNAi) in the middle, and the *mes-4(AAA);lin-35* on the right. All the worms are at the L4 stage. The region inside the box is zoomed at the bottom of the pannel. Neurons of the ventral ganglia are surounded. In the *mes-4(AAA);lin-35* more cells, misexpress MES-4 in comparison with *mes-4(AAA)* and *lin-35;fzr-1*(RNAi). Images are overexposed in order to better distinguish nuclei. Autofluorescence in the head of the *mes-4(AAA)* is observed. Nuclei of neurons in the head ganglia are enclosed by a dash-line.

B. Gonad of a double mutant *mes-4(AAA); lin-35* young adult. Z-stack projection. MES-4::GFP and DAPI staining. Intestinal nuclei are seen crossing the proximal part of the gonad (i). Arrowhead: somatic gonad nuclei. On the right pannel, an oocyte nuclei staining is amplified. Arrow: X chromosome.

pm: pharynx muscles, bm: body muscles, i: inestine, hyp: hypodermal nuclei,

Comparable results were obtained with *mes-4::mCherry* strains. MES-4::mCherry was present in most of the cells of the worm only when both regulators were depleted. In a similar way, few neurons were positive for MES-4.

In order to further analyze interaction of both regulators, double mutants for *lin-35* and the KEN box tagged with GFP were made (*mes-4(AAA);lin-35*). Due to the high number of positive cells observed in this double mutant, and in order to analyze them, instead of z-sacks, one central slide of the head is represented for the KEN box mutant *mes-4(AAA)*; the *lin-35;fzr-1*(RNAi) and the double mutant *mes-4(AAA); lin-35* (**Fig.23**, next page). The head of the *lin-35;*control(RNAi) is observed in **Fig. 22** (previous page).

Although the previous figure is a z-stack it is comparable to these images, as no nuclei in the head were stained.

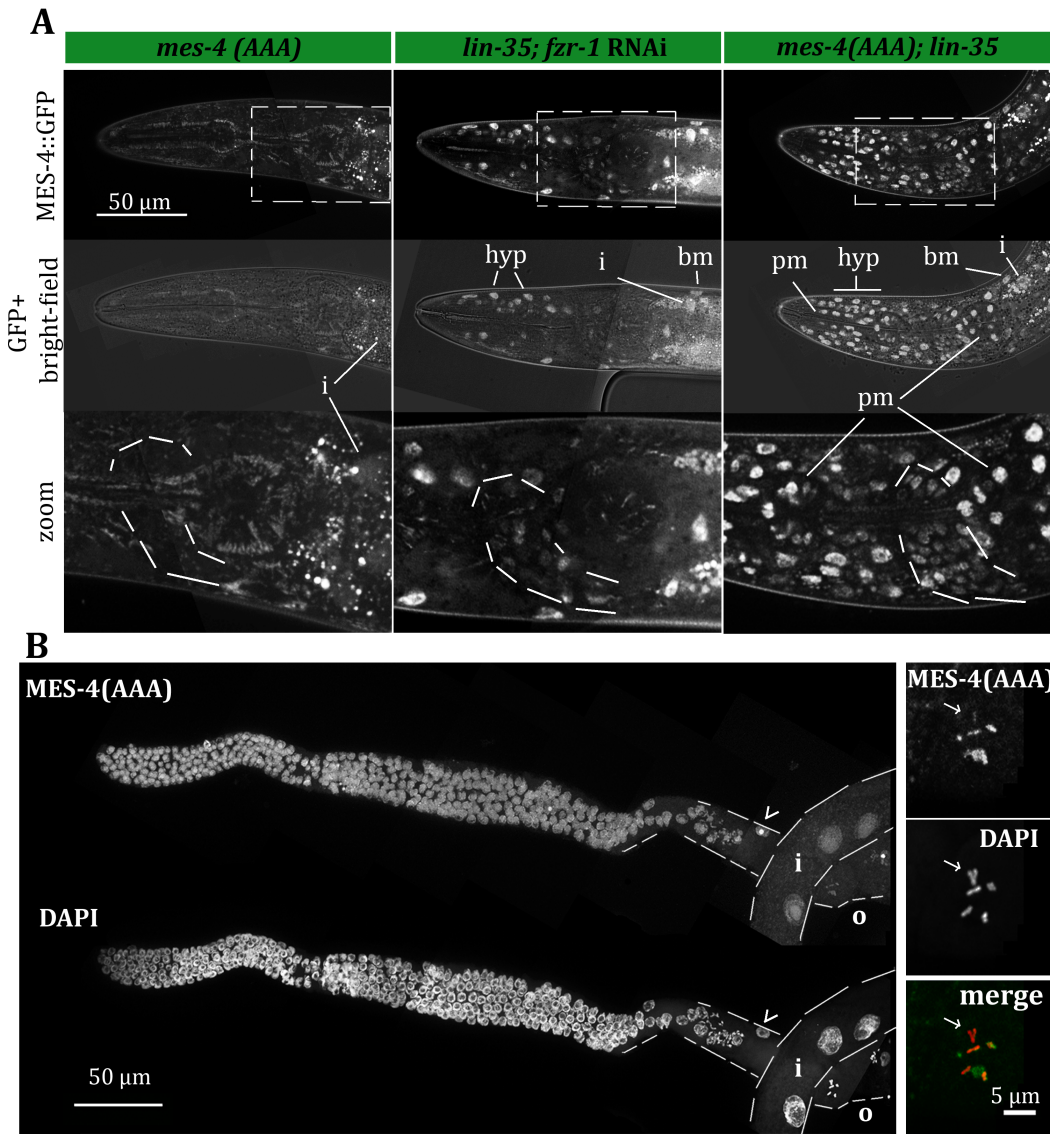

In the *mes-4(AAA);lin-35* double mutants MES-4 was present in almost all the somatic cells, including neurons, body muscles, muscles in the pharynx, intestine, hypodermal and vulval cells. There were other cells that only for position and nuclei shape could not be assessed. However, neurons in the head ganglia were observed with MES-4 misexpression in the *mes-*

4(AAA); lin-35 double mutant, while only few of them were positive after RNAi-treatment in a *lin-35; fzr-1(*RNAi). The differences in somatic pattern between RNAi-treated *lin-35* and the double mutant are possibly due to an incomplete effect of the RNAi, and the commented RNAi low efficiency in neurons.

At the adult stage, MES-4 was not present in somatic tissues in *lin-35* and *mes-4(AAA)* single mutants (except for the somatic gonad in *lin-35*). On the contrary, MES-4 was widely observed in somatic cells of *mes-4(AAA);lin-35* adults. Besides, the gonads of these double mutant adults looked normal by DAPI staining (**Fig. 23** B, previous page), and MES-4 was attached to autosomes, as in a wild type. However, similar to a *lin-35* mutant, nuclei of the somatic gonad of the *mes-4(AAA); lin-35* worms misexpressed MES-4. Despite the presence of MES-4 in all the worm, *mes-4(AAA); lin-35* mutants were viable, although their fertility was lower than in single mutants and the wild type: 62±18 (n=15;mean±SD) for *mes-4(AAA);lin-35* double mutants in comparison to 117±32 (n=13) for *lin-35;* 247±58 (n=15) for *mes-4(AAA)* and 248±19 (n=8) for the wild type (for details see Appendix III). Further phenotypic characterization of these worms is being carried out.

4.2.1. Regulation of MES-4 during embryo development

During embryo development, there are important times at which significant changes take place. At gastrulation (around 28-cells), cells start re-organizing, internalizing the intestine and the only PGC. Afterwards, around the 100-cell stage, this PGC gives rise to two PGCs. At this stage,

zygotic transcription starts in soma, coinciding with a drop in MES-4 levels. Later on, at 550 cells, morphogenesis starts, and the worms elongates. Before hatching, the worms are at the 3-fold stage. We hypothesize that this drop in MES-4 is due to the combination of both: LIN-35 and FZR-1 action. In order to analyze the regulation of MES-4 drop during development through *fzr-1* and *lin-35*, embryos from the single mutants *mes-4(AAA)* and *lin-35*, and double mutants *mes-4(AAA);lin-35* were compared to wild type embryos at different stages. Early embryos were first analyzed (**Fig.24**).

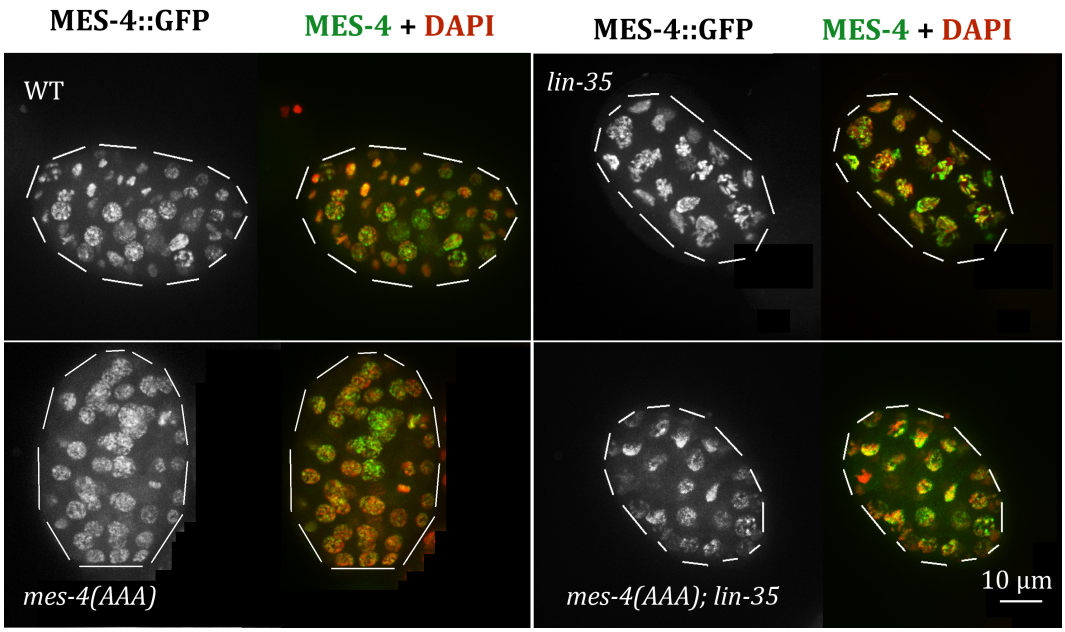

Figure 24. Early embryos

Z-projections. From left to right, wild type embryo, *lin-35* mutant. Down right: *mes-4(AAA)* mutant, and the double mutant *mes-4(AAA); lin-35* on the left. Both, *lin-35* and the double mutant *mes-4(AAA); lin-35* show abnormal cell shapes.

MES-4 was detected in all nuclei of early embryos from the four strains, as observed in **Fig.24** (previous page), except in some abnormal nuclei in the *mes-4(AAA);lin-35* double mutant. Differences started around 100-cell stage, in middle of gastrulation. At this point, the intestine and both PGCs have already migrated to the inside. In order to distinguish the intestinal nuclei by position and shape, only one or two slides from the z-stack were used for the representation (PGCs not always included on these slides). MES-4 presence in embryos around 100-cell and 3-fold stages was compared amongst the four strains.

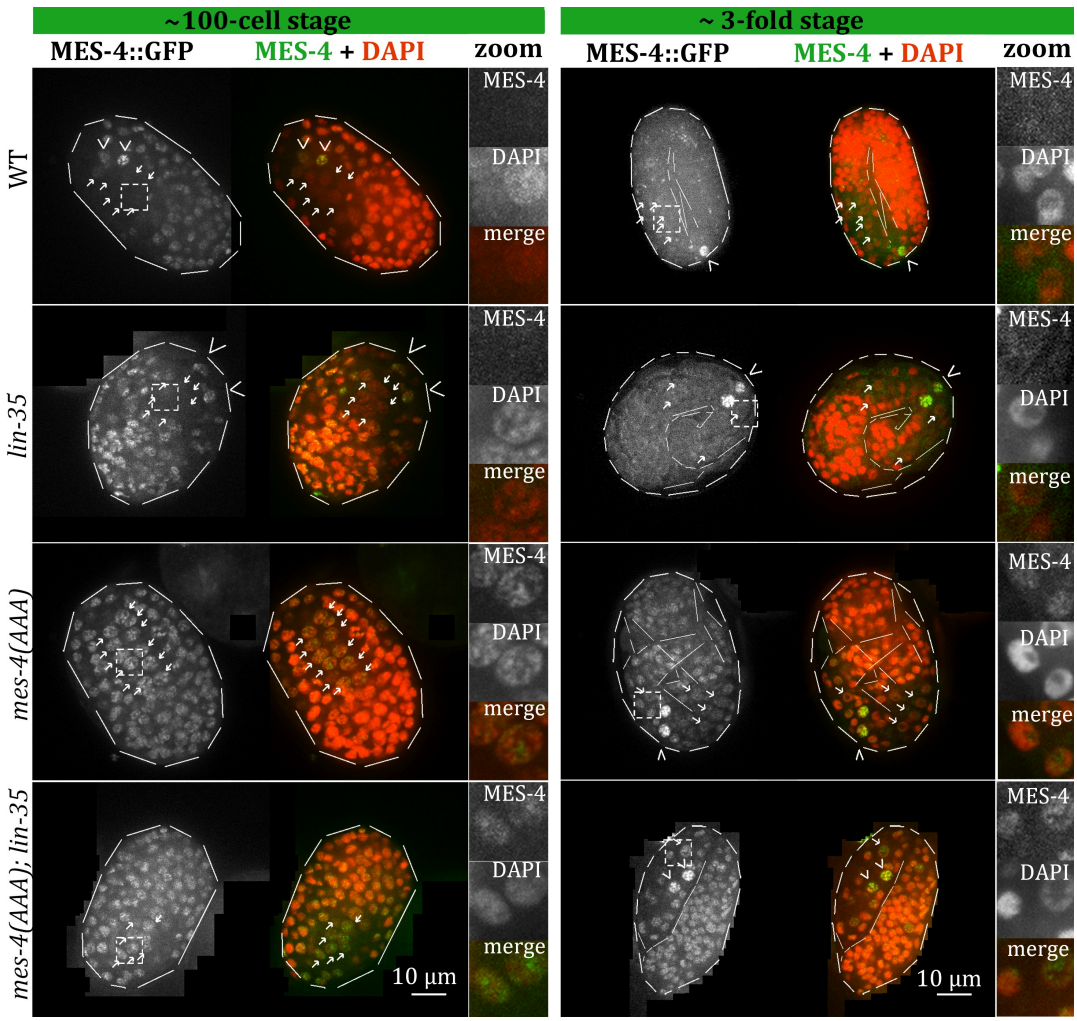

For the wild type and *lin-35* mutant, MES-4 levels dropped in somatic cells between early to 3-fold stage. In between, around the 100-cell stage, MES-4 disappeared from the intestine in the wild type and *lin-35* mutants except for one or two cells. On the contrary, for both, *mes-4(AAA)* mutant and the double mutant *mes-4(AAA);lin-35*, MES-4 was maintained in the intestine and multiple other cells of the embryo until 3-fold stage. Curiously, as shown in the previous section, MES-4 was detected at higher levels in the intestine of *lin-35* larvae, than in *mes-4(AAA)* mutants. These results suggest that the role of FZR-1 during embryonic development is key for MES-4 decay in the intestine, being even more important than LIN-35.

Figure 25. 100-cell and 3-fold stage embryos (previous page)

One or two slides from the z-stack are represented. Embryos from the WT and *lin-35* carry *mes-4::GFP.* Embryos from *mes-4(AAA)* and *mes-4(AAA);lin-35* carry *mes-4(AAA)::GFP*. Images are overexposed for allowing a better visualization. Around 100-cell stage(left), the intestine was observed inside the worm (arrows) as big round nuclei. PGCs contained the higher MES-4 signal. The intestine was positive for MES-4 only in the *mes-4(AAA)* mutant and the *mes-4(AAA); lin-35* double mutant, while not detected in the wild type and *lin-35*.

On the right, 3-fold stage embryos. Arrowheas: PGCs. Arrows: intestinal cells. MES-4 is present in most of the cells of the head, tail and intestine of the *mes-4(AAA)* mutant and the *mes-4(AAA); lin-35* double mutant. Intestinal cells in the box zoomed on the right of each panel.

All the evidences indicate that FZR-1 plays a major role in most cell types, not just in the intestine. Most of the cells of the *mes-4(AAA)* mutant were positive for MES-4 even at the 3-fold stage, in comparison to the undetected MES-4 in *lin-35* mutants or the wild type. Moreover, no great differences were observed in MES-4 distribution between *mes-4(AAA)* mutant and *mes-4(AAA);lin-35,* suggesting that protein degradation is essential for maintenance of MES-4 patterns in the embryo.

Additionally, MES-4 was enriched in PGCs of all the strains, being in all cases higher than in somatic cells at the 3-fold stage. This is not due to an increased transcription, as these cells are transcriptionally silenced (Wang *et al*., 2011), therefore, additional mechanisms may exist.

MES-4 was maintained during embryo development beyond the expected times, presenting a differential regulation in the intestine between embryos and L4 larvae. How is this switch regulated? Do differences start in L1 larvae? Contrary to the idea of MES-4 absence in the wild type larvae, MES-4 should be present, at least, in the intestine of wild type worms. This presence could explain that *fzr-1* RNAi from wild type L1 lead to this faint misexpression of MES-4. If there were no *mes-4* expression at early larval stages, there would be no protein. Consequently, *fzr-1* RNAi from larvae would have no effect, as there is no protein to protect from FZR-1-mediated degradation. Moreover, it would explain as well why *lin-35* worms that have no MES-4 in the intestine during embryo development, misexpress MES-4 at

the L4 stage. At some point between embryo hatch and L4 stage, *mes-4* should be expressed, at least, in the intestine.

4.2.2. Regulation during larvae development

In order to address this question, our first approach was studying L1 larvae looking for MES-4 in soma. The current information about MES-4 localization in larvae comes from few inmmunostaining assays. Protocols used for larvae immunostaining of MES-4 normally use starved L1s. For this reason, the starting point was the analysis of starved L1s. The four strains described before were contrasted amongst them and to the known pattern. Live microscopy was performed for wild type, *lin-35* and *mes-4(AAA)* single mutants and double mutant *mes-4(AAA); lin-35* (**Fig. 26,** next page). From the z-stack only two or three slides were used for the projection in order to avoid as much autofluorescence as possible and centering on the positive cells. In addition, although no DAPI staining was performed for this experiment, DAPI channel was merged to GFP channel in order to allow a better visualization of autofluorescence.

MES-4 was present in the PGCs of starved wild type L1s, as previously described (Fong *et al*., 2002). However, some worms also presented MES-4 in one or two cells at each side near the tail of the worm. For their position, they are possibly neuroblast Q1 on the left side, and the neuroblast Q2 on the right side (**Fig. 26**, next page). However, this localization should be assessed with DAPI staining and specific markers. There were also some unidentified cells positive for MES-4. The pattern was similar for *lin-35* mutants, with no

observed MES-4 in the intestine. MES-4 signal in Q cells observed in the WT, *lin-35* and *mes-4(AAA)* mutants was usually lower than MES-4 at PGCs. This could explain that they were not detected with antibody staining. Moreover, at longer starvation times these cells might be negative.

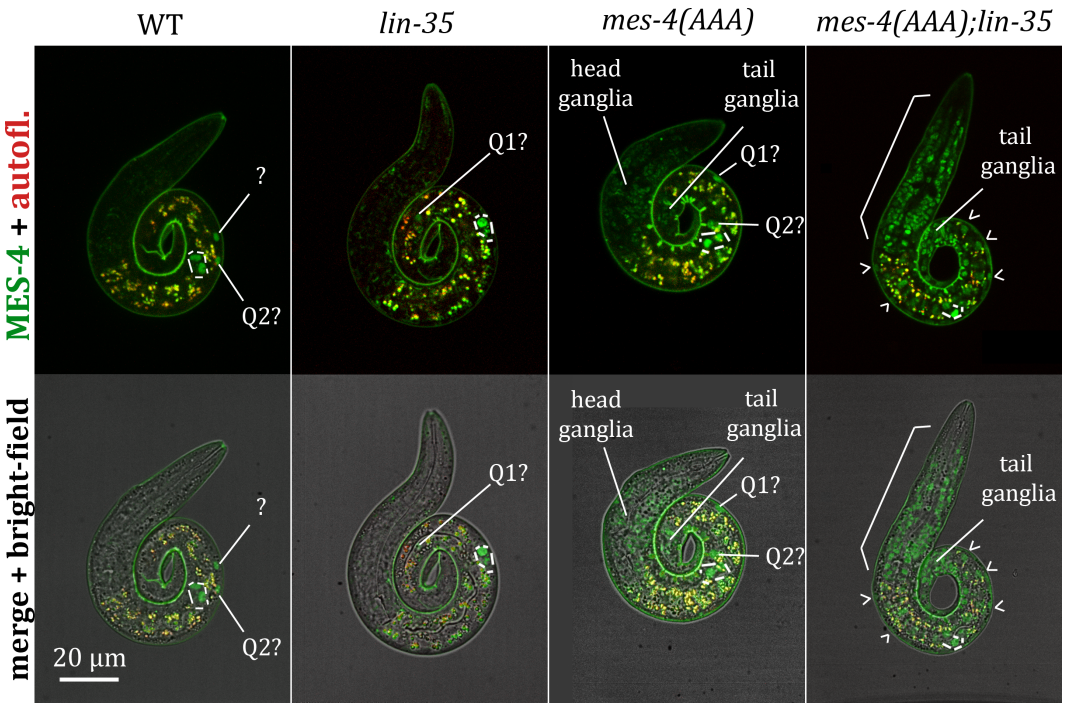

Figure 26. Starved L1s

WT and *lin-35* worms carry *mes-4::GFP.* The strains *mes-4(AAA)* and *mes-4(AAA);lin-35* carry *mes-4(AAA)::GFP*. Autofluorescence of the intestine is shown in red. Merge with DIC is represented on the bottom. Both PGCs (surounded in white) are not always visible, as only one or two slides from the z-stack are represented. Cells positive for MES-4 besides the PGCs are indicated, although additional identification would be needed. Additionaly, the head of the *mes-4(AAA);lin-35* mutant is marked with a square bracket. Arrowheads: multiple cells in the *mes-4(AAA);lin-35* mutant were positive.

Regarding the *mes-4(AAA)* mutant, PGCs and neuroblast were also positive for MES-4, but no the intestinal cells. This suggests that LIN-35 cooperates with FZR-1 during starvation in the intestine. In addition, a group of neurons in the head and tail ganglia of *mes-4(AAA)* mutant also contained MES-4. These cells express *cki-1* at L1 stage, presumably containing some CKI-1 protein that would repress CDK-2/CYE-1 (Baugh and Sternberg, 2006). In our model, this inhibition, would allow FZR-1 activity, therefore, repressing MES-4 in these cells. The fact that MES-4 was observed in these ganglia in *mes-4(AAA)* mutants but not in *lin-35* mutants or the wild type reinforces this idea. Something similar could be happening for seam cells, as *cki-1* is highly expressed here during starvation (Baugh and Sternberg, 2006). However, the absence of MES-4 in seam cells in the *mes-4(AAA)* mutant could be due to the combined repression through FZR-1 and LIN-35. Indeed, only the double mutant *mes-4(AAA); lin-35* presents MES-4 not only in the described cells, but also seam cells, intestine, body muscles, and blast P and Q cells, neurons of the ventral cord and other unidentified nuclei.

This data indicate that LIN-35 and FZR-1 collaborate to ensure a correct pattern for MES-4 during starvation, with FZR-1 playing a major role. Besides, CKI-1 would modulate MES-4 pattern through the inhibition of CDK-2/CYE-1, affecting FZR-1 activity. In addition, different patterns between the *lin-35* and *mes-4(AAA)* single mutants and the double mutant *mes-4(AAA);lin-35* suggest that MES-4 regulation differs amongst tissues in the larva. While in neurons of the head and tail ganglia FZR-1 seem to be more important

than LIN-35, in most of the tissues both, LIN-35 and FZR-1, are needed. For this reason, only when both regulators are eliminated, the protein is detected in all the cells during starvation.

In agreement with this model, when starved L1 worms were fed for 3h, MES-4 reappeared mainly in seam cells in the wild type, *lin-35* and *mes-4(AAA)* (**Fig. 27**), with similar patterns in all of them. Only one or two slides are represented, PGCs and some seam cells not always visible.

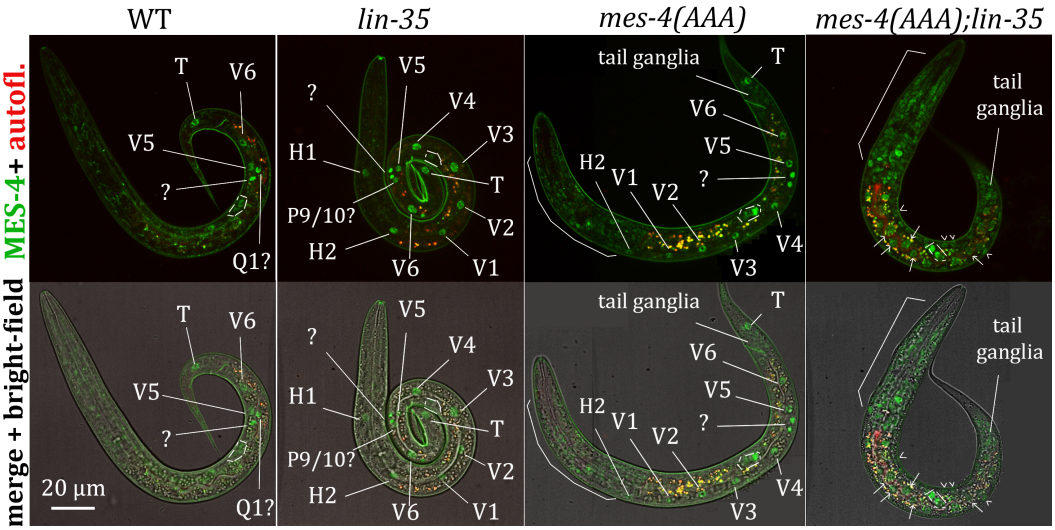

Figure 27. 3h feed L1

MES-4::GFP signal for wild type, single and double mutants. V, H, Q, P9/10 and T cells were positive for MES-4. Unidentified cells also contained MES-4 in all of the strains. Head nuclei containing MES-4 in *mes-4(AAA)* and *mes-4(AAA);lin-35* are marked with a square bracket. Additionally, tail granglia also contained MES-4 in *mes-4(AAA)* and *mes-4(AAA);lin-35* strains. Autofluorescence in the head of the wild type is observed. Arrows: intestinal nuclei. Arrowheads: additional MES-4-positive cells.

In the wild type and the mutants *lin-35* and *mes-4(AAA),* cells from V, H and T cells were positive for MES-4. MES-4 was also detected in other cells that could be Q cells and P9/10, with no appreciable differences between WT and *lin-35* strains. V, H, T, P and Q cells are precursors that would continue dividing giving rise to hypodermal cells, neurons and vulval precursor cells. On the contrary, no signal was detected in the intestinal nuclei at the times observed in the wild type or single mutants *lin-35* and *mes-4(AAA)*. Probably, it would be present at later stages, when intestinal cells start dividing. Additionally, MES-4 was detected in the head and tail ganglia of *mes-4(AAA)* mutants, similarly to the starved *mes-4(AAA)* worm. For the double mutant *mes-4(AAA);lin35*, MES-4 was maintained in all the cells of the worm (**Fig. 27**, previous page).

The data presented here suggest that MES-4 is regulated during development in a cell cycle-dependent manner. In this regulation, the crosstalk between CDK activity and the G1 inhibitors CKI-1, LIN-35 and FZR-1 would act to maintain MES-4 levels low at specific developmental times and in response to external cues, such as starvation. The importance of each regulator in each and tissue and their crosstalk needs to be assessed.

Is this cyclic presence of MES-4 in dividing cells a consequence of its regulation through cell cycle or is it playing an uncovered role in soma? Why does MES-4 need to be switch off? Further analysis of the *mes-4(AAA);lin-35* phenotypes would answer some of these questions.

4.3. mes-4 ectopic overexpression

An alternative and useful tool for answering these questions was the construction of an inducible overexpression system. This would avoid the use of mutant background that would affect also other proteins, centering on the role of MES-4 in soma. First of all, an inducible system was needed in order to allow expression of *mes-4* at the desired stage and the desired tissue. The inducible Q repressive system previously described (Wei *et al*., 2012) was modified in order to achieve a uniform expression in the worm. The modified system was tested with a GFP reporter, and later, *mes-4* was expressed.

The system was composed by two pieces, each one integrated in one chromosome. The first piece contained the repressor (QS) and the activator (QF) connected by a SL2 intergenic region. This construction was expressed under the ubiquitous promoter of *rps-27 (Prps-27)*. The piece containing the *Prps-27::QS::SL2::QF* was integrated in chromosome IV. The QUAS inducible promoter followed by a GFP reporter was integrated in chromosome II (**Fig. 28**, A, next page). Worms carrying both parts of the system were induced and analyzed in comparison with non-induced worms. The reporter was not detected before induction (**Fig. 28**, B, next page). After induction, a strong GFP signal was observed in most of somatic cells, including neurons. Striated muscle presented a strong GFP signal. GFP was not detected in the germline. These observations confirmed that the induction was effective in soma. Moreover, having both, repressor and activator under the same promoter with an SL2 region in between did not alter repression or induction.

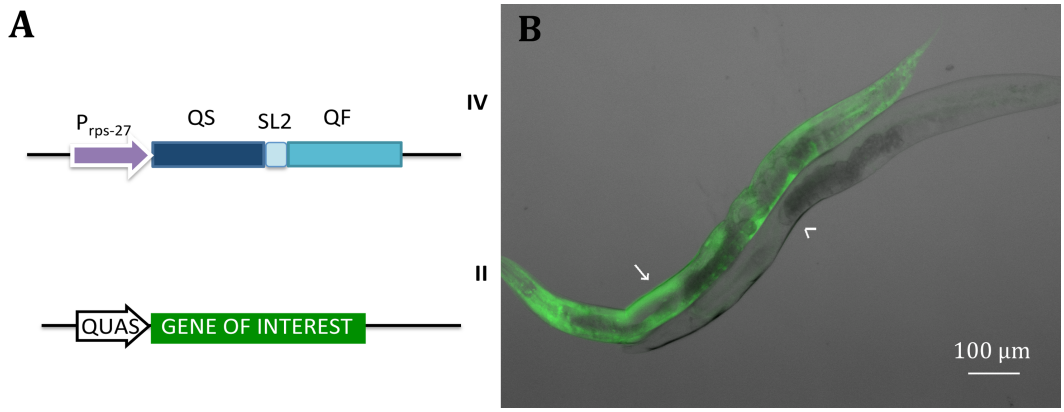

Figure 28. Q repressive system with a GFP reporter integrated in the worm

A. Scheme of both parts of the Q repressive system. The gene of interest in this case was the reporter GFP, in chromosome II, although chromosome V was also used for integration of *mes-4*. **B.** Induced (arrow) against non-induced (arrowhead) worms. 10x objective. Light field and GFP signal overlapped.

Once the system was validated, GFP was substituted by two *mes-4::mCherry* constructions. One construction contained a wild type *mes-4::mCherry* (*mes-4* WT) and the second, a KEN box mutant version of *mes-4::mCherry* (*mes-4* AAA). Both *mes-4* versions placed under the QUAS inducible promoter were integrated on chromosome V. The other part of the system used was the previously described *Prps-27::QS::SL2::QF.* Two strains carrying both parts of the system were constructed. One would overexpress *mes-4* WT, while the other would overexpress *mes-4* AAA.

After induction of both strains, low MES-4 was observed in worms overexpressing the wild type version of the gene (*mes-4* WT). On the

contrary, MES-4 was detected in seam cells, muscles and neurons of the *mes-4* AAA worms. The wild type protein MES-4 WT was observed in a few neurons in the head of the worm. In addition, when the images were overexposed, low levels of MES-4 were detected in seam cells and some neurons in the nerve cord at the L2 stage. Regarding MES-4 AAA, it was present in hypodermal and seam cells, muscles and neurons on the head and the nerve cord. Moreover, their levels were higher than for the wild type protein (**Fig. 29** A, next page). In addition, for ensuring that this was an artifact due to the promoter, *Prps-27* was changed by another ubiquitous promoter: *Peft-3*. All the four strains were tested against control and *fzr-1* RNAi, and nuclei positive for MES-4 were quantified (**Fig. 29** B, next page).

Differences were found between *fzr-1* RNAi and control RNAi for strains with MES-4 WT (p value <0.0001 with an unpaired t-test). On the contrary, no changes were detected between RNAi treatments for MES-4 AAA. However, the number of MES-4-positive cells was higher for the mutant protein than for the wild type treated with *fzr-1* RNAi. These differences could be due to the previously observed incomplete RNAi effect over all the somatic cells. Although the number of analyzed worms was low, comparable patterns and data were observed for both promoters, showing similar trends. Data and statistics can be found in Appendix III.

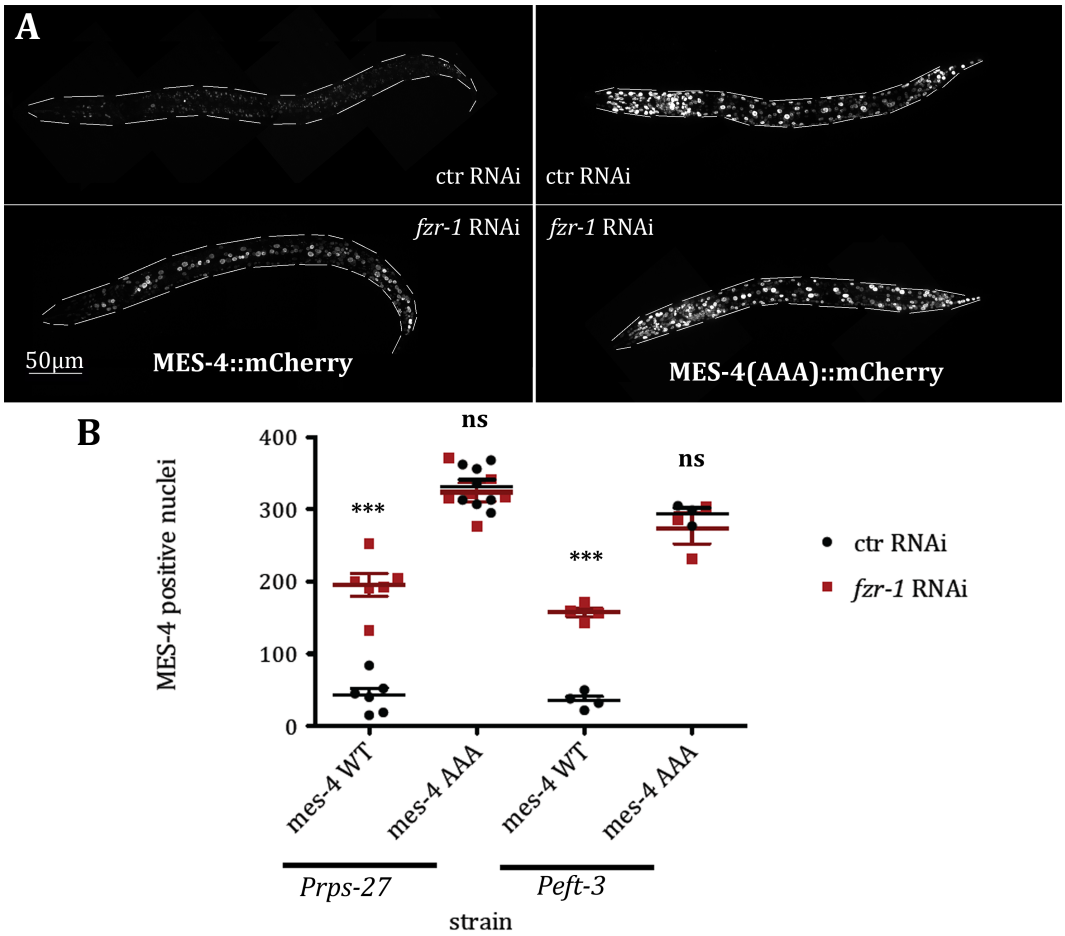

Figure 29. Ectopic *mes-4* expression and RNAi

A. L2 induced worms with MES-4::mCherry and MES-4(AAA)::mCherry treated with control and *fzr-1* RNAi. Promoter: *Prps-27.* Worm silhouette is highlighted, with the head on the left. **B.** Quantification for the strains showed in A (with *Prps-27*) and the strains with *Peft-3* promoter. ***: p value <0.0001, ns: no significant. Unpaired t-test

This inducible system bypassed the regulation at transcriptional level through LIN-35, as neither of the promoters used are regulated by LIN-35. Once induced, the strain overexpressing the mutant version of *mes-4 (mes-4* AAA) should reassemble the double mutant *mes-4(AAA); lin-35*.

Concordantly, MES-4 AAA was broadly observed in the worm. The ectopic expression of the mutant protein eliminates regulation at both, promoter and protein levels. Moreover, the levels of MES-4 in this overexpression were even higher than for the double mutants *mes-4(AAA);lin-35*. For these reasons, the strain with MES-4 AAA in somatic cells was expected to have defects in the tissues affected. However, worms induced at different times, from L1 to L4 and grown with somatic MES-4 AAA had no obvious growing or motor defects (striated muscles and neurons in the nerve cord are responsible for movement). Further experiments are needed to analyze these worms. However, this is a useful tool for analyzing MES-4 function in larval somatic cells without altering other genes.

5. DISCUSSION

The arising crosstalk between cell cycle and chromatin and its influence in plasticity needed to be studied in the context of development. In this Thesis, in order to shed light on this dynamic interaction, the histone methyltransferase MES-4/NSD was studied. Despite MES-4/NSD importance for plasticity and cell cycle maintenance in the germline, there was a gap regarding its regulation.

5.1.1. Control of MES-4 pattern in the germline by APC/C$^{FZR\text{-}1/Cdh1}$

Most of the protein expression patterns observed in the germline are driven by regulation via 3' UTRs (Merritt *et al*., 2008). Indeed, RNA machinery is highly efficient in germ cells, existing redundant RNA pathways controlling self-renewal and differentiation decisions (Brenner and Schedl, 2016; Racher and Hansen, 2012). For instance, MES-3, which acts in PRC2 opposing MES-4 action, presents a pattern analogous to MES-4, and it is negatively regulated at pachytene through GLD-1 binding to its mRNA (Xu *et al*., 2001). Opposite to the expected, we found that in the germline, MES-4 pattern seemed unaffected by this regulation at 3' UTR level. However, we have to be cautious, since recent findings showed that regulatory elements at 5' UTR can mask the effect of 3' UTR regulation (Theil *et al*., 2018). In our strains, only the 3' UTR was changed; therefore, we cannot discard some role of 5' UTR regulatory elements.

However, the pattern of a raising number of germline proteins depends on proteasome and E3 ubiquitin ligases (Burger *et al*., 2013; Gupta *et al*., 2015; Jantsch *et al*., 2007; Starostina *et al*., 2010). For instance, the

chromodomain-containing protein MRG-1/MRG15, which has been proposed to interact with MES-4, is regulated through the proteasome in the germline (Gupta *et al*., 2015; Takasaki *et al*., 2007). Both, MES-4 and MRG-1 patterns are analogous and their outcomes are very similar (Fujita *et al*., 2002; Takasaki *et al*., 2007). Accordingly, we found that MES-4 was also regulated through proteasome, although the E3 ubiquitin ligase responsible for its pattern was APC/C^{FZR-1} instead of RFP-1 as for MRG-1 (Gupta *et al*., 2015). While all indicates that MES-4 and MRG-1 may act together and should be regulated together, Takasaki *et al.* (2007) also observed that their binding to chromosomes was not dependent on each other. This could explain that their regulation, although mediated through the proteasome, depends on different E3 ubiquitin ligases.

Despite this regulation through APC/C-proteasome, for some proteins, proteasome and mRNA cooperate to achieve a correct pattern. Indeed, CYE-1, which has a similar pattern than MES-4, is regulated at mRNA level by GLD-1, and an E3 ubiquitin ligase also regulates its levels (Biedermann *et al*., 2009; Fox *et al*., 2011; Jeong *et al*., 2011). However, the E3 ubiquitin ligase sharpens the drop of CYE-1, and RNAi of this E3 ubiquitin ligase did no lead to a maintenance of CYE-1 through the gonad (Fox *et al*., 2011). On the contrary, MES-4 levels are constant through the gonads of mutants unable to be degraded by APC/C^{FZR-1} (see below). Therefore, our results strongly suggest that APC/C^{FZR-1} regulation is leading MES-4 pattern in the germline. The

presence of regulatory elements at 3' or 5' UTR remains to be elucidated, but they seem to have a minor effect in the studied conditions in the germline.

5.1.2. MES-4 is a direct target of APC/C^{FZR-1} through its KEN box

The main evidence about FZR-1-dependent regulation of MES-4 was the predicted KEN box in its sequence. This KEN box is not conserved in orthologous NDS proteins, as the first 120 residues are not conserved. However, other KEN box was predicted for NSD1 (between the amino acids 1077-1079). It is important to note that despite the existance of a KEN box in a protein sequence, there are additional factors that may contribute to its functionality. One of them is the presence of phosphorylable residues. Phosphorylation of residues adjacent to the KEN box (mainly at -1 position) have been shown to favor APC/C-dependent ubiquitination (Min *et al*., 2013). However, more distant phosphorylated residues can impede APC/C action (Mailand and Diffley, 2005). For MES-4 sequence, there are two serines at -2 and -1 positions. In addition, other potentially phosphorylable residues are present in the protein sequence. Whether if these adjacent and distant residues are phosphorylated or not and if they affect to APC/C regulation, would add new regulatory layers. On the contrary, for NSD1 KEN box, there are no -1 or -2 phosphorylable residues. However, a D-box was also predicted (2223-2226), and it could influence its functionality. If its function is conserved in NSD1 needs further investigation.

Additionally, a KEN box was predicted in the original SEC cassette at the end of the GFP construction (K) and the beginning of the TEV sequence

(EN). This SEC cassette is a valuable tool extensively used for CRISPR-Cas9 transformations in *C. elegans* (Dickinson *et al*., 2015; Koury *et al*., 2018; Perez *et al*., 2017). The presence of this KEN box had some effect although it was not as pronounced as if it was totally functional. This could be explained due to the importance of the phosphorylation of adjacent amino acids. In contrast to the KEN box in MES-4, no phosphorylable residues were adjacent to this box, although there are other phosphorylable residues in the sequence. Besides, the environment of the degron should be important, and this extra-KEN box might only be significant for proteins that are already regulated through APC/C. However, this should be taken into account when using the SEC cassettes for tagging APC/C-regulated proteins.

5.1.3. APC/C^{FZR-1} and MES-4 patterns are integrated with cell cycle regulation in the germline

In *C. elegans,* most of the FZR-1 regulation and functions are inferred from other organisms. Indeed, besides from its role in fertility (Fay *et al*., 2002), this FZR-1-dependent regulation of MES-4 is the first report for FZR-1/Cdh1 activity in the germline of the worm. All the data presented here suggest that MES-4 presence could be considered as a reporter for FZR-1 activity in the germline. This activity would be strong at the pachytene, degrading MES-4 and other proteins, while repressed at the mitotic tip, late pachytene and oocytes. We propose a model in which FZR-1 is inhibited by high CYE-1/CDK activity at the mitotic tip, in a similar way than in mammals (Keck *et al*., 2007). This is coherent with the short G1 of cycling mitotic germ

cells (Fox *et al*., 2011), and high CYE-1 presence in the tip (Brodigan *et al*., 2003; Fox *et al*., 2011) which would impede FZR-1 action at the mitotic zone. In fact, the situation at the mitotic tip is similar to the high cyclin E levels observed in some mammalian tumors in which this inhibition of FZR-1/Cdh1 is more relevant than in a normal cell cycle (Keck *et al*., 2007). Moreover, the possibility of CYE-1 acting not only with CDK-2 but also with CDK-1 previously suggested (Yoon *et al*., 2012) and supported by our results, would explain CYE-1 high levels despite cell cycle phase (Fox *et al*., 2011) and the continued repression of FZR-1.

However, extensive analysis of germline CYE-1 and cell cycle, indicated that the most distal cells of the mitotic tip had lower CYE-1 levels and slower cell cycle than germ nuclei in the middle of the mitotic zone (Chiang *et al*., 2015). Nevertheless, this is not coupled with a change in FZR-1 activity, as MES-4 is seen with the same intensity at these cells. In fact, after *cye-1* depletion, MES-4 is also maintained in the most distal cells, similarly to the reported maintenance of other proliferative markers (Fox and Schedl, 2015; Fox *et al*., 2011). For these proliferative markers, Notch signaling from the DTC has been proposed to be responsible of their maintenance after *cye-1* depletion (Fox and Schedl, 2015). In a similar way, our data suggest that FZR-1 should be inhibited in these cells by other means than CYE-1, being Notch signaling the best candidate.

Taking all this into account, in a wild type germline, Notch signaling would repress FZR-1 and meiotic markers at the most distal cells. Later, CYE-

1 starts increasing, but as Notch signaling decays, GLD-1 starts accumulating. When GLD-1 reaches a threshold, CYE-1 would drop as a consequence of GLD-1 inhibition through *cye-1* mRNA binding (Biedermann *et al*., 2009). At pachytene, SCF^{PROM-1} would decrease CYE-1 levels, sharpening this drop (Fox *et al*., 2011), and CKIs would inhibit any CYE-1/CDK activity left (Kalchhauser *et al*., 2011; Starostina *et al*., 2010). In agreement with our model, MES-4 would be high at the mitotic tip due to FZR-1 repression. This repression would be due to Notch signaling in first place. Later, CYE-1/CDK would phosphorylate and inhibit FZR-1. When CYE-1 starts dropping, FZR-1 activity would increase (dephosphorylation may occur), triggering inhibition of MES-4 and other proteins. FZR-1 would have its maximum activity at pachytene, when no CYE-1 or Notch signaling are present. CKI-1 levels at pachytene would be lower than at the transition zone, where FZR-1 activity starts increasing, consistent with the possible FZR-1-mediated regulation of CKI-1 levels previously proposed (The *et al.,* 2015). In the absence of CYE-1, Notch signaling would extend only to the cells close to the DTC, and meiotic markers would be present at the mitotic tip. Concordantly, FZR-1 extends distally, lowering MES-4 except at the most distal cells, as observed after RNAi of *cye-1/cdk* regualtors.

However, FZR-1 extension did not trigger meiosis start, as MES-4 decays before the transition zone. On one hand, this suggested that MES-4 degradation was not coupled with differentiation start in germline. Similarly, FZR-1 function in germline would not be decisive for differentiation. Actually,

in this same direction, *cye-1* RNAi is critical for differentiation only when other germline factors, such as GLP-1/Notch, are compromised (Fox *et al*., 2011).

Despite this proposed regulatory crosstalk, we cannot discard additional mechanisms. For instance, CYD-1/CDK-4 can also inhibit FZR-1 activity in mammals and worms (The *et al*., 2015; Wan *et al*., 2017), and could be the reason of this retained MES-4 at the tip. Although, CYD-1/CDK-4 role in germline seems to be minor (Fox *et al*., 2011), double depletion of both, CYE-1 and CYD-1 could answer this question. However, all the evidences indicate that CYE-1 plays the major role in cell cycle progression in the germline mitotic zone.

When germ cells reach the late pachytene, CYE-1 levels start increasing (Brodigan *et al*., 2003), coinciding with a decrease of FZR-1 activity. However, in *cye-1, cdk-2* and *cdk-1* RNAi-treated worms, MES-4 presence at late pachytene and oocytes was not altered, indicating that there should be no FZR-1 activity at these zones. Consequently, at this part of the gonad, FZR-1 regulation might be independent on *cye-1*. However, the detected drop in FZR-1 activity could be due to an inhibition of gene or protein production, an increase in protein degradation or an inhibition of its activity. How is this drop in activity is achieved is a question to be answered.

Interestingly, there is a mitogen-activated protein kinase (MAPK) implied in signaling pathways at late pachytene and oocytes: MPK-1/ERK (Lee *et al*., 2007b). It seems to be implied in phosphorylation of GLD-1,

targeting it for SCF-mediated degradation at late pachytene (Kisielnicka *et al*., 2018). Moreover, in human fibroblasts, FZR1 is a direct target of ERK (Wan *et al*., 2017). Therefore, we hypothesize that MPK-1/ERK could be implied in a similar way in lowering FZR-1 levels at late pachytene in the hermaphrodite germline.

Another interesting and unexplored question is if this regulation is taking place in the male germline. Generally, regulatory pathways for hermaphrodites and males are very similar, but there are some known differences. The first one is the more rapid cell cycle in the male germline (Morgan *et al*., 2010). In addition, MKP-1/ERK regulation acts at the transition zone and early pachytene in males, in comparison with its activity at late pachytene and oocytes in hermaphrodite germlines (Lee *et al*., 2007a). It would be interesting to explore how these differences affect FZR-1 and MES-4. Comparison of MES-4 patterns between both germlines would give clues about MPK-1/ERK conserved roles in these events.

5.1.4. APC/C^{FZR-1} possible roles in the germline

Although FZR-1 seems not to be crucial for meiosis start, its pattern seems to be highly regulated. Moreover, FZR-1 total depletion from the germline through injected RNAi drives to worms with defective or without oocytes and sperm (Fay *et al*., 2002). However, this role is not through MES-4 inhibition. Actually, in the MES-4 KEN box mutant with extended MES-4 through pachytene, no defects in fertility were detected. This suggests that FZR-1 has other important targets in the germline and plays a key role in its

development. One possible target is HIM-18/SLX4 (Saito *et al*., 2009). This endonuclease is important for correctly solving homologous recombination (HR) intermediates in the mitosis and meiosis. HR in the germline takes place mainly at the pachytene zone, where planned double strand breaks (DBS) occur (Hayashi *et al*., 2007). HIM-18 has a pattern similar to MES-4, being present at the mitotic tip, decreasing at the transition zone and increasing at late pachytene. Indeed, Saito *et al* (2009) suggested that HIM-18/SLX4 was a possible APC/C substrate due to the presence of a D-box. The study of this possible interplay would shed light on FZR-1 functions and additional targets in the germline.

Mammalian APC/C^{Cdh1} has been reported to favor the repair of DBS by HR (Ha *et al*., 2017). Interestingly, in *C. elegans* germline, HR is always the chosen repair pathway, while decisions between different repairing pathways are thought to take place in somatic cells (Pontier and Tijsterman, 2009). However, HR prevalence in the germline is not due to the inexistence of other mechanisms. For instance, some mutants in components of the synaptonemal complex can repair DSB at pachytene through non-homologous end joining (NHEJ) (Smolikov *et al*., 2007). Although it is tempting to hypothesize that FZR-1 could be involved on these decisions at the germline pachytene, no orthologous for a key target in this choice (USP1) is found in *C. elegans*. However, alternative pathways may exist. Studying why HR is the only choice in germline and if it is achieved through FZR-1 and

alternative mechanisms could reveal if this function is conserved in the worm.

5.1.5. Implications of MES-4 extension in the germline

MES-4 levels drops at pachytene in a wild type background. However, the maintenance of MES-4 during pachytene seems to have no effect on fertility in the worms, as the specific KEN box mutant *mes-4(AAA)* was apparently wild type. Despite this apparent normality, the maintenance of high MES-4 levels through the germline would probably lead to an increased H3K36 di- and trimethylation at the transition zone and pachytene. These marks are important regulators of DNA repair and maintenance of genomic integrity in mammals and worms (Amendola *et al*., 2017; Pfister *et al*., 2014). For instance, both H3K36 HMTs of the worm (MET-1/SETD2 and MES-4/NSD) are necessary for the activation of the synapsis checkpoint (Lamelza and Bhalla, 2012). This suggests that an imbalance in H3K36 methylation levels would affect fertility. Concordantly, mutants of the H3K36me2 demethylase JMJD-5/KDM8 show an increase of this mark and a reduction of fertility after few generations growing at 25°C (Amendola *et al*., 2017). The discordance with the apparent normality of the *mes-4(AAA)* strain could be due to the different temperature, as we conducted this fertility assays at 20°C.

In addition, although MET-1 protein pattern has not been reported, it cooperates with MES-4 in chromosome stability. Possibly, they would have a similar pattern. Indeed, MET-1 has two predicted KEN boxes (residues: 33-

35, 587-589) and one predicted D-box (1164-1167). Moreover, its mammalian orthologous SETD2 is controlled through cell cycle by APC/C^{Cdh1} (Dronamraju *et al*., 2017), and SETD2-dependent trimethylation of H3K36 is essential for HR and maintenance of genomic integrity (Pfister *et al*., 2014). This data suggest that MET-1 could have a similar regulation through ACP/C.

Taking all this into account, lowering H3K36 methylation levels seems to be important for the germline. Further analysis of the KEN box mutant and differences in H3K36 methylation would be needed to gain insights into the significance of MES-4 drop in the germline, its regulation through FZR-1 and the interplay with MET-1.

5.1.6. LIN-35 and APC/C^{FZR-1} are the main controls of MES-4 during development

After the first cell division in the embryo, the germline P lineage is separated from the soma. The P lineage inherits germline-specific components, like the P granules. However, MES-4 distribution is not restricted to the germ lineage until later in development (Bender *et al*., 2006). We show that this restriction consists on an accumulation of MES-4 at PGCs, and an inhibition at transcriptional and protein levels through LIN-35 and FZR-1. The origin of the accumulation of MES-4 at PGCs is currently unknown, as PGCs are transcriptionally inactive before hatching (Wang *et al*., 2011). Nevertheless, the pattern of MRG-1/MRG15 in the embryo is similar, with an accumulation of MRG-1 at PGCs and disappearance in somatic cells during development. This accumulation of MRG-1 is dependent on mRNA

mechanisms (Miwa *et al*., 2015), suggesting that the role of MES-4 UTRs could gain importance for the differential distribution of *mes-4* mRNA between soma and germline.

Besides this possible control, our data suggest that somatic cells regulate MES-4 levels through cell cycle during development. This regulation depends on LIN-35 and FZR-1 dynamics. However, the importance of each regulator varies through development and amongst tissues. FZR-1 regulation seems to be more important during embryonic development than LIN-35, while at the L4 stage their importance is apparently switched. In the embryo, the activity of FZR-1 at the analyzed times would possibly eliminate the excess of MES-4 despite the increased transcription of *mes-4* in *lin-35* mutants. Regarding larvae, both regulators cooperate to achieve the correct MES-4 pattern. Using a GFP::FZR-1 reporter The *et al.* (2015) showed a high FZR-1 presence in the intestine and other tissues in early and starved larvae, including some neurons in the head. The presence of LIN-35::GFP reporter seemed to increase in the intestine at later stages during development (The et al., 2015). Although the presence of these proteins is not always reporter of their activity, this could explain this switch in importance of these regulators at the L4 stage. Analysis of specific lineages and times during embryo and larval developments would shed light on the role of each regulator on MES-4 distribution depending on the stage and lineage.

Curiously, an important S-phase protein from the pre-replication complex, MCM-4/MCM4, is controlled in a similar way by LIN-35 and FZR-1

(Kirienko and Fay, 2007; The *et al*., 2015). MCM-4 was observed in blast cells of feed L1s after 5-7 hours of development (depending on the cell type) (Korzelius *et al*., 2011). However, MES-4 staining was present in some of these blast cells only after 3 hours at the same temperature. This divergence in time between MCM-4 and MES-4 appearance are probably due to experimental procedures. However, the similar patterns and regulation for both proteins opens the possibility of a MES-4-dependent chromatin regulation on *mcm-4* locus. Further study of this difference using one strain with both tagged proteins would allow a more accurate comparison.

Additionally, MES-4 was not present in starved worms except for the PGCs and Q cells. In a similar way, MCM-4 was not detected in starved worms, (Korzelius *et al*., 2011), as expected because cells were not dividing. PGCs are stopped in cell cycle at G2 (Fukuyama *et al*., 2006), with no presumable FZR-1 activity, explaining the maintenance of MES-4. Moreover, PGCs are transcriptionally silent during starvation (Demoinet *et al*., 2017), therefore, no MCM-4 would be produced. On the other hand, Q cells divide short after hatching (4-5 hours) (Sulston and Horvitz, 1977). Indeed, MCM-4 is detected after 5 hour in Q cells descendants (Korzelius et al., 2011). The maintenance of MES-4 during starvation could allow the expression of MCM-4 shortly after feeding, and the rapid division of these cells. Additional experiments would be needed to assess the presence and the importance of MES-4 maintenance in other unidentified cells.

In the seam cells, *cki-1* high transcription during starvation would lead to some CKI-1 protein present in starved cells, inhibiting CDK-cyclin activity (Baugh and Sternberg, 2006) and allowing the repressive action of FZR-1. Although CKI-1 levels seem to be controlled by FZR-1 (The *et al.,* 2015), other mediators might act in CKI-1 regulation. The additional action of LIN-35 in these cells would lead to the observed repression in both mutants.

Taking all these results together, MCM-4 and MES-4 presence in the cells seems to be highly dynamic. It changes through development and amongst tissues in a cell cycle-dependent manner. In addition, both proteins respond to external conditions, allowing the adaptation of the worm to the environment. The significance of MCM-4 dynamic regulation is evident, as it is a cell cycle protein. The importance of MES-4 dynamic regulation remains to be discovered, and suggests that MES-4 has unknown roles in the soma.

Due to the function of MES-4 as a H3K36 HMT, and the existence of a second H3K36 HMT MET-1, MES-4 function in soma is not clear. Moreover, 95% of the H3K36me3 of the worm disappears in *met-1* mutants (quoted in (Ahringer and Gasser, 2018). In addition, MES-4 seems to have no *de novo* activity (Furuhashi *et al*., 2010), and it has been proposed to bind H3K36 methylation deposited by MET-1 or to interact with MRG-1 (Rechtsteiner *et al*., 2010). Interestingly, during wild type development, MES-4 is still bound to germline-expressed genes in somatic cells. This includes those genes specific for germline (like P-granules components) and ubiquitous genes (such as cell cycle or housekeeping genes). Both classes exhibit high MES-4

and high H3K36 methylation (Rechtsteiner *et al*., 2010). However, RNA pol II is low on the germline-specific genes, while it is high on the ubiquitously expressed (Rechtsteiner *et al*., 2010). These data indicate that despite the presence of MES-4 in germline-specific loci, they are being repressed in the soma of the developing embryo.

Feasibly, in somatic cells of the embryo, MES-4 could be marking for both, allowance of rapid activation when needed of ubiquitous genes, or gene silencing of germline-specific genes. We propose that the gene silencing of germline-specific genes would be mainly through DRM/DREAM although other repressors cannot be discarded. This hypothesis would be consistent with the misexpression of germline factors observed in mutants of the DRM complex or the NuRD/Mi2 amongst others (Unhavaithaya *et al*., 2002; Wu *et al*., 2012). Regarding the DRM, the MuvB subcomplex has the inhibitory activity (Goetsch *et al*., 2017). In the germline, EFL-1 and DPL-1 are found in some expressed genes with MES-4 bound (Tabuchi *et al*., 2011), acting as transcriptional activators. In addition, LIN-53/RBAP48 is part the repressive MuvB subcomplex and has been shown to be able to repress some genes on its own (Goetsch *et al*., 2017). However, it is not generally bound to DNA in the germline (Tabuchi *et al*., 2011). This is probably due to the low LIN-35 binding in this tissue (Kudron *et al*., 2013), that would destabilize the complex (Goetsch *et al*., 2017). If no LIN-35 is present, the entire DRM complex would not be present at these loci and no repression is observed. However, some of these genes would be marked with components of the

DRM/DREAM. As cells switch to a somatic fate, LIN-35 would start binding the loci where EFL-1/DPL-1 and LIN-54 are already present, enabling the recruitment of the rest of the DRM, and repressing those genes. This hypothesis would also explain the observed overlap of LIN-35 and MES-4 targets (Wu *et al*., 2012). If these negative regulators were not present, H3K36me and the already present activators EFL-1/DPL-1 would lead to misexpression of MES-4 target genes. RNAi of *mes-4* in these mutants would impair the maintenance of transcriptionally active chromatin on MES-4 targets, and the phenotype would be reverted.

In the wild type, at each round of division, cell cycle regulators would lower MES-4 levels, until being almost undetectable in soma. Therefore, before hatching, all the germline-specific genes would be silenced. In larvae PGCs, which are transcriptionally inactive (Schaner *et al*., 2003), MES-4 has been proposed to act inhibiting expression of germline genes (Rechtsteiner *et al*., 2010), although the mechanisms are unknown. Probably, it could interact with other chromatin regulators for lowering the activating marks H3K4me and H4K8ac, known to be absent from PGCs (Schaner *et al*., 2003). Regarding larvae soma, probably, H3K36 methylation dependent on MES-4 is only maintained on those genes expressed in both, germline and soma: mainly the cell cycle-related genes and housekeeping genes. In addition, PRC2 could be possibly regulated in a similar way. For instance, in mammalian cells, Enhancer of Zeste Homolog 2 (EZH2)/MES-2 is negative regulated through Akt, CDK1 and AMPK phosphorylation (Cha *et al*., 2005; Chen *et al*., 2010;

Wan *et al*., 2018). In addition, Rb also regulates its expression (Bracken *et al*., 2003). PRC2 is also essential for establishing and maintaining the germline chromatin. Consequently, a cell cycle-dependent of MES-4 and PRC2 regulation would allow the progressive change from a germline chromatin landscape to a somatic landscape.

5.1.7. Crosstalk between chromatin, plasticity and cell cycle

During development, chromatin changes allow variations in gene expression. These transcriptional changes also occur through cell cycle, therefore, chromatin-modifying enzymes must be as dynamic as other cell cycle proteins in order to allow these changes. This dynamism enables adaptation to cell cycle and environmental signals. Concordantly, this regulation is not restricted to MES-4 or EZH2. Moreover, SETD2 from mammals and PR-Set7 from *Drosophila* are regulated dependent on cell cycle through different E3 ubiquitin ligases (Dronamraju *et al*., 2017; Zouaz *et al*., 2018). Interestingly, all these chromatin-modifying enzymes have also non-canonical functions. EZH2 has other targets than H3K27 (Cha *et al*., 2005), as well PR-Set7 and NSD proteins have non-canonical targets (Morishita and di Luccio, 2011; Zouaz *et al*., 2018). The high regulation of these HMTs could be not only due to the importance of chromatin landscape, but also to their non-histone targets. For instance, EZH2 (MES-2) is essential for methylation and inhibition of the transcription factor GATA4 (He *et al*., 2012). Although NSD1 methylation of non-histone proteins is controversial (Kudithipudi *et al*.,

2014; Lu *et al*., 2010), studying this possibility for its orthologous MES-4 could shed light on novel MES-4 functions.

The fact that MES-4 is present in stem cells in the gonad, in the embryo and dividing blastomeres in the larvae could indicate that these cells should have some expressed genes in common. Some of these genes are probably cell cycle genes, such as *mcm-4.* Moreover, this regulation through LIN-35/Rb and APC/$C^{FZR\text{-}1/Cdh1}$ is probably taking place for eliminating other plasticity markers.

Coordination of cell cycle, chromatin and differentiation is needed. The crosstalk established for allowing their coordination is more complex than thought. Components of all of them (cell cycle, chromatin and differentiation) can influence each other, in most cases, directly. Moreover, external signals can influence chromatin, cell cycle or differentiation. Consequently, alteration in either, external and internal factors might modify this finely regulated interplay, leading to disease. Extended study of the connections between chromatin, differentiation and cell cycle, and possible direct targets of chromatin modifying enzymes over cell cycle or differentiation factors would raise new therapy possibilities.

6. CONCLUSIONS

1. MES-4 is a direct target of APC/C^{FZR-1} through its KEN box.

2. APC/C^{FZR-1}-mediated degradation drives MES-4 pattern in the germline, with no detected contribution of UTRs.

3. In soma, both G1 inhibitors LIN-35 and APC/C^{FZR-1} control MES-4. This regulation enables a finely control of MES-4 protein levels.

4. LIN-35 and APC/C^{FZR-1} activity on MES-4 seems to be tissue-specific, and this specificity changes throughout development. FZR-1 would be more important during early development, while LIN-35 importance would increase at later stages.

5. The regulation of MES-4 through cell cycle could integrate external signals with chromatin changes.

APPENDIX I –ANATOMY

Considering the worm as a tube, the outer layer would be the body wall, while the inside is the pseudocoelom.

Body wall

The body wall is primarily conformed by the epithelium protected by a collagen cover (cuticle) (Johnstone, 1994). It is composed by a main hypodermal syncytium that covers most of the body of the worm, six small syncytia and three more hypodermal cells around the tail and head. At hatch, two almost symmetric lateral lines of cells interrupt the hypodermis. These are seam cells (hypodermal precursors) and P cells (precursors of the neurons of the ventral nerve cord and the vulval precursor cells- VPCs). Each line contains two seam cells in the head are named H1 and H2. They are followed by V1 to V6 in the body accompanied by a P cell. The last one is the T cell at the tail. Their big nuclei and nucleoli and their position make them distinguishable (**Fig. I**, next page). These cells divide asymmetrically at each molt as stem cells, except for the second molt, that they divide twice: one symmetrically and one asymmetrically. Asymmetrical divisions give rise to one hypodermal cell that fuses to the existing syncytium and a new seam cell. At the last molt, all seam cells exit cell cycle and fuse to form a syncytium, differentiating (Gendreau *et al*., 1994; Sulston and Horvitz, 1977). Seam cells are important for cuticle renovation at each stage and for correct *alae* formation (strip of cuticular crests that extends along the worm) (Thein *et al*., 2003).

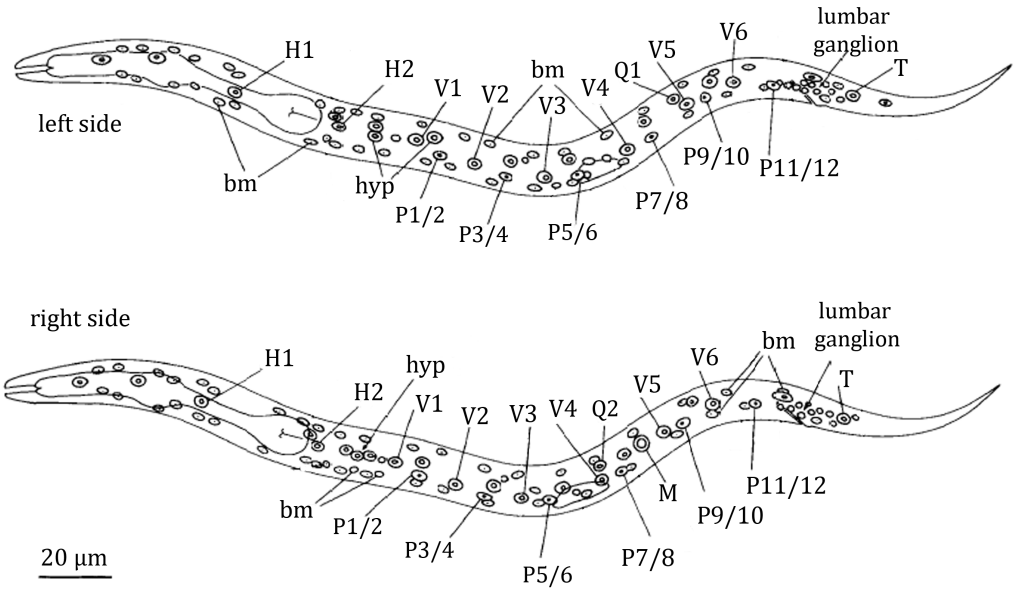

Figure I. L1 larvae lateral views

Simplified from (Sulston and Horvitz, 1977). Precursor cells are shown in the image: H, V, T, P and M. Additionally, body muscles (bm) and hypodermal nuclei from the syncitium are shown (hyp). Lumbar ganglion in the tail also pointe out. Note right-left assymetry.

Both neuroblasts (Q1 and Q2) would divide and migrate early during development. Their neuronal progeny are distributed along the body of the worm (reviewed in (Middelkoop and Korswagen, 2014)). In addition M lineage arises from the M cell (mesoblast) (Sulston and Horvitz, 1977). During larval development, the M cell would give rise to body muscles, muscles of the vulva and coelomycetes (macrophages of the worm distributed through the body).

Although most of the neurons are inside the pseudocoelom grouped in ganglia in the head and the tail, there is a row of neurons in the body wall: the ventral nerve cord (VNC). They are derived from P cells. These cells are situated dorsally near the seam cells, and migrate to the ventral part of the worm at the middle L1. These neurons extend their processes either circumferentially to the dorsal nerve cord (DNC) or longitudinally (White *et al.*, 1986). There are also sensory neurons whose processes run near the epithelium (Chalfie *et al.*, 1985). Processes of VNC and sensory neurons are grouped in the nerve ring, around the pharynx (White *et al.*, 1986).

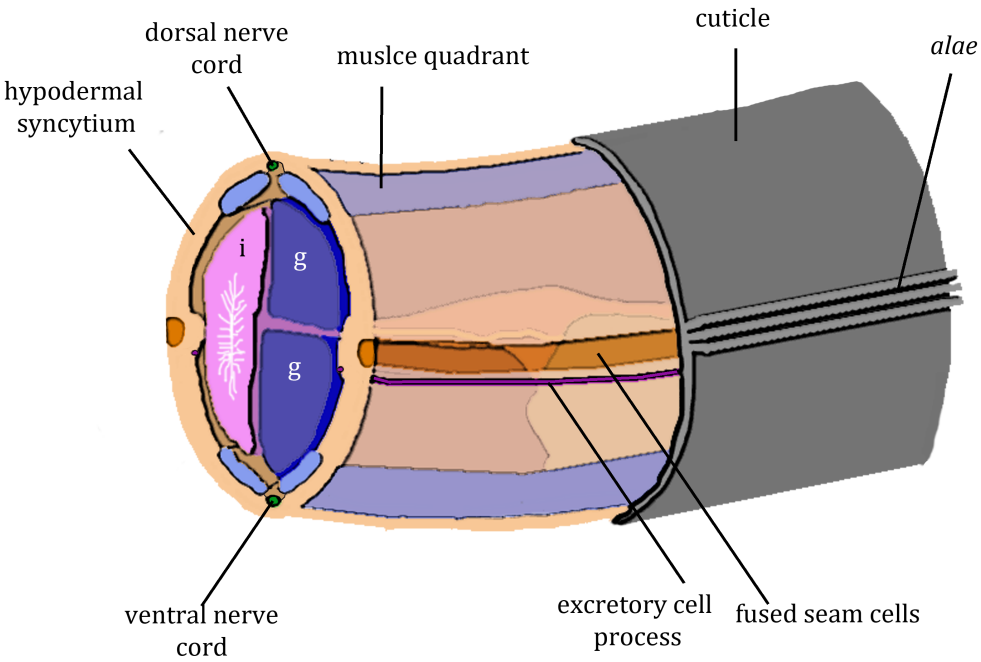

Figure II. Cross section of an adult hermaphrodite

Cuticle covers the body. Flesh color and orange for the hypodermal and seam cell's syncytium respectively. The syncytium is located under the *alae.* Muscle quadrants are shown in light purple. Nerve cords are green. Processes of excretory cell (pink) are at both sides of the tuve. Inside, the intestine (i) and a gonad arm (g).

Four quadrants of muscle strips are situated near the epidermis (**Fig. II,** previous page). They are separated from epidermis and neurons by a basal lamina. In order to receive nervous signals, muscle cells send muscle arms to motor neurons (Sulston and Horvitz, 1977).

Pseudocoelom

This cavity is filled with fluid, and it is not fully lined by mesodermal cells. The alimentary, reproductive and excretory systems are in this space.

The food enters to the organism through the pharynx and passes to the intestine. The movement of ingested food is due to pharynx pumping, as intestine is not innerved (Sulston *et al*., 1983). On the contrary, most of the neurons of the worm are found around the pharynx, in the head ganglia (**Fig.III**) and in the tail (White *et al*., 1986). Microvilli at the gut lumen absorb nutrients. The contents of the intestine are regularly excreted through the rectal valve, which ends at the anus (Thomas, 1990).

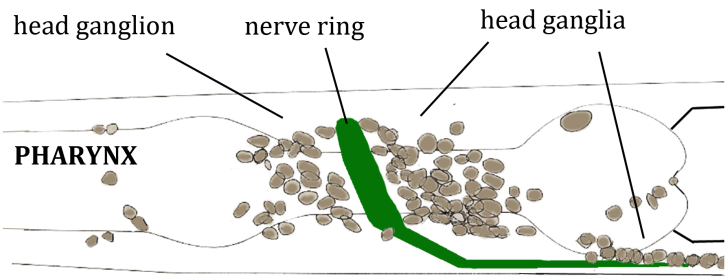

Figure III. Scheme of the head ganglia

Modifyed from (White et al., 1986). Ganglia in the head, near the nerve ring in the pharynx are represented.

Four cells situated in the head form excretory system. However, there are two cell projections that extend along the body, close to the epidermis (see previous page). This is an H-shape system that opens to the outside through the excretory pore. The excretory system is important for waste disposal and osmoregulation of the whole organism. (Nelson and Riddle, 1984)

Finally, the reproductive system is also found in the pseudocoelom. It is detailed in the Introduction.

APPENDIX II –PRIMERS

Table I. Primers for RT-PCR

name	sequence
RT-act1-1	GTCGGTATGGGACAGAAGGA
RT-act1-2	GCTTCAGTGAGGAGGACTGG
RT-mcherry1	GCAAGACTCAAGCCTCCAAG
RT-mcherry2	TTGTCTTCACCTCAGCATCG

Table II. Primers for sgRNA, and templates for *mes-4* tagging

name	sequence	comments
MES4 sg-1	TTTTGTCTCTTTTTGAACTCAAACATTTAGATTTGCAATTCAATTAT	sgRNA in combination with: + CRSP-3 + CRSP-4
MES4 sg-2	GAGTTCAAAAAGAGACAAAAGTTTTAGAGCTAGAAATAGCAAGTTAA	
TEV sg-1	gagaatctgtactttcaatcGTTTTAGAGCTAGAAATAGCAAGTTAA	sgRNA in combination with: + CRSP-3 + CRSP-4
TEV sg-2	gattgaaagtacagattctcAAACATTTAGATTTGCAATTCAATTAT	
CRSP-3	AGTGAATTCCTCCAAGAACTCGTACAAAAATGC	sgRNA in combination with: MES4 sg /TEV sg
CRSP-4	GCCAAGCTTCACAGCCGACTATGTTTGGCGTCG	
MES4-cherry2	ACGTTTAAACCAAAGAAGGCAGTTTATATGATA	1.24 kb of *mes-4* last exon
MES4-cherry3	TTGGCCATCTAGGCCAATCGGTTCAAATCGCTTTGTCTCTTTTTGAACTCGTCCA	
MES4-cherry4	TCTGGCCTGAGTGGCCAAAGTGAAATAATATGCTGTCTCGCCCAA	1.26 kb of *mes-4* 3'UTR
MES4-cherry5	TCGTTTAAACAAAATACCGAAGATCGTGACGAG	

Table II cont. Primers for sgRNA, and templates for *mes-4* tagging

name	sequence	comments
Cherry-1	AGCGGCCTAGCTGGCCAAATGGTCTCAAAGGGT GAAGAAGATAAC	mCherry amplification from pCJF90
Cherry-2	GCATGGCCACTACTTATACAATTCATCCATGCCA CC	
tbb2Sbf-1	ACTCCTGCAGGGATAAATGCAAAATCCTTTCAA GCATT	*tbb-2utr* amplification
tbb2Sbf-2	TGACCTGCAGGAAGCTTGAGACTTTTTTCTTGG CGGCACAATA	
AbRNot-1	ACGCGGCCGCCTGCAGGGCCCATTTCTAAATTT TAGTTTAA	hygromycin resistance (SbfI site for tbb-2 introduction)
AbRNot-2	GTGCGGCCGCGAAACAGTTATGTTTGGTATATT GGGA	
MES4KATE-1	ACGTTGTAAAACGACGGCCAGTCGCCGGCAAAA CCAAAGAAGGCAGTTTATATGATA	1.32 kb left arm for Gibson assembly for GFP
MES4KATE-2	CATCGATGCTCCTGAGGCTCCCGATGCTCCAATC GGTTCAAATCGCTTTGTCTCTTTTTG	
MES4KATE-3	CGTGATTACAAGGATGACGATGACAAGAGAAAA GTGAAATAATATGCTGTCTCGCCC	1.32 kb right arm for Gibson assembly for GFP
MES4KATE-4	GGAAACAGCTATGACCATGTTATGGATTTCAAA CAAAATACCGAAGATCGTGACGAG	
TEV (SacI) fwd	gacgagctctacAAGgtaagtttaaaATAACTTCGTATA	TEV site mutation
TEV (BstXI) rev	CATACCATAAGAGTGGCGACAGTGACC	

Table III. Primers for checking *mes-4* tagging and mutations

NAME	SEQUENCE	COMMENTS
MES4-cherry1	CCAACGCTGCATCTTTCGTTACAA AAGTGT	forward primer for checking the left edge insertion
cherry-LIN REV	GTTATCTTCTTCACCCTTTGAGAC CAT	mCherry tagging: +MES4-cherry1: 1.6 kb
GFP rev SEC	AGTGAACAATTCTTCTCCTTTACT CAT	GFP tagging: +MES4-cherry1: 1.4 kb

Table III cont. Primers for checking *mes-4* tagging and mutations

name	sequence	comments
MES4-cherry6	TTTCTACGAATTTTCAATACTGAGAATGAG	reverse primer for checking the right edge insertion and SEC excision
HYGRO 1	GGATCCAATTACTCTTCAACATCCCTACAT	+MES4-cherry6: right edge insertion checking for both tags
GFP utr DIR	GGAATCACCCACGGAATGGACGAGCTC	+MES4-cherry6: SEC: ----- excision: 1.6 kb
n4760F	TCGACATCAAAATCCGGCTTTGTGACGTCC	*lin-35+*: 1.6 kb *lin-35(n4760)*: 1.0 kb
n4760R	ATACGTCTTAATGCGATTATAATTAACTTC	
GFP(TEV)DIR	ATGAGTAAAGGAGAAGAATTGTTCACT	checking mGFP *versus* GFP+TEV. *BspEI* digestion: GFP: 0.84 + 0.51 + 0.01 pb GFPm: 1.32 + 0.01 pb
MES4UTR-2	ATCCTGCAGGTAATTTGCAAAGGTATTTATTACAGAT	

Table IV. RNAi primers

RNAi	primers		comments
control	-------	-------	Addgene #1654
pas-4	GGGAAATCAATACACACGGATAA	TCGTGCTATCACTATCTTCTCCC	Arhinger's library
pas-5	CGACTATCCCACCTCTTCCA	GTGCGGACGTATTGAATGTG	Arhinger's library
pbs-4	TTGTTTTCATGCCTTTTCAAGAT	GAAAACTGGGAGAAAAGTCACAA	Arhinger's library
pbs-5	GGATCGGATCAGACATCAAATAC	TCAGAATCGAACTCCAAAGATGT	Arhinger's library
pbs-6	GGACGCCGAAATGTAGTCAT	ATTTGAACGCGCAGAAAACT	Arhinger's library
pbs-7	AACATGGAGATACTGAAACGCAT	TCATTGTCGAAATTCACTTCCTT	Arhinger's library
fzy-1	TGTCACAATTGGGTTGCAGT	TCGACGTTGAACAATTGGAA	Arhinger's library
fzr-1	fzr1-1 ACAGGATCCATGGATGAGCAGCAACCGCCAGCC	fzr1-2 TAGAAGCTTCTCGTAACATCAATAATTCCTTCG	constructed
cye-1	AAACGAGACGAAATTCCACG	TGAATCCTCTCTCGTTCGCT	Arhinger's library
cdk-2	cdk2-1 ATCGGTCCGATGAGCCGAGAGATTCGGTCACTCGAA	cdk2-2 ATCGGACCGGCGAAGATTGACTTCTCCTGATGATTGT	constructed
cdk-1	CTCAAAGAGCTCCAGCATCC	CACGGAAGACGATAGGTGGT	Arhinger's library

Table V. Primers for ectopic expression by the QS inducible system

name	sequence	comments
QUAS DIR	ATGGCCACTCAGGCCTATCATGCGGATCCGGGTAATCGCTTAT	QUAS promoter amplification
QUAS REV	TATTAATTAACCTGAAAATGTTCTATGTTATGTTAGT	

Table V cont. Primers for ectopic expression by the QS inducible system

name	sequence	comments
1MES4	AATACTAGTATGCTGCCGAGCTCTGGTGAGTTTAAA	
2MES4	AATTGTTATCGAAACATTCAAATCTCG	
3MES4	TCCGCGCTTTCCATTTGACGTCGTGTT	
4MES4	CTTTGCCAACGAAAAGTAATTCTTGGT	
5MES4	AACCTCTCATGTCAATTGTGCCGGTCT	*mes-4* amplification (with introns)
6MES4	ACGATTATGACAAACGCCCTTTTTCGA	
7MES4	GTCAATATCTCGCCGATGATTATGAAT	
8MES4	TCAAAATGTTGAAACTTAGAAAAAAAG	
9MES4	AATCTGTAAAAAATCAGAATAGAAAGA	
10MES4	AATGGTACCTCAAATCGGTTCAAACCGTTTTGTCTC	
MES4(AAA) DIR	GACTCCAGCgccgctgccTGTGCTCCACAGGACGGTATCGTTGAG	KEN box mutation. Used with QUAS DIR and 2MES4
MES4(AAA) REV	GGAGCACaggcagcggcGCTGGAGTCACctggaattcgatgcat	
tbb2-1	ATAGAGCTCGGATCCGATAAATGCAAAATCCTTTCAAGCATT	*tbb-2*$^{3'UTR}$ amplification
tbb2-2	TCGACGCGTTAATTAACTAGTAGACTTTTTTCTTGGCGGCA	
SL2 Kpn	TGAGGTACCGCTGTCTCATCCTACTTTCAG	SL2 amplification for QS system
SL2 Sac	GCGGAGCTCGCTAGCGATGCGTTGAAGCAGTTTCCCTGAATT	
QF Fwd	ATGCCGCCTAAACGCAAGACACTCAAT	QF amplification
QF Rev	CTATTGCTCATACGTGTTGATATCGCT	

Table IV. Primers for specific MosSCI insertions

name	sequence	comments
MosL II OUT	GTTTACAGAAAGACATTTGAGAATGGC	Insertion chrII MosSCI/ MosSCI Universal: 1.6 kb
MosL IN	ATAATAAACATTTTATCCGTTAACAAT	
QS Fwd	ATGAACACCATCCCGGCACGCCATGTC	Promoter: 0.4 kb
QS rev check	TCAAGATATTTGCGTTGCAATTCCGTT	
QUAS (Sfi) DIR	ATggccactcaggcctATCATGCGGATCCGGG TAATCGCTTAT	Gene of interest (*mes-4*): 1.4 kb
2 MES4	AATTGTTATCGAAACATTCAAATCTCG	
oCF1491	GTCACTCAAACCGATGCAGA	Universal MosSCI chr IV insertion:--- WT/no insertion: 0.4kb
oCF1492	GCAATTTCGGCAATTTCAGT	
ttTi5605 Fwd	TTTCTCAGTTGTGATACGGTTTTT	MosSCI chr II insertion: --- WT/no insertion: 0.4kb
ttTi5605 Rev	CGCTACTTACCGGAAACCAA	

APPENDIX III –STATISTICS

I. Fertility assays for both tagged strains against wild type N2

Table I. Data and summary of fertility assay

N2		*mes-4::GFP*		*mes-4::mCherry*	
25°C	20°C	25°C	20°C	25°C	20°C
168	201	160	214	161	241
168	223	109	247	159	219
176	189	147	212	149	191
163	205	89	159	143	211
145	317	111	259	185	264
110	194	196	297	189	230
136	214	172	216	184	282
135	294	135	177	185	251
89	264	93	298	213	286
139	145	152	307	126	275
152	300	123	246	164	279
114	303	208	274	84	299
165	213	180	217	163	272
212	301	190	-------	174	-------
176	249	-------	-------	-------	-------
n	15	15	14	13	14	13
Mean	**161.13**	**230.07**	**147.50**	**240.23**	**162.79**	**253.85**
SD	37.69	22.23	38.84	46.37	31.54	33.07
SEM	9.73	5.74	10.38	12.86	8.43	9.17

Table II. D'Agostino & Pearson omnibus normality test

	N2		*mes-4::GFP*		*mes-4::mCherry*	
	25°C	20°C	25°C	20°C	25°C	20°C
K2	0.3190	1.6640	1.8110	0.5046	5.7920	1.2480
p value	0.8526	0.4352	0.4043	0.7770	0.0553	0.5358
Passed normality test (α=0.05)?	Yes	Yes	Yes	Yes	Yes	Yes
p value summary	ns	ns	ns	ns	ns	ns

Table III. ANOVA analysis

Source of Variation	% of total variation	p value	p value summary	Significant?
Interaction	0.04	0.9613	ns	No
Strain	1.54	0.2566	ns	No
Temperature	56.39	< 0.0001	***	Yes

II. Fertility assays for wild type, *lin-35, mes-4(AAA) and mes-4(AAA); lin-35*

All the strains contain mes-4 tagged with GFP, considering *mes-4::GFP* strain the wild type and *lin-35;mes-4::GFP* as *lin-35*. The AAA strain is the KEN box mutant tagged with GFP, and *AAA; lin-35* is the double mutant.

Table IV. Data and summary of fertility assay at 20°C

WT	*lin-35*	*AAA*	*AAA lin-35*
214	86	201	84
259	74	215	53
253	138	174	77
270	88	295	78
260	160	252	90
254	125	213	67
244	146	206	48
227	152	162	36
-------	87	255	62
-------	118	187	44
-------	142	336	60
-------	142	263	41
-------	70	314	54
-------	-------	296	50
-------	-------	333	91

n	8	13	15	15
Mean	**247.63**	**117.54**	**246.80**	**62.33**
SD	18.60	32.18	57.93	18.01
SEM	6.58	8.93	14.96	4.65

Table V. D'Agostino & Pearson omnibus normality test

	WT	*lin-35*	*mes-4(AAA)*	*mes-4(AAA); lin-35*
K2	1.6620	4.7030	2.5890	2.1430
p value	0.4357	0.0952	0.2741	0.3426
Passed normality test (α=0.05)?	Yes	Yes	Yes	Yes
p value summary	ns	ns	ns	ns

Table VI. Unpaired t-test with Welch's correlation

Due to the differences in variances, unpaired t-test without assuming equal variances was performed. F test confirmed these differences.

	WT *vs* *AAA/lin-35*	*lin-35 vs* *AAA/lin-35*	*AAA vs* *AAA/lin-35*	WT *vs AAA*	WT *vs lin-35*
p value	< 0.0001	< 0.0001	< 0.0001	0.9603	< 0.0001
p value summary	***	***	***	ns	***
Means signif. different? (p <0.05)	Yes	Yes	Yes	No	Yes
One- or two-tailed p value?	Two-tailed	Two-tailed	Two-tailed	Two-tailed	Two-tailed
Welch's correlation (t. df)	t=23.00 df=14	t=5.485 df=18	t=11.78 df=16	t=0.05049 df=18	t=11.73 df=18

F test to compare variances

P value	0.8655	0.0418	< 0.0001	0.0056	0.1537
P value summary	ns	*	***	**	ns
Are variances signif. different?	No	Yes	Yes	Yes	No

III. Overexpression of MES-4

Table VII. Nuclei positive for MES-4 in soma

	Prps-27				***Peft-3***			
	MES-4(WT)		MES-4(AAA)		MES-4(WT)		MES-4(AAA)	
RNAi	ctr	*fzr-1*	ctr	*fzr-1*	ctr	*fzr-1*	ctr	*fzr-1*
	15	132	356	343	50	171	277	304
	19	192	362	316	32	157	305	285
	52	190	307	371	22	159	299	232
	40	252	295	276	38	143	-----	-----
	45	201	313	317	-----	-----	-----	-----
	84	205	336	321	-----	-----	-----	-----
	-----	-----	368	-----	-----	-----	-----	-----
	-----	-----	313	-----	-----	-----	-----	-----
n	6	6	8	6	4	4	3	3
Mean	**42.50**	**195.33**	**331.25**	**323.83**	**35.50**	**157.50**	**293.67**	**273.67**
SD	25.03	38.44	28.03	35.18	11.71	11.47	14.74	37.31
SEM	10.22	15.69	9.91	14.36	5.85	5.74	8.51	21.54

Table VII. Unpaired t-test

	Prp-27		***Peft-3***	
	MES-4 WT	MES-4 AAA	MES-4 WT	MES-4 AAA
	ctr *vs fzr-1*	ctr *vs fzr-1*	ctr *vs fzr-1*	ctr *vs fzr-1*
p value	< 0.0001	0.6580	< 0.0001	0.4366
p value summary	***	ns	***	ns
Means signif. different? (p <0.05)	Yes	No	Yes	No
One- or two-tailed p value?	Two-tailed	Two-tailed	Two-tailed	Two-tailed
t. df	t=8.161 df=10	t=0.4539 df=12	t=14.89 df=6	t=0.8634 df=4

7. REFERENCES

Ahringer, J., and Gasser, S.M. (2018). Repressive Chromatin in Caenorhabditis elegans: Establishment, Composition, and Function. Genetics *208*, 491-511.

Amendola, P.G., Zaghet, N., Ramalho, J.J., Vilstrup Johansen, J., Boxem, M., and Salcini, A.E. (2017). JMJD-5/KDM8 regulates H3K36me2 and is required for late steps of homologous recombination and genome integrity. PLoS Genetics *13*, e1006632.

Asikainen, S., Vartiainen, S., Lakso, M., Nass, R., and Wong, G. (2005). Selective sensitivity of Caenorhabditis elegans neurons to RNA interference. NeuroReport *16*, 1995-1999.

Ausubel, F.M., Brent, R., Kingston, R.E., Moore, D.D., Seidman, J.G., Smith, J.A., and Struhl, K., eds. (1997). Current Protocols in Molecular Biology (New York: Ed. Wiley).

Bar-On, O., Shapira, M., Skorecki, K., Hershko, A., and Hershko, D.D. (2010). Regulation of APC/C (Cdh1) ubiquitin ligase in differentiation of human embryonic stem cells. Cell Cycle *9*, 1986-1989.

Bashir, T., Dorrello, N.V., Amador, V., Guardavaccaro, D., and Pagano, M. (2004). Control of the SCFSkp2–Cks1 ubiquitin ligase by the APC/CCdh1 ubiquitin ligase. Nature *428*, 190.

Batchelder, C., Dunn, M.A., Choy, B., Suh, Y., Cassie, C., Shim, E.Y., Shin, T.H., Mello, C., Seydoux, G., and Blackwell, T.K. (1999). Transcriptional repression by the Caenorhabditis elegans germ-line protein PIE-1. Genes and Development *13*, 202-212.

Baugh, L.R., and Sternberg, P.W. (2006). DAF-16/FOXO Regulates Transcription of *cki-1*/Cip/Kip and Repression of *lin-4* during *C. elegans* L1 Arrest. Current Biology *16*, 780-785.

Belinsky, S.A., Nikula, K.J., Palmisano, W.A., Michels, R., Saccomanno, G., Gabrielson, E., Baylin, S.B., and Herman, J.G. (1998). Aberrant methylation of p16(INK4a) is an early event in lung cancer and a potential biomarker for early diagnosis. Proceedings of the National Academy of Sciences of the United States of America *95*, 11891-11896.

Bender, L.B., Suh, J., Carroll, C.R., Fong, Y., Fingerman, I.M., Briggs, S.D., Cao, R., Zhang, Y., Reinke, V., and Strome, S. (2006). MES-4: an autosome-associated histone methyltransferase that participates in silencing the X chromosomes in the C. elegans germ line. Development *133*, 3907-3917.

Berger, C., Kannan, R., Myneni, S., Renner, S., Shashidhara, L.S., and Technau, G.M. (2010). Cell cycle independent role of Cyclin E during neural cell fate specification in Drosophila is mediated by its regulation of Prospero function. Developmental Biology *337*, 415-424.

Biedermann, B., Wright, J., Senften, M., Kalchhauser, I., Sarathy, G., Lee, M.-H., and Ciosk, R. (2009). Translational Repression of Cyclin E Prevents Precocious Mitosis and Embryonic Gene Activation during C. elegans Meiosis. Developmental Cell *17*, 355-364.

Blais, A., van Oevelen, C.J.C., Margueron, R., Acosta-Alvear, D., and Dynlacht, B.D. (2007). Retinoblastoma tumor suppressor protein–dependent methylation of histone H3 lysine 27 is associated with irreversible cell cycle exit. The Journal of cell biology *179*, 1399-1412.

Boxem, M., and van den Heuvel, S. (2001). *lin-35* Rb and *cki-1* Cip/Kip cooperate in developmental regulation of G1 progression in *C. elegans*. Development *128*, 4349.

Bracken, A.P., Pasini, D., Capra, M., Prosperini, E., Colli, E., and Helin, K. (2003). EZH2 is downstream of the pRB-E2F pathway, essential for proliferation and amplified in cancer. The EMBO Journal *22*, 5323-5335.

Brehm, A., Miska, E.A., McCance, D.J., Reid, J.L., Bannister, A.J., and Kouzarides, T. (1998). Retinoblastoma protein recruits histone deacetylase to repress transcription. Nature *391*, 597.

Brenner, J.L., and Schedl, T. (2016). Germline Stem Cell Differentiation Entails Regional Control of Cell Fate Regulator GLD-1 in Caenorhabditis elegans. Genetics *202*, 1085-1103.

Brenner, S. (1974). The Genetics of CAENORHABDITIS ELEGANS. Genetics *77*, 71-94.

Brodigan, T.M., Liu, J.i., Park, M., Kipreos, E.T., and Krause, M. (2003). Cyclin E expression during development in caenorhabditis elegans. Developmental Biology *254*, 102-115.

Buck, S.H., Chiu, D., and Saito, R.M. (2009). The cyclin-dependent kinase inhibitors, cki-1 and cki-2, act in overlapping but distinct pathways to control cell-cycle quiescence during C. elegans development. Cell cycle (Georgetown, Tex) *8*, 2613-2620.

Budirahardja, Y., and Gönczy, P. (2009). Coupling the cell cycle to development. Development *136*, 2861-2872.

Burger, J., Merlet, J., Tavernier, N., Richaudeau, B., Arnold, A., Ciosk, R., Bowerman, B., and Pintard, L. (2013). CRL2LRR-1 E3-Ligase Regulates Proliferation and Progression through Meiosis in the Caenorhabditis elegans Germline. PLoS Genetics *9*, e1003375.

Busanello, A., Battistelli, C., Carbone, M., Mostocotto, C., and Maione, R. (2012). MyoD regulates p57(kip2) expression by interacting with a distant cis-element and modifying a higher order chromatin structure. Nucleic Acids Research *40*, 8266-8275.

Byerly, L., Cassada, R.C., and Russell, R.L. (1976). The life cycle of the nematode Caenorhabditis elegans: I. Wild-type growth and reproduction. Developmental Biology *51*, 23-33.

Calder, A., Roth-Albin, I., Bhatia, S., Pilquil, C., Lee, J.H., Bhatia, M., Levadoux-Martin, M., McNicol, J., Russell, J., Collins, T.*, et al.* (2012). Lengthened G1 Phase Indicates Differentiation Status in Human Embryonic Stem Cells Stem Cells and Development *22*, 279-295.

Calo, E., Quintero-Estades, J.A., Danielian, P.S., Nedelcu, S., Berman, S.D., and Lees, J.A. (2010). Rb regulates fate choice and lineage commitment in vivo. Nature *466*, 1110-1114.

Capowski, E.E., Martin, P., Garvin, C., and Strome, S. (1991). Identification of Grandchildless Loci Whose Products Are Required for Normal Germ-Line Development in the Nematode Caenorhabditis Elegans. Genetics *129*, 1061-1072.

Ceol, C.J., and Horvitz, H.R. (2001). dpl-1 DP and efl-1 E2F Act with lin-35 Rb to Antagonize Ras Signaling in C. elegans Vulval Development. Molecular Cell *7*, 461-473.

Cha, T.-L., Zhou, B.P., Xia, W., Wu, Y., Yang, C.-C., Chen, C.-T., Ping, B., Otte, A.P., and Hung, M.-C. (2005). Akt-Mediated Phosphorylation of EZH2 Suppresses Methylation of Lysine 27 in Histone H3. Science *310*, 306-310.

Chai, J., Charboneau, A.L., Betz, B.L., and Weissman, B.E. (2005). Loss of the hSNF5 Gene Concomitantly Inactivates p21CIP/WAF1 and p16INK4a Activity

Associated with Replicative Senescence in A204 Rhabdoid Tumor Cells. Cancer research *65*, 10192.

Chalfie, M., Sulston, J.E., White, J.G., Southgate, E., Thomson, J.N., and Brenner, S. (1985). The neural circuit for touch sensitivity in Caenorhabditis elegans. The Journal of Neuroscience *5*, 956.

Chen, S., Bohrer, L.R., Rai, A.N., Pan, Y., Gan, L., Zhou, X., Bagchi, A., Simon, J.A., and Huang, H. (2010). Cyclin-dependent kinases regulate epigenetic gene silencing through phosphorylation of EZH2. Nature Cell Biology *12*, 1108-1114.

Chiang, M., Cinquin, A., Paz, A., Meeds, E., Price, C.A., Welling, M., and Cinquin, O. (2015). Control of *Caenorhabditis elegans* germ-line stem-cell cycling speed meets requirements of design to minimize mutation accumulation. BMC Biology *13*.

Coulson, M., Robert, S., Eyre, H.J., and Saint, R. (1998). The Identification and Localization of a Human Gene with Sequence Similarity to Polycomb like of *Drosophila melanogaster*. Genomics *48*, 381-383.

Crittenden, S.L., Bernstein, D.S., Bachorik, J.L., Thompson, B.E., Gallegos, M., Petcherski, A.G., Moulder, G., Barstead, R., Wickens, M., and Kimble, J. (2002). A conserved RNA-binding protein controls germline stem cells in Caenorhabditis elegans. Nature *417*, 660.

Crittenden, S.L., Leonhard, K.A., Byrd, D.T., and Kimble, J. (2006). Cellular Analyses of the Mitotic Region in the Caenorhabditis elegans Adult Germ Line. Molecular biology of the cell *17*, 3051-3061.

Cuende, J., Moreno, S., Bolanos, J.P., and Almeida, A. (2008). Retinoic acid downregulates Rae1 leading to APC(Cdh1) activation and neuroblastoma SH-SY5Y differentiation. Oncogene *27*, 3339-3344.

Cui, M., Fay, D.S., and Han, M. (2004). lin-35/Rb cooperates with the SWI/SNF complex to control Caenorhabditis elegans larval development. Genetics *167*, 1177-1185.

DeGregori, J., Kowalik, T., and Nevins, J.R. (1995). Cellular targets for activation by the E2F1 transcription factor include DNA synthesis- and G1/S-regulatory genes. Molecular and cellular biology *15*, 4215-4224.

Demoinet, E., Li, S., and Roy, R. (2017). AMPK blocks starvation-inducible transgenerational defects in Caenorhabditis elegans. Proceedings of the National Academy of Sciences of the United States of America *114*, E2689-E2698.

Dernburg, A.F., McDonald, K., Moulder, G., Barstead, R., Dresser, M., and Villeneuve, A.M. (1998). Meiotic Recombination in C. elegans Initiates by a Conserved Mechanism and Is Dispensable for Homologous Chromosome Synapsis. Cell *94*, 387-398.

Dickinson, D.J., Pani, A.M., Heppert, J.K., Higgins, C.D., and Goldstein, B. (2015). Streamlined Genome Engineering with a Self-Excising Drug Selection Cassette. Genetics *200*, 1035.

Dickinson, D.J., Ward, J.D., Reiner, D., and Goldstein, B. (2013). Engineering the *Caenorhabditis elegans* genome using Cas9-triggered homologous recombination. Nature Methods *10*, 1028-1034.

Doré, L.C., Chlon, T.M., Brown, C.D., White, K.P., and Crispino, J.D. (2012). Chromatin occupancy analysis reveals genome-wide GATA factor switching during hematopoiesis. Blood *119*, 3724-3733.

Dronamraju, R., Jha, D.K., Eser, U., Adams, A.T., Dominguez, D., Choudhury, R., Chiang, Y.-C., Rathmell, W.K., Emanuele, M.J., Churchman, L.S.*, et al.* (2017). Set2 methyltransferase facilitates cell cycle progression by maintaining transcriptional fidelity. Nucleic Acids Research, gkx1276-gkx1276.

Duronio, R.J., and O'Farrell, P.H. (1995). Developmental control of the G1 to S transition in *Drosophila*: cyclin E is a limiting downstream target of E2F. Genes & Development *9*, 1456-1468.

Edgar, B.A., and O'Farrell, P.H. (1990). The Three Postblastoderm Cell Cycles of Drosophila Embryogenesis Are Regulated in G2 by string. Cell *62*, 469-480.

Erdelyi, P., Wang, X., Suleski, M., and Wicky, C. (2017). A Network of Chromatin Factors Is Regulating the Transition to Postembryonic Development in *Caenorhabditis elegans*. G3: Genes|Genomes|Genetics *7*, 343.

Fay, D.S. (2005). Classical genetic methods. In WormBook: The Online Review of C elegans Biology [Internet] (Pasadena (CA)).

Fay, D.S., Keenan, S., and Han, M. (2002). fzr-1 and lin-35/Rb function redundantly to control cell proliferation in C. elegans as revealed by a nonbiased synthetic screen. Genes Dev *16*, 503-517.

Feng, H., Zhong, W., Punkosdy, G., Gu, S., Zhou, L., Seabolt, E.K., and Kipreos, E.T. (1999). CUL-2 is required for the G1-to-S-phase transition and mitotic chromosome condensation in Caenorhabditis elegans. Nature Cell Biology *1*, 486.

Ferres-Marco, D., Gutierrez-Garcia, I., Vallejo, D.M., Bolivar, J., Gutierrez-Aviño, F.J., and Dominguez, M. (2006). Epigenetic silencers and Notch collaborate to promote malignant tumours by Rb silencing. Nature *439*, 430.

Fischer, M., Uxa, S., Stanko, C., Magin, T.M., and Engeland, K. (2017). Human papilloma virus E7 oncoprotein abrogates the p53-p21-DREAM pathway. Scientific Reports *7*, 2603.

Fong, Y., Bender, L., Wang, W., and Strome, S. (2002). Regulation of the different chromatin states of autosomes and X chromosomes in the germ line of C. elegans. Science *296*, 2235-2238.

Fox, P.M., and Schedl, T. (2015). Analysis of Germline Stem Cell Differentiation Following Loss of GLP-1 Notch Activity in Caenorhabditis elegans. Genetics *201*, 167-184.

Fox, P.M., Vought, V.E., Hanazawa, M., Lee, M.-H., Maine, E.M., and Schedl, T. (2011). Cyclin E and CDK-2 regulate proliferative cell fate and cell cycle progression in the C. elegans germline. Development (Cambridge, England) *138*, 2223-2234.

Friedland, A.E., Tzur, Y.B., Esvelt, K.M., Colaiacovo, M.P., Church, G.M., and Calarco, J.A. (2013). Heritable genome editing in C. elegans via a CRISPR-Cas9 system. Nat Meth *10*, 741-743.

Frigola, J., Song, J., Stirzaker, C., Hinshelwood, R.A., Peinado, M.A., and Clark, S.J. (2006). Epigenetic remodeling in colorectal cancer results in coordinate gene suppression across an entire chromosome band. Nature Genetics *38*, 540.

Frøkjær-Jensen, C., Davis, M.W., Ailion, M., and Jorgensen, E.M. (2012). Improved Mos1-mediated transgenesis in C. elegans. Nature Methods *9*, 117-118.

Frøkjær-Jensen, C., Davis, M.W., Hopkins, C.E., Newman, B.J., Thummel, J.M., Olesen, S.-P., Grunnet, M., and Jorgensen, E.M. (2008). Single-copy insertion of transgenes in *Caenorhabditis elegans*. Nature Genetics *40*, 1375-1383.

Fujita, M., Takasaki, T., Nakajima, N., Kawano, T., Shimura, Y., and Sakamoto, H. (2002). MRG-1, a mortality factor-related chromodomain protein, is required maternally for primordial germ cells to initiate mitotic proliferation in C. elegans. Mechanisms of Development *114*, 61-69.

Fujita, M., Takeshita, H., and Sawa, H. (2007). Cyclin E and CDK2 repress the terminal differentiation of quiescent cells after asymmetric division in C. elegans. PLoS ONE *2*.

Fukushige, T., and Krause, M. (2005). The myogenic potency of HLH-1 reveals wide-spread developmental plasticity in early C. elegans embryos. Development *132*, 1795.

Fukuyama, M., Gendreau, S.B., Derry, W.B., and Rothman, J.H. (2003). Essential embryonic roles of the CKI-1 cyclin-dependent kinase inhibitor in cell-cycle exit and morphogenesis in C. elegans. Developmental Biology *260*, 273-286.

Fukuyama, M., Rougvie, A.E., and Rothman, J.H. (2006). C. elegans DAF-18/PTEN mediates nutrient-dependent arrest of cell cycle and growth in the germline. Current biology : CB *16*, 773-779.

Furuhashi, H., Takasaki, T., Rechtsteiner, A., Li, T., Kimura, H., Checchi, P.M., Strome, S., and Kelly, W.G. (2010). Trans-generational epigenetic regulation of C. elegans primordial germ cells. Epigenetics & chromatin *3*, 15.

Garvin, C., Holdeman, R., and Strome, S. (1998). The phenotype of mes-2, mes-3, mes-4 and mes-6, maternal-effect genes required for survival of the germline in Caenorhabditis elegans, is sensitive to chromosome dosage. Genetics *148*, 167-185.

Gaydos, L.J., Rechtsteiner, A., Egelhofer, T.A., Carroll, C.R., and Strome, S. (2012). Antagonism between MES-4 and Polycomb repressive complex 2 promotes appropriate gene expression in C. elegans germ cells. Cell Rep *2*, 1169-1177.

Gendreau, S.B., Moskowitz, I.P.G., Terns, R.M., and Rothman, J.H. (1994). The Potential to Differentiate Epidermis Is Unequally Distributed in the AB Lineage during Early Embryonic Development in C. elegans. Developmental Biology *166*, 770-781.

Giordano-Santini, R., Milstein, S., Svrzikapa, N., Tu, D., Johnsen, R., Baillie, D., Vidal, M., and Dupuy, D. (2010). An antibiotic selection marker for nematode transgenesis. Nature Methods *7*, 721-723.

Goetsch, P.D., Garrigues, J.M., and Strome, S. (2017). Loss of the Caenorhabditis elegans pocket protein LIN-35 reveals MuvB's innate function as the repressor of DREAM target genes. PLoS Genetics *13*, e1007088.

González-Aguilera, C., Palladino, F., and Askjaer, P. (2013). *C. elegans* epigenetic regulation in development and aging. Briefings in Functional Genomics.

Grishok, A., and Sharp, P.A. (2005). Negative regulation of nuclear divisions in Caenorhabditis elegans by retinoblastoma and RNA interference-related genes. Proceedings of the National Academy of Sciences of the United States of America *102*, 17360-17365.

Gupta, P., Leahul, L., Wang, X., Wang, C., Bakos, B., Jasper, K., and Hansen, D. (2015). Proteasome regulation of the chromodomain protein MRG-1 controls the balance between proliferative fate and differentiation in *C. elegans* germ line. Development *142*, 291-302.

Ha, K., Ma, C., Lin, H., Tang, L., Lian, Z., Zhao, F., Li, J.-M., Zhen, B., Pei, H., Han, S.*, et al.* (2017). The anaphase promoting complex impacts repair choice by protecting ubiquitin signalling at DNA damage sites. Nature Communications *8*, 15751.

Hajkova, P., Erhardt, S., Lane, N., Haaf, T., El-Maarri, O., Reik, W., Walter, J., and Surani, M.A. (2002). Epigenetic reprogramming in mouse primordial germ cells. Mechanisms of Development *117*, 15-23.

Hanahan, D. (1983). Studies on Transformation of *Escherichia coli* with Plasmids. J Mol Biol *166*, 557-580.

Hao, B., Zheng, N., Schulman, B.A., Wu, G., Miller, J.J., Pagano, M., and Pavletich, N.P. (2005). Structural Basis of the Cks1-Dependent Recognition of p27Kip1 by the SCFSkp2 Ubiquitin Ligase. Molecular Cell *20*, 9-19.

Harper, J.W., Adami, G.R., Wei, N., Keyomarsi, K., and Elledge, S.J. (1993). THE P21 CDK-INTERACTING PROTEIN CIP1 IS A POTENT INHIBITOR OF G1 CYCLIN-DEPENDENT KINASES. Cell *75*, 805-816.

Hayashi, M., Chin, G.M., and Villeneuve, A.M. (2007). C. elegans Germ Cells Switch between Distinct Modes of Double-Strand Break Repair During Meiotic Prophase Progression. PLoS Genetics *3*, e191.

He, A., Shen, X., Ma, Q., Cao, J., von Gise, A., Zhou, P., Wang, G., Marquez, V.E., Orkin, S.H., and Pu, W.T. (2012). PRC2 directly methylates GATA4 and represses its transcriptional activity. Genes Dev *26*, 37-42.

Hedgecock, E.M., and White, J.G. (1985). Polyploid tissues in the nematode Caenorhabditis elegans. Developmental Biology *107*, 128-133.

Hinds, P.W., Mittnacht, S., Dulic, V., Arnold, A., Reed, S.I., and Weinberg, R.A. (1992). Regulation of retinoblastoma protein functions by ectopic expression of human cyclins. Cell *70*, 993-1006.

Hirsh, D., Oppenheim, D., and Klass, M. (1976). Development of the reproductive system of Caenorhabditis elegans. Developmental Biology *49*, 200-219.

Hodgkin, J., Horvitz, H.R., and Brenner, S. (1979). Nondisjunction Mutants of the Nematode CAENORHABDITIS ELEGANS. Genetics *91*, 67-94.

Hong, Y., Roy, R., and Ambros, V. (1998). Developmental regulation of a cyclin-dependent kinase inhibitor controls postembryonic cell cycle progression in Caenorhabditis elegans. Development *125*, 3585-3597.

Horton, L., Qian, Y., and Templeton, D. (1995). G1 cyclins control the retinoblastoma gene product growth regulation activity via upstream mechanisms. Cell Growth Differ *6*, 395-407.

Huang, T., Kuersten, S., Deshpande, A.M., Spieth, J., MacMorris, M., and Blumenthal, T. (2001). Intercistronic Region Required for Polycistronic Pre-mRNA Processing in Caenorhabditis elegans. Molecular and cellular biology *21*, 1111-1120.

Jacobs, H.W., Richter, D.O., Venkatesh, T.R., and Lehner, C.F. (2002). Completion of Mitosis Requires Neither fzr/rap nor fzr2, a Male Germline-Specific Drosophila Cdh1 Homolog. Current Biology *12*, 1435-1441.

Jantsch, V., Tang, L., Pasierbek, P., Penkner, A., Nayak, S., Baudrimont, A., Schedl, T., Gartner, A., and Loidl, J. (2007). Caenorhabditis elegans prom-1 Is Required for Meiotic Prophase Progression and Homologous Chromosome Pairing. Molecular biology of the cell *18*, 4911-4920.

Jeong, J., Verheyden, J.M., and Kimble, J. (2011). Cyclin E and Cdk2 Control GLD-1, the Mitosis/Meiosis Decision, and Germline Stem Cells in Caenorhabditis elegans. PLoS Genetics *7*, e1001348.

Johnson, D.G., Schwarz, J.K., Cress, W.D., and Nevins, J.R. (1993). Expression of transcription factor E2F1 induces quiescent cells to enter S phase. Nature *365*, 349.

Johnstone, I.L. (1994). The cuticle of the nematode Caenorhabditis elegans: A complex collagen structure. BioEssays *16*, 171-178.

Kalchhauser, I., Farley, B.M., Pauli, S., Ryder, S.P., and Ciosk, R. (2011). FBF represses the Cip/Kip cell-cycle inhibitor CKI-2 to promote self-renewal of germline stem cells in C. elegans. The EMBO Journal *30*, 3823-3829.

Kamath, R.S., and Ahringer, J. (2003). Genome-wide RNAi screening in Caenorhabditis elegans. Methods *30*, 313-321.

Kaneko, S., Li, G., Son, J., Xu, C.-F., Margueron, R., Neubert, T.A., and Reinberg, D. (2010). Phosphorylation of the PRC2 component Ezh2 is cell cycle-regulated and up-regulates its binding to ncRNA. Genes & Development *24*, 2615-2620.

Kato, J.-y., Matsushime, H., Hiebert, S.W., Ewen, M.E., and Sherr, C.J. (1993). Direct binding of cyclin D to the retinoblastoma gene product (pRb) and pRb phosphorylation by the cyclin D-dependent kinase CDK4. Genes & Development *7*, 331-342.

Keck, J.M., Summers, M.K., Tedesco, D., Ekholm-Reed, S., Chuang, L.-C., Jackson, P.K., and Reed, S.I. (2007). Cyclin E overexpression impairs progression through mitosis by inhibiting APC(Cdh1). The Journal of cell biology *178*, 371-385.

Kemphues, K.J., Priess, J.R., Morton, D.G., and Cheng, N. (1988). Identification of genes required for cytoplasmic localization in early C. elegans embryos. Cell *52*, 311-320.

Kimble, J., and Hirsh, D. (1979). The postembryonic cell lineages of the hermaphrodite and male gonads in Caenorhabditis elegans. Developmental Biology *70*, 396-417.

Kimble, J.E., and White, J.G. (1981). On the control of germ cell development in Caenorhabditis elegans. Developmental Biology *81*, 208-219.

Kipreos, E.T., Lander, L.E., Wing, J.P., He, W.W., and Hedgecock, E.M. (1996). cul-1 Is Required for Cell Cycle Exit in C. elegans and Identifies a Novel Gene Family. Cell *85*, 829-839.

Kirienko, N.V., and Fay, D.S. (2007). Transcriptome profiling of the C. elegans Rb ortholog reveals diverse developmental roles. Dev Biol *305*, 674-684.

Kisielnicka, E., Minasaki, R., and Eckmann, C.R. (2018). MAPK signaling couples SCF-mediated degradation of translational regulators to oocyte meiotic progression. Proceedings of the National Academy of Sciences *115*, E2772-E2781.

Klass, M.R. (1977). Aging in the nematode Caenorhabditis elegans: Major biological and environmental factors influencing life span. Mechanisms of Ageing and Development *6*, 413-429.

Korf, I., Fan, Y., and Strome, S. (1998). The Polycomb group in Caenorhabditis elegans and maternal control of germline development. Development *125*, 2469-2478.

Korzelius, J., The, I., Ruijtenberg, S., Portegijs, V., Xu, H., Horvitz, H.R., and van den Heuvel, S. (2011). C. elegans MCM-4 is a general DNA replication and checkpoint component with an epidermis-specific requirement for growth and viability. Developmental Biology *350*, 358-369.

Kostic, I., Li, S., and Roy, R. (2003). cki-1 links cell division and cell fate acquisition in the C. elegans somatic gonad. Developmental Biology *263*, 242-252.

Koury, E., Harrell, K., and Smolikove, S. (2018). Differential RPA-1 and RAD-51 recruitment in vivo throughout the C. elegans germline, as revealed by laser microirradiation. Nucleic Acids Research *46*, 748-764.

Krüger, A.V., Jelier, R., Dzyubachyk, O., Zimmerman, T., Meijering, E., and Lehner, B. (2015). Comprehensive single cell-resolution analysis of the role of chromatin regulators in early C. elegans embryogenesis. Developmental Biology *398*, 153-162.

Kudithipudi, S., Lungu, C., Rathert, P., Happel, N., and Jeltsch, A. (2014). Substrate specificity analysis and novel substrates of the protein lysine methyltransferase NSD1. Chemistry & biology *21*, 226-237.

Kudron, M., Niu, W., Lu, Z., Wang, G., Gerstein, M., Snyder, M., and Reinke, V. (2013). Tissue-specific direct targets of Caenorhabditis elegans Rb/E2F dictate distinct somatic and germline programs. Genome Biology *14*, R5.

Labouesse, M., and Mango, S.E. (1999). Patterning the C. elegans embryo: moving beyond the cell lineage. Trends in Genetics *15*, 307-313.

Lamelza, P., and Bhalla, N. (2012). Histone Methyltransferases MES-4 and MET-1 Promote Meiotic Checkpoint Activation in Caenorhabditis elegans. PLoS Genetics *8*, e1003089.

Latorre, I., Chesney, M.A., Garrigues, J.M., Stempor, P., Appert, A., Francesconi, M., Strome, S., and Ahringer, J. (2015). The DREAM complex promotes gene body H2A.Z for target repression. Genes Dev *29*, 495-500.

Lee, M.-H., Ohmachi, M., Arur, S., Nayak, S., Francis, R., Church, D., Lambie, E., and Schedl, T. (2007a). Multiple Functions and Dynamic Activation of MPK-1 Extracellular Signal-Regulated Kinase Signaling in Caenorhabditis elegans Germline Development. Genetics *177*, 2039-2062.

Lee, M.-H., Ohmachi, M., Arur, S., Nayak, S., Francis, R., Church, D., Lambie, E., and Schedl, T. (2007b). Multiple Functions and Dynamic Activation of MPK-1 Extracellular Signal-Regulated Kinase Signaling in Caenorhabditis elegans Germline Development. Genetics *177*, 2039-2062.

Li, V.C., and Kirschner, M.W. (2014). Molecular ties between the cell cycle and differentiation in embryonic stem cells. Proceedings of the National Academy of Sciences of the United States of America *111*, 9503-9508.

Liu, L., Michowski, W., Inuzuka, H., Shimizu, K., Nihira, N.T., Chick, J.M., Li, N., Geng, Y., Meng, A.Y., Ordureau, A.*, et al.* (2017). G1 cyclins link proliferation, pluripotency and differentiation of embryonic stem cells. Nat Cell Biol *19*, 177-188.

Liu, T., Rechtsteiner, A., Egelhofer, T.A., Vielle, A., Latorre, I., Cheung, M.-S., Ercan, S., Ikegami, K., Jensen, M., Kolasinska-Zwierz, P.*, et al.* (2011). Broad chromosomal domains of histone modification patterns in C. elegans. Genome research *21*, 227-236.

Liu, Z., Yuan, F., Ren, J., Cao, J., Zhou, Y., Yang, Q., and Xue, Y. (2012). GPS-ARM: Computational Analysis of the APC/C Recognition Motif by Predicting D-Boxes and KEN-Boxes. PLoS ONE *7*, e34370.

Lu, T., Jackson, M.W., Wang, B., Yang, M., Chance, M.R., Miyagi, M., Gudkov, A.V., and Stark, G.R. (2010). Regulation of NF-kappaB by NSD1/FBXL11-dependent reversible lysine methylation of p65. Proceedings of the National Academy of Sciences of the United States of America *107*, 46-51.

Lu, X., and Horvitz, H.R. (1998). lin-35 and lin-53, two genes that antagonize a C. elegans Ras pathway, encode proteins similar to RB and its Binding Protein RBAp48. Cell *95*, 981-991.

Lukas, J., Herzinger, T., Hansen, K., Moroni, M.C., Resnitzky, D., Helin, K., and Bartek, J. (1997). Cyclin E-induced S phase without activation of the pRb/E2F pathway. Genes & Development, 1479-1492.

MacDonald, L.D., Knox, A., and Hansen, D. (2008). Proteasomal regulation of the proliferation vs. meiotic entry decision in the Caenorhabditis elegans germ line. Genetics *180*, 905-920.

Mailand, N., and Diffley, J.F.X. (2005). CDKs Promote DNA Replication Origin Licensing in Human Cells by Protecting Cdc6 from APC/C-Dependent Proteolysis. Cell *122*, 915-926.

Mango, S.E., Lambie, E.J., and Kimble, J. (1994). The pha-4 gene is required to generate the pharyngeal primordium of Caenorhabditis elegans. Development *120*, 3019.

Martins, T., Meghini, F., Florio, F., and Kimata, Y. (2017). The APC/C Coordinates Retinal Differentiation with G1 Arrest through the Nek2-Dependent Modulation of Wingless Signaling. Developmental Cell *40*, 67-80.

McCarter, J., Bartlett, B., Dang, T., and Schedl, T. (1999). On the Control of Oocyte Meiotic Maturation and Ovulation inCaenorhabditis elegans. Developmental Biology *205*, 111-128.

McClurg, U.L., Nabbi, A., Ricordel, C., Korolchuk, S., McCracken, S., Heer, R., Wilson, L., Butler, L.M., Irving-Hooper, B.K., Pedeux, R.*, et al.* (2018). Human ex vivo prostate tissue model system identifies ING3 as an oncoprotein. British Journal Of Cancer.

Mello, C.C., Draper, B.W., Krause, M., Weintraub, H., and Priess, J.R. (1992). The pie-1 and mex-1 genes and maternal control of blastomere identity in early C. elegans embryos. Cell *70*, 163-176.

Merritt, C., Rasoloson, D., Ko, D., and Seydoux, G. (2008). 3' UTRs are the primary regulators of gene expression in the C. elegans germline. Current biology : CB *18*, 1476-1482.

Meshorer, E., Yellajoshula, D., George, E., Scambler, P.J., Brown, D.T., and Misteli, T. (2006). Hyperdynamic Plasticity of Chromatin Proteins in Pluripotent Embryonic Stem Cells. Developmental Cell *10*, 105-116.

Middelkoop, T.C., and Korswagen, H.C. (2014). Development and migration of the C. elegans Q neuroblasts and their descendants. WormBook : the online review of C elegans biology, 1-23.

Min, M., Mayor, U., and Lindon, C. (2013). Ubiquitination site preferences in anaphase promoting complex/cyclosome (APC/C) substrates. Open Biology *3*, 130097.

Miwa, T., Takasaki, T., Inoue, K., and Sakamoto, H. (2015). Restricted distribution of mrg-1 mRNA in C. elegans primordial germ cells through germ granule-independent regulation. Genes to Cells *20*, 932-942.

Morgan, C.T., Noble, D., and Kimble, J. (2013). Mitosis-meiosis and sperm-oocyte fate decisions are separable regulatory events. PNAS *110*, 3411-3416.

Morgan, D.E., Crittenden, S.L., and Kimble, J. (2010). The *C. elegans* adult male germline: stem cell and sexual dimorphism. Dev Biol *346*, 204-214.

Morishita, M., and di Luccio, E. (2011). Cancers and the NSD family of histone lysine methyltransferases. Biochimica et Biophysica Acta (BBA) - Reviews on Cancer *1816*, 158-163.

Munshi, A., Shafi, G., Aliya, N., and Jyothy, A. (2009). Histone modifications dictate specific biological readouts. Journal of Genetics and Genomics *36*, 75-88.

Naoe, H., Chiyoda, T., Ishizawa, J., Masuda, K., Saya, H., and Kuninaka, S. (2013). The APC/C activator Cdh1 regulates the G2/M transition during differentiation of placental trophoblast stem cells. Biochem Biophys Res Commun *430*, 757-762.

Nelson, F.K., and Riddle, D.L. (1984). Functional study of the Caenorhabditis elegans secretory-excretory system using laser microsurgery. Journal of Experimental Zoology *231*, 45-56.

Nevins, J.R. (2001). The Rb/E2F pathway and cancer. Human Molecular Genetics *10*, 699-703.

Nurse, P., Thuriaux, P., and Nasmyth, K. (1976). Genetic control of the cell division cycle in the fission yeast Schizosaccharomyces pombe. Molecular and General Genetics MGG *146*, 167-178.

Ohtani, K., DeGregori, J., and Nevins, J.R. (1995). Regulation of the cyclin E gene by transcription factor E2F1. Proceedings of the National Academy of Sciences of the United States of America *92*, 12146-12150.

Papaevgeniou, N., and Chondrogianni, N. (2014). The ubiquitin proteasome system in Caenorhabditis elegans and its regulation. Redox Biology *2*, 333-347.

Papp, B., and Müller, J. (2006). Histone trimethylation and the maintenance of transcriptional ONand OFF states by trxG and PcG proteins. Genes & Development *20*, 2041-2054.

Pardee, A.B. (1974). A Restriction Point for Control of Normal Animal Cell Proliferation. Proceedings of the National Academy of Sciences of the United States of America *71*, 1286-1290.

Patel, T., Tursun, B., Rahe, D.P., and Hobert, O. (2012). Removal of Polycomb Repressive Complex 2 makes *C. elegans* germ cells susceptible to direct conversion into specific somatic cell types. Cell Reports *2*, 1178-1186.

Pauklin, S., and Vallier, L. (2013). The Cell-Cycle State of Stem Cells Determines Cell Fate Propensity. Cell *155*, 135-147.

Perez, M.F., Francesconi, M., Hidalgo-Carcedo, C., and Lehner, B. (2017). Maternal age generates phenotypic variation in Caenorhabditis elegans. Nature *552*, 106.

Petrella, L.N. (2014). Natural Variants of C. elegans Demonstrate Defects in Both Sperm Function and Oogenesis at Elevated Temperatures. PLoS ONE *9*, e112377.

Petrella, L.N., Wang, W., Spike, C.A., Rechtsteiner, A., Reinke, V., and Strome, S. (2011). synMuv B proteins antagonize germline fate in the intestine and ensure C. elegans survival. Development *138*, 1069-1079.

Pfister, Sophia X., Ahrabi, S., Zalmas, L.-P., Sarkar, S., Aymard, F., Bachrati, Csanád Z., Helleday, T., Legube, G., La Thangue, Nicholas B., Porter, Andrew C.*, et al.* (2014). SETD2-Dependent Histone H3K36 Trimethylation Is Required for Homologous Recombination Repair and Genome Stability. Cell Reports *7*, 2006-2018.

Pfleger, C.M., and Kirschner, M.W. (2000). The KEN box: an APC recognition signal distinct from the D box targeted by Cdh1. Genes & Development *14*, 655-665.

Polyak, K., Kato, J.Y., Solomon, M.J., Sherr, C.J., Massague, J., Roberts, J.M., and Koff, A. (1994). p27Kip1, a cyclin-Cdk inhibitor, links transforming growth factor-beta and contact inhibition to cell cycle arrest. Genes & Development, 9-22.

Pontier, D.B., and Tijsterman, M. (2009). A robust network of double-strand break repair pathways governs genome integrity during C. elegans development. Current biology : CB *19*, 1384-1388.

Porta-de-la-Riva, M., Fontrodona, L., Villanueva, A., and Cerón, J. (2012). Basic Caenorhabditis elegans Methods: Synchronization and Observation. Journal of Visualized Experiments : JoVE, 4019.

Priess, J., and Thomson, J.N. (1987). Cellular interactions in early C. elegans embryos, Vol 48.

Quintin, S., Michaux, G., McMahon, L., Gansmuller, A., and Labouesse, M. (2001). The Caenorhabditis elegans Gene lin-26 Can Trigger Epithelial Differentiation without Conferring Tissue Specificity, Vol 235.

Racher, H., and Hansen, D. (2012). PUF-8, a Pumilio Homolog, Inhibits the Proliferative Fate in the Caenorhabditis elegans Germline. G3: Genes|Genomes|Genetics *2*, 1197-1205.

Rayasam, G.V., Wendling, O., Angrand, P.-O., Mark, M., Niederreither, K., Song, L., Lerouge, T., Hager, G.L., Chambon, P., and Losson, R. (2003). NSD1 is essential for early post-implantation development and has a catalytically active SET domain. The EMBO Journal *22*, 3153-3163.

Rechtsteiner, A., Ercan, S., Takasaki, T., Phippen, T.M., Egelhofer, T.A., Wang, W., Kimura, H., Lieb, J.D., and Strome, S. (2010). The histone H3K36 methyltransferase MES-4 acts epigenetically to transmit the memory of germline gene expression to progeny. PLoS Genet *6*, e1001091.

Reddy, K.L., Zullo, J.M., Bertolino, E., and Singh, H. (2008). Transcriptional repression mediated by repositioning of genes to the nuclear lamina. Nature *452*, 243.

Reynaud, E.G., Pelpel, K., Guillier, M., Leibovitch, M.P., and Leibovitch, S.A. (1999). p57(Kip2) Stabilizes the MyoD Protein by Inhibiting Cyclin E-Cdk2 Kinase Activity in Growing Myoblasts. Molecular and cellular biology *19*, 7621-7629.

Ross, J.M., and Zarkower, D. (2003). Polycomb Group Regulation of Hox Gene Expression in C. elegans. Developmental Cell *4*, 891-901.

Ruijtenberg, S., and van den Heuvel, S. (2015). G1/S Inhibitors and the SWI/SNF Complex Control Cell-Cycle Exit during Muscle Differentiation. Cell *162*, 300-313.

Sadasivam, S., and DeCaprio, J.A. (2013). The DREAM complex: master coordinator of cell cycle-dependent gene expression. Nature Reviews *13*, 585-595.

Saito, T.T., Youds, J.L., Boulton, S.J., and Colaiácovo, M.P. (2009). Caenorhabditis elegans HIM-18/SLX-4 Interacts with SLX-1 and XPF-1 and Maintains Genomic Integrity in the Germline by Processing Recombination Intermediates. PLoS Genetics *5*, e1000735.

Santamaría, D., Barrière, C., Cerqueira, A., Hunt, S., Tardy, C., Newton, K., Cáceres, J.F., Dubus, P., Malumbres, M., and Barbacid, M. (2007). Cdk1 is sufficient to drive the mammalian cell cycle. Nature *448*, 811.

Schaner, C.E., Deshpande, G., Schedl, P.D., and Kelly, W.G. (2003). A Conserved Chromatin Architecture Marks and Maintains the Restricted Germ Cell Lineage in Worms and Flies. Developmental Cell *5*, 747-757.

Schnabel, H., and Schnabel, R. (1990). An organ-specific differentiation gene, pha-1, from Caenorhabditis elegans. Science *250*, 686-688.

Schwarz, C., Johnson, A., Koivomagi, M., Zatulovskiy, E., Kravitz, C.J., Doncic, A., and Skotheim, J.M. (2018). A Precise Cdk Activity Threshold Determines Passage through the Restriction Point. Mol Cell *69*, 253-264 e255.

Sczaniecka, M., Feoktistova, A., May, K.M., Chen, J.-S., Blyth, J., Gould, K.L., and Hardwick, K.G. (2008). The Spindle Checkpoint Functions of Mad3 and Mad2 Depend on a Mad3 KEN Box-mediated Interaction with Cdc20-Anaphase-promoting Complex (APC/C). The Journal of Biological Chemistry *283*, 23039-23047.

Shen, X., Kim, W., Fujiwara, Y., Simon, M.D., Liu, Y., Mysliwiec, M.R., Yuan, G.-C., Lee, Y., and Orkin, S.H. (2009). Jumonji modulates Polycomb activity and self-renewal versus differentiation of stem cells. Cell *139*, 1303-1314.

Singh, Amar M., Sun, Y., Li, L., Zhang, W., Wu, T., Zhao, S., Qin, Z., and Dalton, S. (2015). Cell-Cycle Control of Bivalent Epigenetic Domains Regulates the Exit from Pluripotency. Stem Cell Reports *5*, 323-336.

Smolikov, S., Eizinger, A., Hurlburt, A., Rogers, E., Villeneuve, A.M., and Colaiácovo, M.P. (2007). Synapsis-Defective Mutants Reveal a Correlation Between Chromosome Conformation and the Mode of Double-Strand Break Repair During Caenorhabditis elegans Meiosis. Genetics *176*, 2027-2033.

Starostina, N.G., Simpliciano, J.M., McGuirk, M.A., and Kipreos, E.T. (2010). CRL2LRR-1 Targets a CDK Inhibitor for Cell Cycle Control in C. elegans and Actin-Based Motility Regulation in Human Cells. Developmental Cell *19*, 753-764.

Stead, E., White, J., Faast, R., Conn, S., Goldstone, S., Rathjen, J., Dhingra, U., Rathjen, P., Walker, D., and Dalton, S. (2002). Pluripotent cell division cycles are driven by ectopic Cdk2, cyclin A/E and E2F activities. Oncogene *21*, 8320.

Strome, S., Kelly, W.G., Ercan, S., and Lieb, J.D. (2014). Regulation of the X chromosomes in Caenorhabditis elegans. Cold Spring Harbor perspectives in biology *6*.

Strome, S., and Updike, D. (2015). Specifying and protecting germ cell fate. Nature reviews Molecular cell biology *16*, 406-416.

Strome, S., and Wood, W.B. (1983). Generation of asymmetry and segregation of germ-line granules in early C. elegans embryos. Cell *35*, 15-25.

Sulston, J.E., and Horvitz, H.R. (1977). Post-embryonic cell lineages of the nematode, Caenorhabditis elegans. Developmental Biology *56*, 110-156.

Sulston, J.E., Schierenberg, E., White, J.G., and Thomson, J.N. (1983). The embryonic cell lineage of the nematode Caenorhabditis elegans. Developmental Biology *100*, 64-119.

Sutterluty, H., Chatelain, E., Marti, A., Wirbelauer, C., Senften, M., Muller, U., and Krek, W. (1999). p45(SKP2) promotes p27(Kip1) degradation and induces S phase in quiescent cells. Nature Cell Biology *1*, 207-214.

Swaffer, M.P., Jones, A.W., Flynn, H.R., Snijders, A.P., and Nurse, P. (2016). CDK Substrate Phosphorylation and Ordering the Cell Cycle. Cell *167*, 1750-1761.e1716.

Tabuchi, T.M., Deplancke, B., Osato, N., Zhu, L.J., Barrasa, M.I., Harrison, M.M., Horvitz, H.R., Walhout, A.J.M., and Hagstrom, K.A. (2011). Chromosome-Biased Binding and Gene Regulation by the Caenorhabditis elegans DRM Complex. PLoS Genetics *7*, e1002074.

Takasaki, T., Liu, Z., Habara, Y., Nishiwaki, K., Nakayama, J., Inoue, K., Sakamoto, H., and Strome, S. (2007). MRG-1, an autosome-associated protein, silences X-linked genes and protects germline immortality in Caenorhabditis elegans. Development *134*, 757-767.

The, I., Ruijtenberg, S., Bouchet, B.P., Cristobal, A., Prinsen, M.B., van Mourik, T., Koreth, J., Xu, H., Heck, A.J., Akhmanova, A.*, et al.* (2015). Rb and FZR1/Cdh1 determine CDK4/6-cyclin D requirement in C. elegans and human cancer cells. Nat Commun *6*, 5906.

Theil, K., Herzog, M., and Rajewsky, N. (2018). Post-transcriptional regulation by 3' UTRs can be masked by regulatory elements in 5' UTRs. Cell Reports *22*, 3217-3226.

Thein, M.C., McCormack, G., Winter, A.D., Johnstone, I.L., Shoemaker, C.B., and Page, A.P. (2003). Caenorhabditis elegans exoskeleton collagen COL-19: An adult-specific marker for collagen modification and assembly, and the analysis of organismal morphology. Developmental Dynamics *226*, 523-539.

Thomas, J.H. (1990). Genetic Analysis of Defecation in Caenorhabditis Elegans. Genetics *124*, 855-872.

Thomas, J.O., and Kornberg, R.D. (1975). An octamer of histones in chromatin and free in solution. Proceedings of the National Academy of Sciences of the United States of America *72*, 2626-2630.

Timmons, L., and Fire, A. (1998). Specific interference by ingested dsRNA. Nature *395*, 854-854.

Tursun, B., Patel, T., Kratsios, P., and Hobert, O. (2011). Direct Conversion of *C. elegans* germ cells into specific neuron types. Science *331*, 304-308.

Unhavaithaya, Y., Shin, T.H., Miliaras, N., Lee, J., Oyama, T., and Mello, C.C. (2002). MEP-1 and a Homolog of the NURD Complex Component Mi-2 Act Together to Maintain Germline-Soma Distinctions in C. elegans. Cell *111*, 991-1002.

Updike, D., and Strome, S. (2010). P granule assembly and function in Caenorhabditis elegans germ cells. Journal of andrology *31*, 53-60.

Updike, D.L., and Strome, S. (2009). A genomewide RNAi screen for genes that affect the stability, distribution and function of P granules in Caenorhabditis elegans. Genetics *183*, 1397-1419.

van den Heuvel, S., and Dyson, N.J. (2008). Conserved functions of the pRB and E2F families. Nature Reviews Molecular Cell Biology *9*, 713.

Walter, J., Schermelleh, L., Cremer, M., Tashiro, S., and Cremer, T. (2003). Chromosome order in HeLa cells changes during mitosis and early G1, but is stably maintained during subsequent interphase stages. The Journal of cell biology *160*, 685-697.

Wan, L., Chen, M., Cao, J., Dai, X., Yin, Q., Zhang, J., Song, S.J., Lu, Y., Liu, J., Inuzuka, H.*, et al.* (2017). The APC/C E3 Ligase Complex Activator FZR1 Restricts BRAF Oncogenic Function. Cancer discovery *7*, 424-441.

Wan, L., Xu, K., Wei, Y., Zhang, J., Han, T., Fry, C., Zhang, Z., Wang, Y.V., Huang, L., Yuan, M.*, et al.* (2018). Phosphorylation of EZH2 by AMPK Suppresses PRC2 Methyltransferase Activity and Oncogenic Function. Molecular Cell *69*, 279-291.e275.

Wan, L., Zou, W., Gao, D., Inuzuka, H., Fukushima, H., Berg, Anders H., Drapp, R., Shaik, S., Hu, D., Lester, C., *et al.* (2011). Cdh1 Regulates Osteoblast Function through an APC/C-Independent Modulation of Smurf1. Molecular Cell *44*, 721-733.

Wang, D., Kennedy, S., Conte Jr, D., Kim, J.K., Gabel, H.W., Kamath, R.S., Mello, C.C., and Ruvkun, G. (2005a). Somatic misexpression of germline P granules and enhanced RNA interference in retinoblastoma pathway mutants. Nature *436*, 593-597.

Wang, S., Fisher, K., and Poulin, G.B. (2011). Lineage specific trimethylation of H3 on lysine 4 during C. elegans early embryogenesis. Developmental Biology *355*, 227-238.

Wang, W., Nacusi, L., Sheaff, R.J., and Liu, X. (2005b). Ubiquitination of p21Cip1/WAF1 by SCFSkp2: Substrate Requirement and Ubiquitination Site Selection. Biochemistry *44*, 14553-14564.

Ward, S., Hogan, E., and Nelson, G.A. (1983). The initiation of spermiogenesis in the nematode Caenorhabditis elegans. Developmental Biology *98*, 70-79.

Wei, X., Potter, C.J., Luo, L., and Shen, K. (2012). Controlling gene expression with the Q repressible binary expression system in *Caenorhabditis elegans*. Nature Methods *9*.

White, J.G., Southgate, J.N., Thomson, S., and Brenner, S. (1986). The structure of the nervous system of the nematode *Caenorhabditis elegans*. Philosophical Transactions of the Royal Society of London B, Biological Sciences *314*, 1-340.

Williams, B.D., Schrank, B., Huynh, C., Shownkeen, R., and Waterston, R.H. (1992). A Genetic Mapping System in Caenorhabditis Elegans Based on Polymorphic Sequence-Tagged Sites. Genetics *131*, 609-624.

Wu, X., Shi, Z., Cui, M., Han, M., and Ruvkun, G. (2012). Repression of germline RNAi pathways in somatic cells by Retinoblastoma pathway chromatin complexes. PLoS Genetics *8*.

Xu, L., Paulsen, J., Yoo, Y., Goodwin, E.B., and Strome, S. (2001). Caenorhabditis elegans MES-3 is a target of GLD-1 and functions epigenetically in germline development. Genetics *159*, 1007-1017.

Ye, Y., Li, M., Gu, L., Chen, X., Shi, J., Zhang, X., and Jiang, C. (2016). Chromatin remodeling during in vivo neural stem cells differentiating to neurons in early Drosophila embryos. Cell Death And Differentiation *24*, 409.

Yoon, S., Kawasaki, I., and Shim, Y.-H. (2012). CDC-25.1 controls the rate of germline mitotic cell cycle by counteracting WEE-1.3 and by positively regulating CDK-1 in Caenorhabditis elegans. Cell Cycle *11*, 1354-1363.

Yuan, W., Xu, M., Huang, C., Liu, N., Chen, S., and Zhu, B. (2011). H3K36 Methylation Antagonizes PRC2-mediated H3K27 Methylation. The Journal of Biological Chemistry *286*, 7983-7989.

Zhang, J., Wan, L., Dai, X., Sun, Y., and Wei, W. (2014). Functional characterization of Anaphase Promoting Complex/Cyclosome (APC/C) E3 ubiquitin ligases in tumorigenesis. Biochimica et biophysica acta *1845*, 277-293.

Zhang, P., Wong, C., Liu, D., Finegold, M., Harper, J.W., and Elledge, S.J. (1999). p21(CIP1) and p57(KIP2) control muscle differentiation at the myogenin step. Genes & Development *13*, 213-224.

Zhou, Z., Thomsen, R., Kahns, S., and Nielsen, A.L. (2010). The NSD3L histone methyltransferase regulates cell cycle and cell invasion in breast cancer cells. Biochemical and Biophysical Research Communications *398*, 565-570.

Zouaz, A., Fernando, C., Perez, Y., Sardet, C., Julien, E., and Grimaud, C. (2018). Cell-cycle regulation of non-enzymatic functions of the Drosophila methyltransferase PR-Set7. Nucleic Acids Research, gky034-gky034.

INTERNET-BASED RESOURCES:

NCBI Blast server: https://blast.ncbi.nlm.nih.gov/

Wormbase (WS258): www.wormbase.org